Abstract

Han, Xiaogang **Development of Monte Carlo Code for Coincidence Prompt Gamma-ray Neutron Activation analysis** (under the direction of Professor Robin P. Gardner)

Prompt Gamma-Ray Neutron Activation Analysis (PGNAA) offers a non-destructive, relatively rapid on-line method for determination of elemental composition of bulk and other samples. However, PGNAA has an inherently large background. These backgrounds are primarily due to the presence of the neutron excitation source. It also includes neutron activation of the detector and the prompt gamma rays from the structure materials of PGNAA devices. These large backgrounds limit the sensitivity and accuracy of PGNAA.

Since most of the prompt gamma rays from the same element are emitted in coincidence, a possible approach for further improvement is to change the traditional PGNAA measurement technique and introduce the gamma-gamma coincidence technique. It is well known that the coincidence techniques can eliminate most of the interference backgrounds and improve the signal-to-noise ratio. A new Monte Carlo code, CEARCPG has been developed at CEAR to simulate gamma-gamma coincidence spectra in PGNAA experiment. Compared to the other existing Monte Carlo code CEARPGA I and CEARPGA II, a new algorithm of sampling the prompt gamma rays produced from neutron capture reaction and neutron inelastic

scattering reaction, is developed in this work. All the prompt gamma rays are taken into account by using this new algorithm. Before this work, the commonly used method is to interpolate the prompt gamma rays from the pre-calculated gamma-ray table. This technique works fine for the single spectrum. However it limits the capability to simulate the coincidence spectrum. The new algorithm samples the prompt gamma rays from the nucleus excitation scheme. The primary nuclear data library used to sample the prompt gamma rays comes from ENSDF library.

Three cases are simulated and the simulated results are benchmarked with experiments. The first case is the prototype for ETI PGNAA application. This case is designed to check the capability of CEARCPG for single spectrum simulation. The second case and the third case are designed for coincidence simulation. CEARCPG is also applied to optimize the design of coincidence PGNAA device. Additionally, a new coincidence PGNAA application is also proposed in this work. The possible extensions of this code are also discussed.

The funding of this work is provided by the Center for Engineering Application of Radioisotopes (CEAR) at North Carolina State University (NCSU) and Nuclear Engineering Education Research.

Development of Monte Carlo code for Coincidence Prompt Gamma-ray Neutron Activation Analysis

By

Xiaogang Han

A dissertation Submitted to the Graduate Faculty of
North Carolina State University
in partial fulfillment of the
requirement for the Degree of
Doctor of Philosophy

Nuclear Engineering

Raleigh, North Carolina

August 8, 2005

Approved by:

Prof. Robin P. Gardner, Chair	**Dr. Man-Sung Yim**
Dr. Avneet Sood	**Dr. Wenye Wang**

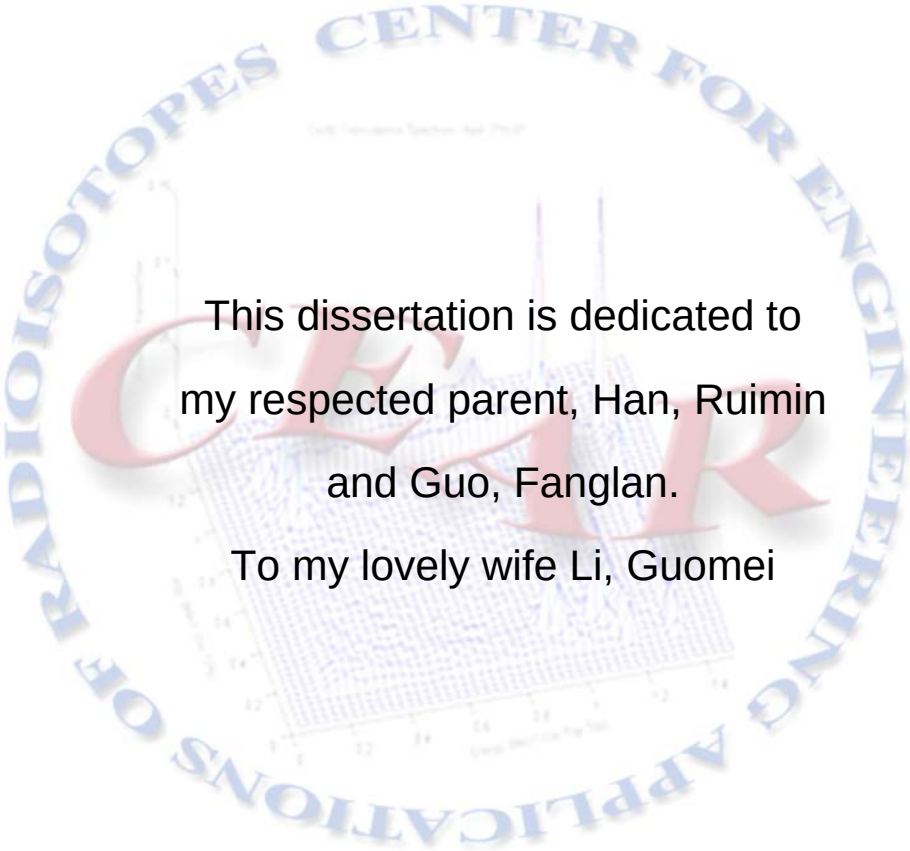

This dissertation is dedicated to

my respected parent, Han, Ruimin

and Guo, Fanglan.

To my lovely wife Li, Guomei

Biography

Han, Xiaogang, son of Han, Ruimin and Guo, Fanglan, was born in HuaYin, a small town near HuaShan Mountain in ShanXi province, China, on March 26, 1974. In September 1991, he was accepted by the department of physics of SiChuan University. He met his future wife there. It is the most important thing during his university life. He earned his B.S. degree in July 1995. After that, he worked as a research assistant in China Institute of Atomic Energy (CIAE) for six years.

In 2001, he began his graduate study in the Nuclear Engineering Department at North Carolina State University and worked as a research assistant.

The Author got married to Guomei Li in March 2000, a millennium wedding.

Acknowledgement

First of all, I would like to express my deep gratitude to my advisor, Professor Robin Gardner for your guidance throughout this work. I also want to thank you for your financial support that makes me and my wife reunion when I pursue my PhD degree at NCSU alone. Dr Avneet, I would like to say thank you for your helpful instruction and discussion for this work. I also would like to thank Gerald D. Wicks, for your assistance for experiment work. Special thanks are given to Dr. Guo, Weijun and Dr. Wallid Metwally, for their instructive discussion and suggestion. I would like to extend my thanks to all those who helped me, including faculties and staff members of the Department of Nuclear Engineering, graduate students and my friends.

Finally I want to express my innermost feelings to my parent, Han, Ruimin and Guo, Fanglan. I want to appreciate that they brought life to me, to appreciate them to give me warm family and to guide me to be a righteous man. I need to express my deepest and most sincere appreciation to my wife, my best friend and my lover, for her self-giving love and for her comfort to me.

TABLE OF CONTENTS

LIST OF FIGURES

List of Tables

1 Introduction

1.1 Overview

The traditional method for measuring the compositions of coal involves laboratory analysis of samples weighting of the order of 1g. Not only is this process slow, tedious and expensive if continuous sampling, but also the inhomogeneous nature of coal results in the average compositions of the small sample not being representative of the bulk material. Therefore, a need exists for an instrument which can determine an “on-line” basis for the amounts of the major elements in bulk materials, such as coal. The analysis should be performed continuously and automatically on samples of mass flow rates that may exceed several hundred tons per hour.

A technique known as PGNAA (prompt gamma neutron activation analysis) is used to measure the raw material element composition (Molnar et al. 1993, Molnar and Lindstrom 1998). Some extensive experiments have been performed to analyze the composition of bulk coal (Gozani et al 1998, Duffey et al 1978,. Reynolds, 1979, Marshall III, 1989, Gozani, 1977) and mineral deposits from deep sea vents on the Pacific floor (Perry 1999). The PGNAA phenomenon is based on the radioactive capture reaction between a neutron and the nucleus of any atom. Neutron radioactive capture reaction is a purely nuclear process and can be used for the characterization of material composition. The neutron interacts with the target nucleus and a compound nucleus is formed in excited state. The excited compound nucleus then de-excites quickly (less than 10^{-14}

seconds) to the ground level by emitting gamma rays that are unique for each element.

Prompt gamma-ray neutron activation analysis (PGNAA) is different from the neutron activation analysis (NAA). Neutron induced prompt gamma-ray activation analysis (PGNAA) exploits the prompt capture gamma rays directly, while the neutron activation analysis (NAA) utilizes the delayed gamma rays from the radioactive daughter nucleus (Fig. 1-1).

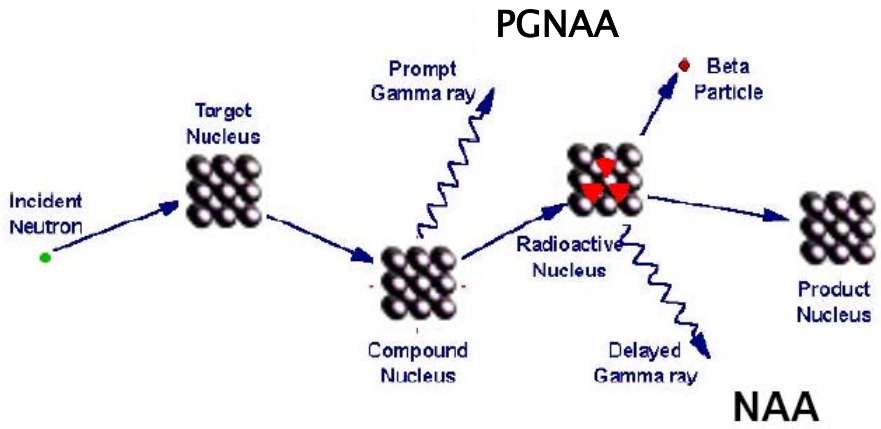

Figure 1- 1 The neutron capture and gamma emission process

Compared with the traditional chemical analysis, PGNAA is a nondestructive, simultaneous method and applicable to all elements. However, PGNAA suffers from relatively complicated gamma spectra and the interference from the neutron source, the structure material, the natural background, pulse summing and pulse pile-up effects (Metwally 2004). The interferences from the neutron source are listed as follows:

1. Fission gamma rays emitted from the neutron source (for example: ^{252}Cf spontaneous neutron source)

2. Gamma rays produced by neutron interaction with the materials of detector. (Gardner 2000). For NaI detector, it includes the prompt gamma rays of NaI and the decay gamma rays of radioisotopes ^{128}I and ^{24}Na.
3. Gamma rays produced by the construction materials of PGNAA analyzer

The interferences from background are listed as follows:

1. Potassium-40 which emits the gamma rays with energy 1.461 MeV
2. Natural Uranium and Thorium decay chain which emits gamma rays with energy 1.764 MeV, 2.204 MeV, 2.614 MeV etc.
3. Cosmic radiation which will generate high-energy continuous distribution gamma rays.

Hydrogen, both in sample or non-sample region, is a common material that can cause problems in many typical cases of PGNAA. When the hydrogen nucleus is bombarded by neutron, a single-energy gamma ray with energy 2.223 MeV will be emitted when the excited hydrogen nucleus de-excites. The magnitude of hydrogen peak is much higher than the peaks of other interested element. At the same time, the increased counting rates from hydrogen can significantly increase the dead time of PGNAA analyzer system and reduce the sensitivity of PGNAA analyzer. Figure 1-2 shows the typical spectrum of PGNAA analysis. The calculated interference spectra are plotted. It takes almost 58% of the total spectrum.

Other factors that cause the complexity of PGNAA system are the summing and pulse pile-up effects. The summing effect can be seen if two (or more) gamma rays are emitted at the same time (in coincidence) and are detected by detector simultaneously, additional peaks may also appear in the recorded pulse-height spectrum. This can lead to errors when analyzing the result.

Pulses from a radiation detector are randomly spaced in time which can lead to an overlap among pulses when counting rates are high. This effect is generally called pulse pile-up and will lead to distortions in the recorded spectrum (Metwally 2003).

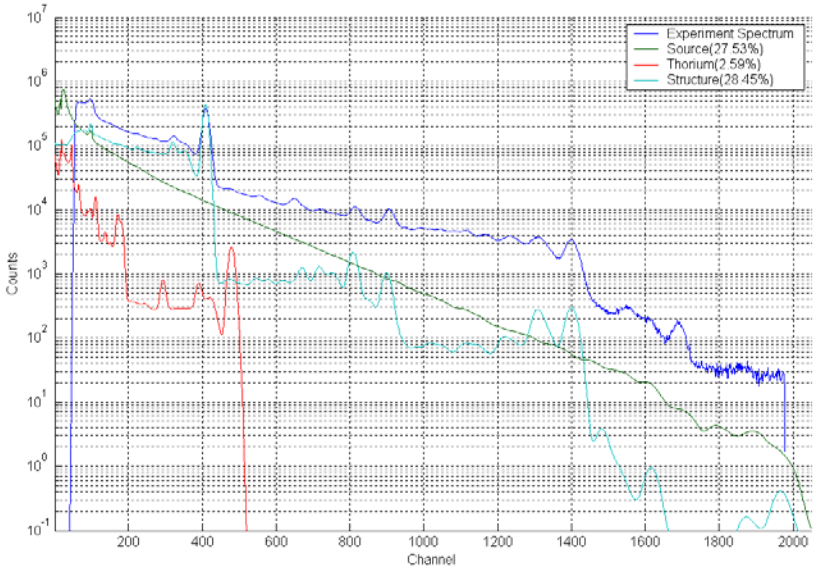

Figure 1- 2 The typical spectrum of PGNAA analysis

Summing effects and pulse pile-up effect add a source of complexity to the spectrum and cause interference with quantitative measurement. For example, they may lead to false amounts when elemental analysis is performed using full

energy peaks or Library Least Squares (LLS) method (Marshall and Zumberge, 1989).

One of possible improvement is to change the single detector measurement technique to gamma-gamma coincidence technique (Metwally 2004, Gardner 2000). The gamma-gamma coincidence technique is a well-developed technique and widely used in the nuclear structure study (Wapstra 1979). It is well known that the gamma-gamma coincidence technique can reduce the interference from background, pulse-pile effect, the summing effect, and improve the signal-to-noise ratio. Fortunately, most of prompt gamma rays are emitted in coincidence. Applying gamma-gamma coincidence technique for PGNAA analysis is a definitely newly developing study. The biggest disadvantage of gamma-gamma coincidence measurement is the low counting rate. Optimization of the coincidence PGNAA application is one of objectives of this work. The last experimental work was done by Walid A. Metwally (2004).

1.2 Review of PGNAA analysis methods

To make the quantitative analysis of the measured PGNAA gamma spectrum, there are two popular methods. They are peak analysis and Library Least Squares (LLS). Robin. P. Gardner compared these two methods in 1997. (Gardner 1997). In his study, analyses for elements Al, Si, and Fe were made by using the single peak analysis and the elemental library least-squares method. It shows that the library least-squares method is about 2.5 times better than the single peak analysis method.

1.2.1 Single peak analysis

For the single peak analysis, peak intensities are not only related to the elemental weight fraction but also related to the matrix effect correction methods. The matrix effect is from the attenuation of prompt gamma-rays. Compare to the X-ray Fluorescence, the matrix effect of PGNAA analysis is less significant due to the high energy of the prompt gamma-rays. However, PGNAA analysis still suffers from the matrix effect for some selected elements. For example, the mercury, the most popular characteristic prompt gamma-rays used for mercury analysis is 0.367 MeV and might be attenuated by the bulk sample before they enter the detector. The counts of full energy peaks might be distorted due to the matrix effect.

The matrix effect correction for the quantification of elemental weight fractions can be handled with one of two methods: the empirical coefficients method and fundamental parameters method (Bertin 1978, Jenkins 1988). The disadvantage lies in the requirement of measurements on a number of carefully prepared standard samples to determine the empirical coefficients, which is very time consuming and expensive. And quite often, these empirical coefficients are system dependent and can not transfer to the systems. The fundamental parameters method was initially proposed in the early of 1950s' and invested further (Criss and Birks 1968, Gillam and Heal 1952), which attempts to model the sample matrix effect with a complete mathematical model. In principle, the fundamental parameters method is an absolute method and does not require measurements on standard samples. However, since calculations required are

extremely complex, the practical application of this approach usually makes use of pure element standards to that of the unknown sample, to cancel some number of unknown fundamental parameters that are required and simplify the calculation. So, these methods are not absolute. In contrast to these traditional methods, the Monte-Carlo Library Least-Squares method can solve the matrix problem automatically since all the matrix effect will be included when using the Monte Carlo code to generate the spectrum since the Monte Carlo code already took the matrix effect into account during the calculation.

1.2.2 Monte Carlo Library Least-Square fitting analysis

The PGNAA technique is very similar to the energy-dispersive X-ray fluorescence (EDXRF) analysis in many ways. However, it is at the earlier stage of its development. Compared to the EDXRF, PGNAA can be used to analyze the larger sized sample because the neutron and prompt gamma rays are easier to penetrate through the sample than X-rays. An approach to the non-linear analysis problem for PGNAA has been developed recently, which shows this promise. The method is called the Monte Carlo Library Least-Squares (MCLLS) approach. It requires that one have a very accurate forward model which enables one to calculate the pulse-height spectrum obtained with a PGNAA system when the geometrical and sample composition variables are known. This approach has been developed and successfully tested for the PGNAA analysis of bulk coal on (simulated) conveyor belts. The MCLLS approach consists of the following. (Shyu et al., 1988, 1993)

1. The pulse-height spectrum is generated by the Monte Carlo code using assumed values of the sample composition (and density).

2. The prompt gamma-ray pulse-height spectrum for each element is separately recorded to serve as library spectra--this is just a bookkeeping problem within the code.

3. A linear library least-squares (LLS) analysis is performed and the elemental analysis so obtained is compared with the initially assumed values.

4. If the LLS elemental composition is close enough to the assumed values that the linearity assumption is valid, then they are taken as the final measured values--if not, the LLS values are taken as the next iteration of assumed values and steps 1 through 3 are repeated until the linearity assumption is valid.

For Library Least-square method, it is based on the assumption that any unknown sample spectrum is the sum of the products of the elemental amount and the library spectrum of each element for every channel. It is given by:

$$y_i = \sum_{j=1}^{m} x_j a_{ij} + e_i \qquad \text{i= 1,2,3,....n} \qquad (1.1)$$

Where y_i is the unknown sample spectrum or counting rate in channel i of the unknown sample, x_j is the amounts of component j in the unknown sample, a_{ij} is the library spectra of component j in counting rate in channel per unit amount, and e_i is the random error in channel i due to statistical counting rate fluctuations. Expression (1.1) is actually a set of linear equations that can be solved for x_j by

minimizing the reduced Chi-Square χ_v^2 which is given by

$$\chi_v^2 = \sum_{i=1}^{n} \frac{e_i^2}{(n-m)\sigma_i^2} \qquad (1.2)$$

Where (n-m) is the number of degrees of freedom, and σ_i^2 is the variance of the random error in each channel. The set of equations for estimating σ_i^2 can be found in the reference (Arinc. et. al 1975). Compared to the single peak analysis method, this approach has following advantages:

1. Elemental library spectra are acquired by Monte Carlo simulation instead of by extensive and time consuming experiments
2. Overlapping peaks in the sample spectrum are automatically resolved
3. The entire spectrum information is available to be utilized
4. The matrix effect is automatically corrected
5. The measurement uncertainty is directly available from the least-squares fit

1.3 Overview of previous experiment work

One of the earliest gamma-gamma coincidence measurements was done by Kim, Speecke and Hoste(1965) and Kim and Hoste(1965). In their paper, they tried to determine the concentration of copper, silver and antimony in bismuth. Their results were based on scalar counts and yielded results with considerable errors.

The usefulness of the gamma-gamma coincidence technique in elemental

analysis has already been demonstrated by Ehmann and Vance (1991), Meyer (1987), Meyer et al. (1993), Jakubek et al.(1998), and Koeberl and Huber (2000). They found it is especially useful in determining Ir and Se in geological samples at the ppm level. Their main goal was to improve the sensitivity of the method by suppressing the continuous background and reducing spectral interference.

The conventional method of doing gamma-gamma coincidence detection is to require a coincidence relation with a selected full-energy peak; here we call this the peak-coincidence method. This constraint reduces the spectrum to the signals of those gamma photons which are in a cascade relation with that peak. It lowers the background substantially, increasing the peak to the background ratio. However, the peak counting rate is also reduced, since it is proportional to the product of two full-energy peak efficiencies. A significant disadvantage is that this method is extremely time consuming due to the low coincidence count rate.

Other useful attempts were done by Ember (2002 and 2004), Gardner and Metwally (2000 and 2004). In Ember's work (2002), they proposed to define a coincidence relation not with a single peak, but with a selected part of the spectrum containing several peaks and a part of their Compton continuum to increase the coincidence efficiency. In his work, he also mentioned the matrix problem when he quantitatively analyzed the recorded spectrum. But there are no mentions of the approach indicated in his paper. In PGNAA, a frequent problem is the presence of a few strong gamma-ray emitted in an element of no interest. Their Compton continuum may mask the lower energy transitions of trace elements. Ember thought the most "problematic" elements are hydrogen

and boron. Hydrogen is dominant in biological samples and solutions. Boron is widely used in heat resistant glasses. Actually, the geometry of sample (thickness), homogeneity of sample can introduce the matrix problem that will shield part of prompt gamma rays and introduce distortion in the final recorded spectrum.

Fortunately, as mentioned previously, the MCLLS method can fix the matrix problem automatically because when generate the elemental library spectra, the Monte Carlo code will account for the shielding (attenuation) prompt gamma rays and the interference from the elements. In Gardner's (2000) work, a feasibility study was done by using the coincidence counting approach. Their main concern was to apply this approach to PGNAA application. They used NIM (Nuclear Instrument Module) modules, NaI detectors, reactor neutron source and Cf-252 spontaneous fission neutron source. The results showed that the coincidence measurement can efficiently reduce the background and increase the signal-to-noise (S/N) ratio. A crude Monte Carlo simulation was also performed to coincidence spectrum of sulfur sample. In Metwally's (2004) work, CAMAC modules based on the SPARROW multi-parameter data acquisition system was used. In his work, elemental library least-square fitting was performed for a mixture of radioisotopes sample. The LLS method was applied to the coincidence data as well as the normal signal spectrum data. The results showed that the fitting results of coincidence spectra are much closer to the original activity values than the fittings of the single spectra. In addition, greatly reduction of the background, summing and pulse pile up effects was observed in his work.

1.4 Review of previous MC work

Monte Carlo simulation for the PGNAA device has been conducted for several years. Before 1991, the roles that Monte Carlo simulation played in the PGNAA systems were mostly focused on predicting the spectral responses that could be used to compare with experimental spectrum or optimize the PGNAA analyzer systems in their design stage. A variety of specific Monte Carlo simulation codes were reported in the past. They are: McPNL, developed in CEAR which modeled the spectral response of dual-spaced gamma-gamma litho-density logging tools (Mickael, Gardner, and Verghese, 1988), McDN, developed in CEAR (Mickael, Gardner, and Verghese, 1988), and MOCA (Pinault and Gateau, 1989) etc. However, the concept of MCLLS algorithm (Shyu 1991, Shyu, Gardner and Verghese, 1993) greatly extended the application of Monte Carlo simulation, since it made possible to use simulated elemental library spectra to apply the Least-Square fitting to analyze the unknown sample spectra. The application of MCLLS algorithm has been reported in a paper (Shyu, Gardner and Verghese, 1993), where elemental library spectra were generated by a specific Monte Carlo code, CEARPGA I.

CEARPGA I is the first specific purpose Monte Carlo code publicly reported to implement MCLLS algorithm for PGNAA analyzer. It was developed on the basis of many previous research work on modeling PGNAA devices, which mostly were done at CEAR of North Carolina State University. It inherits many features from its previous versions. Clark first developed a Monte Carlo code to model the system of borehole geometry (Clark, Gardner and Verghese, 1982), which

incorporated the correlated sampling approach that allow to calculate the reference sample and comparison samples simultaneously. It used continuous energy treatment of neutron transport by using piecewise fitted neutron cross sections of ENDF/B-V. Yuan modeled the system of transmission geometry (Yuan, Gardner and Verghese, 1987), where some features extracted from those used in the previous version. These new features included implicit capture scheme for gamma-ray generation and Russian roulette for particle termination. A further improvement (Jin, Gardner and Verghese, 1987) was done for modeling the complete pulse-height spectral response of PGNAA of bulk media and borehole configuration, where Ge (Li) detector response function was first used to generate the pulse-height spectrum when all the simulation histories were finished. To implement the Monte Carlo library least squares algorithm, Shyu modified Jin's Monte Carlo code to extend the capability of generating elemental library spectra (Shyu, Gardner and Verghese, 1993). A further improvement were done later by Guo (1997) who added the functions of generating the gamma-ray library spectra from neutron inelastic scattering reaction and radioisotope decay gamma-ray library, and included the NaI detector response functions obtained by another Monte Carlo simulation code developed by Peplow, Gardner and Verghese (1994).

The CEARPGA I was developed with much effort on accuracy and efficiency. The major variance reduction techniques used include:

1) Russian roulette. This technique is used in conjunction with the expected value technique to randomly terminate the neutron or gamma-ray history if its cumulative weight falls below a specified value.

2) Truncated exponential probability density function. This technique is used for those particles that reach the system boundary and could fly out of the system along their current flight direction. In this case, the flight distance to the next interaction is sampled from the truncated exponential probability density function to force the next interaction to occur before it escapes out of the system.

3) Direction biasing. The flight directions of the gamma rays are sampled in a transformed fictitious probability density functions that result in sampling more frequently along their last flight directions. For the initial flight direction of a gamma ray at the site of its emission, it is always biased toward the detector.

4) Discrete importance function This technique is used to increase the neutron capture interaction sampling frequency for those elements whose capture interaction cross sections are less than one tenth of the elastic interaction cross section.

5) Stratified sampling approach. This technique is employed to force all the important prompt gamma rays of a given element from the radioactive capture interaction to be emitted and the resultant prompt gamma rays are tracked independently.

6) Expected value splitting approach. This approach is employed to make the gamma ray of interest to score at every interaction site by splitting it into two parts or two sub-particles. One of which is assumed to directly go to the detector

without any interaction along its flight path with the expected weight assigned to that process, the other with remaining weight will have one or more interactions based on normally tracking process.

7) Correlated sampling. This technique is used to predict the change in the detector response due to the slight composition variation of the sample. It is implemented during the normal process of particle tracking.

8) Detector response function. By this technique, the process of tracking any gamma ray stops once it reaches the detector and the score of the gamma ray incident on detector is tallied and is converted to detector pulse height responses after all the simulation histories finish. This technique is considered to be very powerful and can save as much as 50% of the total tracking time for each gamma ray history in the Monte Carlo simulation (Gardner, 2000). The detector response functions are usually more accurate since the Monte Carlo simulation code with which the detector response functions are calculated often has more accurate models.

Based on the CEARPGA I, Zhang developed the next generation code CEARPGA II (Zhang, 2003). In his code, he did some modification of CEARPGA I. The major modifications are listed in the following:

1) Solve the Big Weight Problem of code CEARPGA I.
2) Implement the new detector response function of NaI detector. The new detector response function is generated by using code g03 (Gardner 2002).
3) Add the neutron activation libraries of NaI detector.
4) Add the libraries spectra of Natural background.

5) Implement a new general geometry package adopt from MCNP4

6) Use new gamma-ray cross section

7) Add the annihilation gamma-ray tracking

The biggest contribution of Dr. Zhang is to solve the big weight problem in code CEARPGA I by using analogy interpolation method.

Before we introduce the analogy interpolation method used in code CEARPGA II, let us review the reasons that cause the big weight problem in code CEARPGA I. The main reason is the impact of variance reduction technique used in code CEARPGA I. As we know, most of variance reduction techniques are based on sampling fictitious probability distributions rather than true ones, such as biasing direction, truncated exponential function, expected value splitting techniques etc. To correct the resulting error, each time when a fictitious probability distribution is sampled, a weight-adjusting factor has to be calculated as follows:

$$W_{adj} = \frac{f(x)}{f'(x)} \qquad (1.1)$$

Where $f(x)$ is the true probability distribution function. x represents any value of random variable of concern, and $f'(x)$ is the biasing sampling probability density function. This weigh-adjusting factor guarantees the final estimate of the parameter concerned to be unchanged.

Expected value splitting approach used in CEARPGA I was identified to be the main reason for the big weight problem encountered in the simulation of ETI coal analyzer system (Gardner, 2000). This technique basically divides the

gamma ray of interest into two particles, no matter where it is emitted. One particle goes directly to the detector without any further collisions and the other carries the rest of the weight and will travel as usual in the system. The detection probability of the non-scattered gamma ray is calculated through the following formula (Shyu 1991):

$$P = \int_{v_{\min}}^{v_{\max}} \int_{\rho_{\min(v)}}^{\rho_{\max(v)}} p_1(v,\rho) \times p_2(v,\rho) \times p_3(v,\rho) d\rho dv \quad (1.2)$$

Where p_1 is the probability of scattering toward the detector through the angles (v,ρ) , p_2 is the probability that the gamma ray will be transmitted to the detector at the direction angles (v,ρ) without collision and p_3 is the detection efficiency of the detector, and (v,ρ) is the direction angle of the gamma ray. The detailed description of how to approximate *p* in the Monte Carlo codes was discussed in the reference (Shyu, 1991). Here only qualitative discussion is done. From the expression for non-scattered detection probability, it can be found that the first term p_1 is associated with angles subtended by the detector. The closer the gamma ray is to the detector, the larger p_1 is. The second term p_2 is related to the distance to the detector, the closer the gamma ray to the detector, the greater probability the gamma ray has to reach the detector without interaction. This implies that the relative position of the origin of gamma rays to the detector has a big impact on the evaluation of the non-scattered detection probability and distorts the final pulse-height spectra.

The analogy linear interpolation approach that is used in code CEARPGA II is a combination of analogy Monte Carlo simulation method and the linear

interpolation technique (Wenchao Zhang 2003). This approach is intended to maintain high calculation efficiency while eliminating the big weight problem. The basic idea of analogy linear interpolation approach is using the analogy method to generate the output table of pre-selected pseudo gamma rays and then using linear interpolation technique to generate the output spectra of true prompt gamma rays of interested elements. The generated output gamma spectra will be acted as input library spectra of the next analysis (LLS). A set of pseudo gamma rays are selected whose energy range can cover all energy region of true prompt gamma rays in PGNAA. In code CEARPGA II, 24 pseudo gamma rays are selected with energy of 0.5, 1.0, 1.5, 2.0 …… 12.0 MeV respectively.

As what we expect, the analogy linear interpolation can eliminate the big weight problem. However, another error will be introduced when applying analog linear interpolation method to generate the true elemental spectra, especially at low – energy region because the lowest pseudo gamma rays energy is 0.5 MeV.

The biggest limitation of code CEARPGA I and CEARPGA II is that they are all originally designed to simulate the single library elemental spectra. The algorithm used to generate the neutron-induced gamma-ray limits its capability of simulating coincidence measurement. Before this work, there is no any existing Monte Carlo code can be used to simulate the coincidence spectra.

CEARCPG is developed at CEAR for this purpose. CEARCPG is the first specific Monte Carlo code for elemental analysis by using coincidence technique. It can generate the single library spectra and the coincidence spectra of interested elements at the same time. The single library spectra and coincidence

spectra will be served as elemental library spectra for the next step, Library Least – Square fitting.

2 Physics

2.1 Neutron Physics

2.1.1 Sampling the neutron from the neutron source

The default built-in neutron source in the CEARCPG is the ^{252}Cf spontaneous neutron source, which is one of the most commonly used thermal neutron sources in PGNAA analyzers. The basic information of ^{252}Cf is presented in Table 2-1. For each fission, there is about 80% fission gamma rays emitted with half life of 10^{-11} sec or less and about 15% emitted with half life of 10^{-9} to 10^{-10} sec.

Table 2- 1. The characteristics of spontaneous fission source ^{252}Cf

Decay mode	α decay	96.9%
	Spontaneous fission	3.1%
Half life	α decay	2.731±0.007 a
	Spontaneous fission	85.5±0.5 a
	Average	2.646±0.004 a
Yield of spontaneous fission neutrons(#/μg.s)	2.34×10^{6}	
Average energy of neutron(MeV)	2.158±0.017	
$\bar{\nu}$ (#of neutrons/spontaneous fission)	3.731±0.008	
Yield of fission gamma rays(#/μg.s)	1.3×10^{7}	

In CEARCPG, it is assumed to be a point source specified by both its location (x, y, z) and source strength in the input file. The probability distribution function for its neutron energies is given by the normalized Cf 252 fission

spectrum (Green, Mitchell and Steen, 1973):

$$X(E) = \frac{2}{\sqrt{\pi}} \frac{\sqrt{E}}{T^{3/2}} E^{-E/T} \qquad (2.1)$$

Where T=1.406 MeV

The energy is then sampled as suggested by Carter and Cashwell (1975; Shyu 1991):

$$E = T[-\ln \xi_1 - (\ln \xi_2) \cos^2(\frac{\pi}{2} \xi_3)] \qquad (2.2)$$

Where ξ_1, ξ_2 , ξ_2 are three random numbers between 0 and 1

The initial neutron direction is assumed to be isotropic. The direction is sampled by the introduction of two independent random variables, the polar angle θ (or μ=cosθ) and the azimuthal angle ϕ . It is described as follows.

$$\begin{aligned} \mu &= 2\xi_1 - 1 \\ \phi &= 2\pi\xi_2 \end{aligned} \qquad (2.3)$$

Where ξ_1, ξ_2 are two random numbers between 0 and 1

The direction cosines (Ω_1 ,Ω_2 , Ω_3) of the direction in the Cartesian system can thus be obtained by,

$$\begin{aligned} \Omega_1 &= \sqrt{1-\mu^2} \cos\phi \\ \Omega 2 &= \sqrt{1-\mu^2} \sin\phi \\ \Omega 3 &= \mu \end{aligned} \qquad (2.4)$$

In CEARCPG, the neutron source energy and initial direction is sampled in the subroutine named CF252. The algorithm of sampling the fission gamma-ray will be detailed discussed in the part of photon physics

2.1.2 Sampling the Neutron Flight Path Length to Next Collision

Before sampling the neutron flight distance, the distance of the cell boundary along the flight direction is calculated first, the next cell that neutron enters along the flight direction will be determined and the cell boundary is intersected along the flight direction has to be checked to determine whether this boundary is part of the whole system boundary. Depending on the wall boundary condition, the neutron flight length is sampled from either a truncated exponential function or a normal exponential function.

If the cell boundary turns out to be the system boundary, the truncated exponential probability density function will be applied so as to avoid the neutron escaping out of the system and force an interaction to occur before the neutron reaches the system boundary. The truncated exponential probability density function is described by

$$p(x) = \frac{\Sigma_t \exp(-\Sigma_t x)}{1 - \exp(-\Sigma_t D)}, \qquad \text{For } 0 \le x \le D \tag{2.5}$$

Where Σ_t is the macroscopic total cross section of the cell and D is the distance to the cell boundary. In this case, the sampled flight distance d is determined by

$$d = -\frac{1}{\Sigma_t} \ln\{1 - \xi[1 - \exp(-\Sigma_t D)]\} \tag{2.6}$$

Where ξ is the random number between 0 and 1. Note that the neutron weight must be adjusted in this case due to the biased sampling by multiplying the associated adjusting factor as given below:

$$W_{adj} = 1 - \exp(-\Sigma_t D) \qquad (2.7)$$

If the cell boundary is not the system boundary, the normal exponential probability density function as shown below will be used to determine the flight distanced d:

$$p(x) = \Sigma_t \exp(-\Sigma_t x), \text{ For } 0 \le x \le \infty \qquad (2.8)$$

and the distance d is determined by

$$d = -\frac{1}{\Sigma_t} \ln \xi \qquad (2.9)$$

This distance d is to be compared with the distance to the cell boundary D to determine whether it is necessary to continue the sampling process for the flight distance. If $d \le D$, the next interaction position will be in the same cell or on its boundary, this indicates that the sampling process of flight distance to the next interaction is completed, and the next interaction position is calculated by

$$\begin{aligned} x &= x_0 + d\Omega_1 \\ y &= y_0 + d\Omega_2 \\ z &= z_0 + d\Omega_3 \end{aligned} \qquad (2.10)$$

Where (x_0, y_0, z_0) is the current position. If $d \ge D$, it means that the neutron will enter the new cell abutting the current cell along its flight direction, and the sampling process for the flight distance of the neutron will continue. In this case the neutron will move to the cell boundary at the following new position (x, y, z):

$$\begin{aligned} x &= x_0 + D\Omega_1 \\ y &= y_0 + D\Omega_2 \\ z &= z_0 + D\Omega_3 \end{aligned} \qquad (2.11)$$

Note that the neutron will keep the same flight direction before it reaches the

next interaction position.

2.1.3 Sampling the Neutron Interaction Type

Among all types of neutron interactions, the inelastic scattering interaction, elastic scattering interaction and radioactive capture interaction are sampled explicitly in the current code while the rest interaction types such as (n, α) reaction etc, are treated implicitly by adjusting neutron weights accordingly. The probability mass functions for neutron interaction types can be expressed by their cross sections. Let Σ_1, Σ_2, Σ_3, ., Σ_n be the macroscopic total cross sections for interaction types 1,2, 3, and n respectively. The probability mass function for interaction type i is given by

$$p_i = \frac{\Sigma_i}{\sum_{j=1}^{n} \Sigma_j}, \quad \text{For i=1,2,…n} \qquad (2.12)$$

Explicit sampling is adopted to force neutron to undergo elastic scattering or inelastic scattering and radioactive capture reaction. The aim of this method is to increase the number of neutron scattering and capture interaction in order to increase the accuracy. By using this technique, at each interaction position, the neutron will be divided into two parts. The first one will undergo neutron inelastic scattering or elastic scattering reaction selected by analog sampling. The scattered neutron will travel into the next iteration until the neutron will be killed by Russian Roulette. The second one must undergo neutron radioactive capture reaction. In physics, for the neutron radioactive capture reaction, neutron will be

absorbed to compose the compound nucleus and there is no chance for neutron to survive from neutron capture reaction. In simulation, the neutron must be killed in neutron radioactive capture reaction. The weight of neutron of both part will be adjust to keep the total weight balanced. If we refer the cross section of neutron inelastic, elastic and radioactive capture with symbol Σ_{inel}, Σ_{el}, and Σ_{cp}. the neutron's weight of the first part will be:

$$W_1 = W_0 \frac{\Sigma_{inel} + \Sigma_{el}}{\Sigma_{TOT}} \qquad (2.12)$$

Where W_0 is the original weight of neutrons, Σ_{TOT} is the total macroscopic cross section.

The neutron's weight of the second part will be:

$$W_1 = W_0 \frac{\Sigma_{cp}}{\Sigma_{TOT}} \qquad (2.13)$$

The next step is to sample the interaction type between the neutron inelastic scattering reaction and the elastic scattering reaction. A random number ξ between 0 and 1 is sampled. The neutron inelastic scattering will be sampled if $\xi \le \frac{\Sigma_{inel}}{\Sigma_{inel} + \Sigma_{el}}$, otherwise the elastic scattering reaction will be sampled.

2.1.4 Sampling the Collision Isotope

There are two steps to sample the collision isotope in CEARCPG. The first step is to sample the collision element and the second step is to sample the collision isotope of the element already selected in step 1. Sampling the collision

element could be sorted into two categories, the zones other than the sample zone and the sample zone. If the neutron interaction position is in the zones other than sample zone, the collision element is sample by using analog method. The probability function used to sample the collision element can be described as follows,

$$p_j = \frac{\Sigma_{ij}}{\sum_{k=1}^{m} \Sigma_{ik}} \qquad \text{For j = 1,..., m} \qquad (2.14)$$

Where m is the total number of the element containing in the material of current cell i. Σ_{ij} is the total macroscopic cross section of j^{th} element in cell i. The element j is sampled if

$$\sum_{k=1}^{j-1} p_k \le \xi < \sum_{k=1}^{j} p_k \qquad (2.15)$$

where ξ is the random number between 0 and 1.

In the second step, the probability function of sampling collision isotope is given by

$$p_l = \frac{\Sigma_l}{\sum_{h=1}^{n} \Sigma_{lh}} \qquad \text{For h=1 ,..., n} \qquad (2.16)$$

Where n is the isotope number of element j. Σ_{lh} is the macroscopic cross section of n^{th} isotope of element j. isotope l is sampled if

$$\sum_{h=1}^{l-1} p_l \le \xi < \sum_{h=1}^{l} p_l \qquad (2.17)$$

If the neutron collision position locates in the sample zone, stratified sampling technique is used to force all elements to be interacted with neutron.

The method of sampling the collision isotope is the same as the method described in equation 2.16 and 2.17. Stratified sampling technique will guarantee each elemental library spectrum has the same statistics.

2.1.5 Sampling the Prompt Gamma Rays from neutron capture interaction

There are several modes for excited nucleus to de-excite. The direct way is emitting gamma rays (Prompt gamma, for example), and also can de-excite by transfer the excess energy to the bounded electrons. Usually a K shell electron is emitted, but an electron in the L-shell (or a higher shell) can also be emitted (called internal conversion). The electron hole that appears will soon be filled by another outer shell electron. This can result in the emission of an X-ray photon or the emission of an Auger electron. Break-up reaction is another way for excited nucleus to de-excite, for example, to de-excite by emitting alpha particle.

Only the first de-excited mode is taken into account in CEARCPG since prompt gamma rays are emitted during de-exciting. Besides the neutron capture reaction, gamma-ray also could be produced through neutron inelastic reaction with another mechanism which is needed to be treated in another way.

For neutron capture reaction, the nuclear structure data are adopted to sample the prompt gamma rays of given isotope. The primary nuclear structure data come from the ENSDF nuclear data library (BNL 2005) and the PGAA (IAEA database 2005) nuclear data library. The isotopes covered in CEARCPG are presented in appendix B. Figure 2-1 is typical ENSDF file and structure

scheme of isotope ^{12}C obtained from $^{12}C(n, \gamma)^{13}C$ reaction.

The ENSDF data library for neutron capture reaction part contains:

1) The Q value of neutron capture reaction,
2) The energy and relative intensity of each prompt gamma ray,
3) The structure information of each prompt gamma ray that indicates prompt gamma ray generating from which level and ending at which level, and
4) The life time of each excited level, mostly, the life time of excited level is fs magnitude. All these prompt gamma rays can be regarded as in coincidence.

According to the file and the scheme of $^{12}C(n, \gamma)^{13}C$ reaction, we know there are six prompt gamma rays generating from $^{12}C(n, \gamma)^{13}C$ reaction. They are listed in Table 2-2.

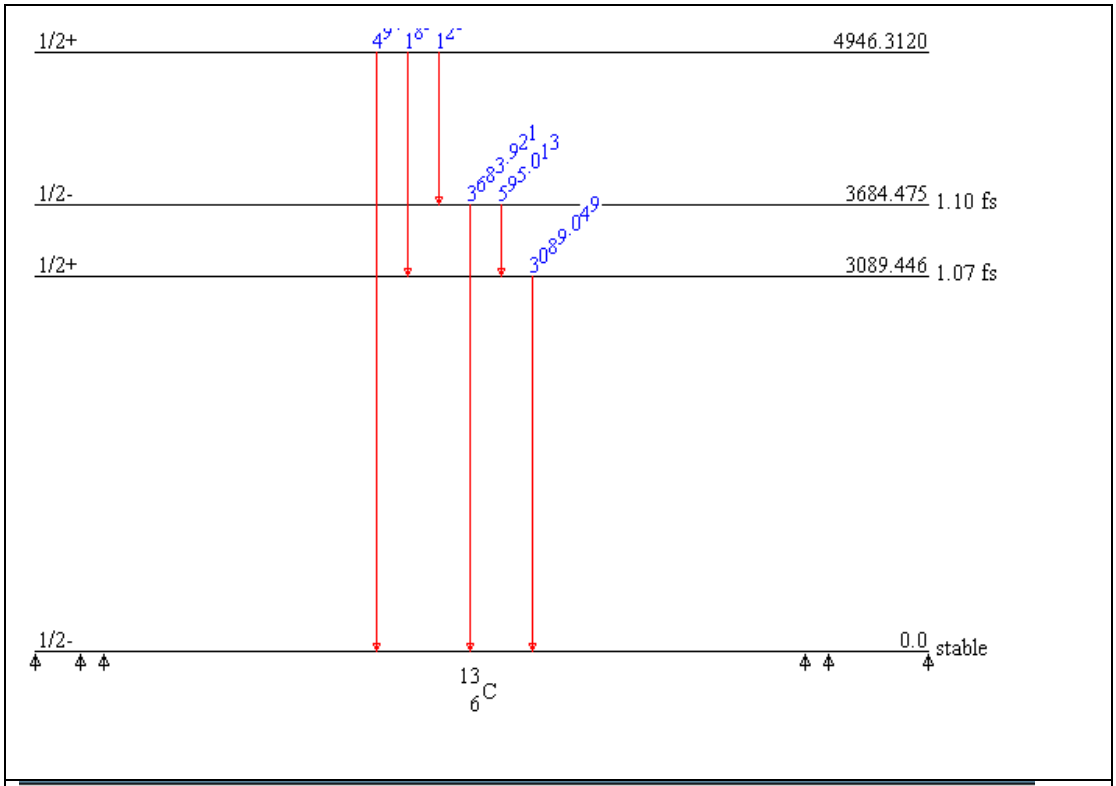


```
13C    *12C(N,G) E=TH                  1982MU14                  91NP      200006
13  6 I     4          6          0          0          0                    0
      H TYP=FUL$AUT=F. AJZENBERG-SELOVE, J.H. KELLEY AND C.D. NESARAJA$
    2 H CIT=NP A523, 1 (1991)$CUT=1-Jul-1990$
     c  Target J|p=0+.
     c  1982Mu14: measured E|g and I|g, deduced S(n).
     c  Evaluated S(n)=4946.31 keV (1995Au04).
     cL E          From E|g using least-squares fit to data.
     cL J,T        From 1996FiZY, except as noted.
     cG E          From 1996FiZY, except as noted.
     cG E(A)       From level energy differences.
     cG RI         Intensities per 100 neutron captures from 1982Mu14.
      N 1
     PN
   1  L 0.0          1/2-                STABLE
   2  L 3089.446   161/2+                1.07 FS   10
   1  G 3089.049   20 0.43    2
   3  L 3684.475   171/2-                1.10 FS    9
   2  G  595.013   11 0.24    1
   1  G 3683.921   2332.14    64
 S 4  L 4946.3120  231/2+
 S 4 cL J          from s-wave neu
   3  G 1261.764   1232.36    44
   2  G 1858.716   12 0.16    1
   1  G 4945.301   3 67.47    92
```

Level energy

Level life time

Relative intensity

Energy of Gamma ray generated from level 3

Ending level

Figure 2- 1. The typical structure scheme of ^{13}C from $^{12}C(n,\gamma)^{13}C$ reaction

Table 2- 2. The prompt gamma rays generated from $^{12}C(n, \gamma)^{13}C$ reaction

Energy(MeV)	Relative ratio(%)	Structure	
		Begin (level)	End (level)
3.089	0.43	2	1
0.595	0.24	3	2
3.683	32.14	3	1
1.261	32.36	4	3
1.856	0.16	4	2
4.945	67.47	4	1

Since the excited nucleus can de-excite through the internal conversion. For each level, intensity balance (Zhou 1999) checking must be done before sampling the prompt gamma rays. In physics, the total numbers of gamma rays falling into a certain level should equal the numbers of gamma rays out of that level plus internal conversion. It also can be shown as following equation:

$$\text{For } j^{th} \text{ level, } \sum_{i=1}^{m} I_{i,j} \approx \sum_{k=1}^{n} I_{k,j}\left(1+\alpha_j\right) \qquad (2.18)$$

Where $I_{i,j}$ is the intensity of gamma rays that fall into j^{th} level. $I_{k,j}$ is the intensity of gamma rays out of the j^{th} level. α_j is internal conversion coefficient of level j . Right now, CEARCPG doesn't take into account the X-rays or the Auger electron which are generated from the internal conversion. Only the prompt gamma rays are considered in CEARCPG. If there is a significant internal conversion effect for a certain level, the weight of sampled gamma rays must be adjusted. The adjusted weight of gamma ray can be expressed as follows:

$$W_1 = W_0 \frac{\sum_{k=1}^{n} I_{k,j}}{\sum_{i=1}^{m} I_{i,j}} \qquad (2.19)$$

Where $I_{i,j}$ and $I_{k,j}$ are the same as that described in equation 2.18

For neutron capture reaction, the energy of the highest level is the Q value of that reaction. When sampling the prompt gamma rays from the scheme of ^{13}C, the starting level should be the highest level. Prompt gamma rays are sampled based on their relative intensity. Gamma ray j will be sampled if

$$\sum_{h=1}^{j-1} R_l \le \xi < \sum_{h=1}^{j} R_l \qquad (2.19)$$

Where R_l is the normalized intensity of gamma rays.

Let's look at the scheme of ^{13}C, If we assume the gamma ray of 1.56 MeV is sampled and we know this gamma ray falls into the second level, then the starting point of sampling the next prompt gamma ray will be moved to the second level. The nucleus will de-excite to the ground level by emitting gamma ray with energy 3.089 MeV. In this example, two prompt gamma rays are sampled, one is 1.56MeV and the other is 3.089 MeV and we know these two gamma rays are emitted in coincidence.

2.1.6 Sampling the Gamma Rays from neutron inelastic scattering interaction

The treatment of inelastic scattering depends upon the particular inelastic reaction. Inelastic reactions are defined as (n,y) reactions such as (n, n'γ), (n, 2n), (n, f), (n, n' α) in which y includes at least one neutron. In CEARCPG, only interaction (n,n' γ) reaction is considered because the excited nucleus will de-excite by emitting gamma rays. Flag LR (ENDF manual 2001) shows which level will de-excite by emitting gamma rays. To sample the gamma rays from neutron inelastic scattering reaction is a little complicated than the sampling of neutron

capture reaction. ENDF nuclear data library must be used to determine the excited level first. In ENDF file, Flag LR indicates the decay mode. If LR is zero, it means this excited level will decay by emitting gamma rays. The excited level is sampled explicitly based on the cross section of each level. Once the excited level is determined, the scheme from ENSDF nuclear data library is used to sample the gamma rays. The method of sampling gamma rays is the same as the method of sampling the gamma rays from radioactive capture reaction. Figure 2-2 shows the part of scheme of ^{16}O excited level.

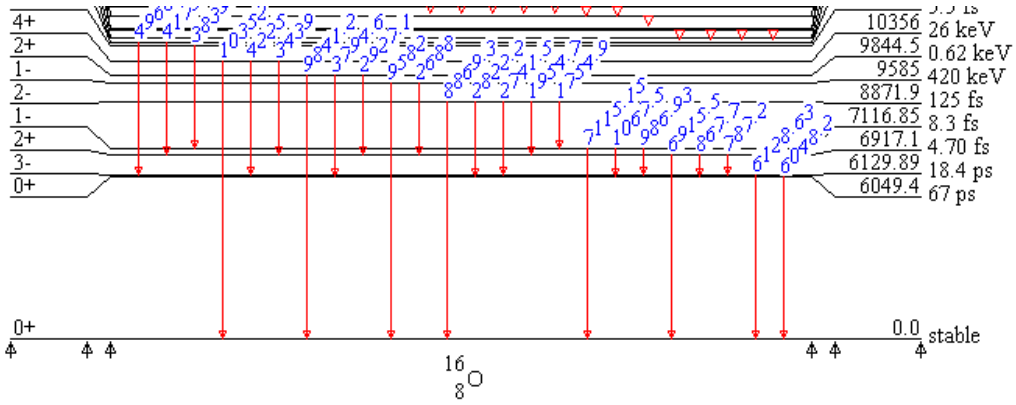

Figure 2- 2. The scheme of ^{16}O

According to the ENDF file of ^{16}O, the flag LR of the second level is 40. It means this level will de-excite through electron-positron formation. The flag LR of the third level is zero. It means it will de-excite by emitting gamma ray with energy 6.129 MeV. The detailed information of flag LR can be found in ENDF manual. Explicit sampling will force the levels with LR=0 to be sampled. The neutrons weight must be adjusted by using the following equation.

$$W_1 = W_0 \frac{\sum_{j=1}^{m} \Sigma_j}{\Sigma_{inel}} \qquad (2.20)$$

Where W_0 is the original weight of neutron. Σ_{inel} is the macroscopic cross section of neutron inelastic scattering reaction. Σ_j is the macroscopic cross section of level j which de-excites by emitting gamma-rays. m the total number of excited level which de-excite by emitting gamma rays. Analog method is used to sample the excited level.

For the example of ^{16}O, based on the cross section of each level, If the third level is sampled, there is only one gamma ray will be sampled with energy 6.128 MeV.

2.1.7 Sampling Neutron Energy and Direction after Scattering

Neutron interaction with element can be generally classified as scattering or absorption interaction. The scattering collisions result in the changes in the energy as well as the direction-of-flight of the neutron. The mathematical models used to simulate these mechanisms are described in the next sections.

Neutron Elastic scattering reaction

Direction of scattered neutrons

According to the ENDF manual, the angular distribution of emitting particles are recorded in the file 4 which indicator MF is 4. Flag MT indicates the reaction type. For example MT=2 means neutron elastic scattering reaction, MT=102 means neutron radioactive capture reaction.

The angular distributions can be expressed as normalized probability distribution, i.e.

$$\int_{-1}^{1} f(\mu, E)d\mu = 1 \qquad (2.21)$$

Where f(μ,E)dμ is the probability that a particle of incident energy E will be scattered into the interval dμ about an angle μ. The units of f(μ,E) are (unit cosine)$^{-1}$. Since the angular distribution of scattered neutrons is generally assumed to have azimuthal symmetry, the distribution may be represented as a Legendre polynomial series

$$f(\mu, E) = \frac{2\pi}{\sigma_s(E)}\sigma(\mu, E) = \sum_{i=1}^{NL} \frac{2l+1}{2} a_l(E) P_l(E) \qquad (2.22)$$

Where μ = cosine of the scattered angle in either the laboratory or the center-of-mass system

E = energy of the incident particle in the laboratory system

σ_s(E) = the scattering cross section, e.g., elastic scattering at energy E as given in File 3 for the particular reaction type (MT)

l = order of the Legendre polynomial

σ (μ,E) = differential scattering cross section

a_l = the l^{th} Legendre polynomial coefficient and it is understood that a0 =1.0.

The angular distributions may be given by one of two methods, and in either the center-of-mass (CM) or laboratory (LAB) systems. Using the first method, the distributions are given by tabulating the normalized probability distribution, f(μ,E), as a function of incident energy. Using the second method, the Legendre polynomial expansion coefficients, al(E), are tabulated as a function of incident

neutron energy. Several Flags in File 4 indicate the method of data recording. The most important flags are listed as follows,

LTT Flag to specify the representation used and it may have the following values:

LTT=0, all angular distributions are isotropic

LTT=l, the data are given as Legendre expansion coefficients, al(E)

LTT=2, the data are given as normalized probability distributions, f(μ,E)

LTT=3, low energy region is represented by as Legendre coefficients; higher region is represented by tabulated data.

LI Flag to specify whether all the angular distributions are isotropic

LI=0, not all isotropic

LI=1, all isotropic

LCT Flag to specify the frame of reference used

LCT=l, the data are given in the LAB system

Several subroutines are written in CEARCPG to deal with different situations. When the data are recorded as Legendre coefficients, the rejection method is used to sample the value μ according to the incident energy. When data are recorded as tabulated table, the interpolation method is used to sample the value μ. If the angular is isotropic, the μ_{cm} is sampled randomly. If the data are recorded in CM system, transformation must be performed to transfer the value of μ from the center-of-mass system to the Laboratory system according to the following equation,

$$\mu_{lab} = \frac{1 + A\mu_{com}}{\sqrt{A^2 + 2A\mu_{com} + 1}} \qquad (2.23)$$

The incident particle direction cosines (uo,vo,wo) are rotated to a new outgoing target-at-rest system cosines (u, v, w) through a polar angle whose cosine is μ_{lab}, and through an azimuthal angle sampled uniformly. For random numbers ξ_1 and ξ_2 on the interval [-1,1) with rejection criterion $\xi_1^2\xi_2^2 \leq 1$, the rotation scheme is (Ivam Lux and Laszlo Koblinger 1991)

$$u = u_o\mu_{lab} + \frac{\sqrt{1-\mu_{lab}^2}(\xi_1 u_o w_o - \xi_2 o)}{\sqrt{(\xi_1^2+\xi_2^2)(1-w_o^2)}}$$

$$v = v_o\mu_{lab} + \frac{\sqrt{1-u_{lab}^2}(\xi_1 v_o w_o + \xi_2 u_o)}{\sqrt{(\xi_1^2+\xi_2^2)(1-w_o^2)}}$$

$$w = w_o\mu_{lab} - \frac{\xi_1\sqrt{(1-\mu_{lab}^2)(1-w_o^2)}}{\sqrt{(\xi_1^2+\xi_2^2)}} \quad .$$

If $1-w_o^2 - 0$, then

$$u = u_o\mu_{lab} + \frac{\sqrt{1-\mu_{lab}^2}(\xi_1 u_o v_o + \xi_2 w_o)}{\sqrt{(\xi_1^2+\xi_2^2)(1-\upsilon_o^2)}}$$

$$v = v_o\mu_{lab} - \frac{\xi_1\sqrt{(1-\mu_{lab}^2)(1-v_o^2)}}{\sqrt{(\xi_1^2+\xi_2^2)}}$$

$$w = w_o\mu_{lab} + \frac{\sqrt{1-\mu_{lab}^2}(\xi_1 w_o v_o - \xi_2 u_o)}{\sqrt{(\xi_1^2+\xi_2^2)(1-v_o^2)}} \quad . \qquad (2.24)$$

Energy of scattered neutrons

Once the particle direction is sampled from the appropriate angular distribution tables, then the exiting energy, Eout, is dictated by two-body kinematics:

$$E_{out} = \frac{1}{2}E_{in}[(1-\alpha)\mu_{cm} + 1 + \alpha]$$

$$= E_{in}\left[\frac{1 + A^2 + 2A\mu_{cm}}{(1+A)^2}\right] \quad , \qquad (2.25)$$

Where Ein = incident neutron energy, μcm = center-of-mass cosine of the angle between incident and exiting particle directions,

$$\alpha = \left(\frac{A-1}{A+1}\right)^2 \qquad (2.26)$$

and A=mass of collision nuclide in unites of the mass of a neutron

Neutron Inelastic scattering

Direction of scattered neutron

The method of sampling the direction of scattered neutron is the same as the method used for neutron elastic scattering reaction. ENDF file contains the date of each excited level that used to sample the μ_{cm}. the detailed explanation can be referred the ENDF manual. Only the data of that level de-excite by emitting gamma rays are stored when the problem setup.

Energy after inelastic scattering

According to the manual of MCNP5, ENDF law 3 is used to calculate the neutrons energy after inelastic scattering. The law 3 can be expressed as:

$$E_{out} = \left(\frac{A}{A+1}\right)^2\left[E_{in} - \frac{Q(A+1)}{A}\right] \qquad (2.27)$$

For (n,n', γ) reaction, the Q value should equal the energy of excited level.

Thermal Neutron Scattering

Neutron scattering at thermal energies is modeled by free gas model (Carter and Cashwell, 1975). In this model, neutrons are assumed to be transport in mono-atomic gas, the latter having an isotropic Maxwellian distribution of velocities. The effective scattering cross- section in the LAB system for a neutron of kinetic energy E is

$$\sigma_s^{eff}(E) = \frac{1}{v_n} \int\int \sigma_s(v_{rel}) v_{rel}\, p(V, \mu_t) dV d\mu_t \qquad (2.28)$$

Here, v_{rel} is the relative velocity between a neutron moving with a scalar velocity v_n and a target nucleus moving with a scalar velocity V and μ_t is the cosine of the angle between the neutron and the target direction of flight vectors. The scattering cross section for this relative velocity is denoted by $\sigma_s(v_{rel})$ and $p(V, \mu_t)$ is the probability density function for the Maxwellian distribution of target velocities,

$$p(V, \mu_t) = \frac{4}{\sqrt{\pi}} \beta^3 V^2 \exp(-\beta^2 V^2) \qquad (2.29)$$

with β define as

$$\beta = \sqrt{\frac{A}{2kT}} \qquad (2.30)$$

Where A is the atomic mass of target nucleus in the unit of neutron mass, k is the Boltzmann constant and T is the equilibrium temperature of the target nuclei.

According to the free gas kernel model, the probability density function, $f(\mu_t)$

for the cosine of the angle between the target and the neutron direction of flight vectors is given as follows (Carter and Cashwell 1975). Let $\beta = \sqrt{\frac{A}{2kT}}$, $a = \beta v_n$ and $b = \beta V$ where b is sampled uniformly between 0 to 3 as an approximation, then

$$f(\mu_t) = C\sqrt{\left(a^2 + b^2 - 2ab\mu_t\right)} \qquad (2.31)$$

Where A is the mass of the target nucleus in the unit of the mass of a neutron, k is the Boltzmann constant, T is the equilibrium temperature of the target nuclei, V_n is the neutron moving velocity and V is the target nucleus moving velocity. Then μ_t is sampled by:

$$\mu_t = \frac{1}{2ab}\left(a^2 + b^2 - \{|a-x|^3 - \xi[|a-x|^3 - (a+x)^3]\}^{2/3}\right) \qquad (2.32)$$

Where ξ is the random number.

Let (u, v, w) denote the incident neutron direction of flight. The target direction cosines (u_t, v_t, w_t) are obtained with an assumption that the azimuth angle is of a uniform distribution on the cone about w_t. The scattering is assumed to be isotropic in the COM system, and the new direction-of-flight in this system is thus sampled uniformly on the unit sphere, and is denoted by (u_0 ,v_0 ,w_0). The kinematics of the collision process yields the final energy, E', and the neutron direction cosines in the Lab system (Carter and Cashwell 1975, Shyu 1991)

$$
\begin{aligned}
E' &= \frac{E}{(A+1)^2}\left(\bar{x}^2+\bar{y}^2+\bar{z}^2\right) \\
u' &= \frac{\bar{x}}{\left(\bar{x}^2+\bar{y}^2\bar{z}^2\right)^{1/2}} \\
v' &= \frac{\bar{y}}{\left(\bar{x}^2+\bar{y}^2+\bar{z}^2\right)^{1/2}} \\
w' &= \frac{\bar{z}}{\left(\bar{x}^2+\bar{y}^2+\bar{z}^2\right)^{1/2}}
\end{aligned}
\qquad (2.33)
$$

Where

$$
\begin{aligned}
\bar{x} &= u + A\left(\delta u_0 + \frac{b}{a}u_t\right) \\
\bar{y} &= v + A\left(\delta v_0 + \frac{b}{a}uv_t\right) \\
\bar{z} &= w + A\left(\delta w_0 + \frac{b}{a}w_t\right) \\
\delta &= \left(1+\frac{b^2}{a^2}-\frac{2b\mu_t}{a}\right)^{1/2}
\end{aligned}
\qquad (2.34)
$$

2.2 Photon Physics

In CEARCPG, the gamma rays are mainly from (1) gamma rays from the neutron source, (2) from the neutron radioactive capture reaction, (3) from the neutron inelastic scattering reaction, (4) from the natural background and the NaI detector activation.

2.2.1 Overview of photo interaction

Simple photon treatment is used in CEARCPG. This method is very similar to the simple mode used in MNCP. The CEARCPG ignores the coherent scattering and fluorescent photon from the photoelectron absorption. CEARCPG only

considers the photoelectron effect, pair production, Compton scattering from free electron. Total cross section σ_t is regarded as the sum of the three components,

$$\sigma_t = \sigma_{pe} + \sigma_{pp} + \sigma_s \qquad (2.35)$$

Photoelectron effect

In the photoelectron absorption process, a photon undergoes an Interaction with an absorber atom in which the photon completely disappears. In its place, an energetic photoelectron is ejected by the atom from one of its bound shells. The CEARCPG considers the ejected free electron deposit its all energy locally.

Pair production

If the gamma rays energy exceeds twice the rest-mass energy of an electron (1.02 MeV), the process of pair production is energetically possible. In the interaction (which must take place in the coulomb field of a nucleus), the photon disappears and is replaced by an electron-positron pair. All the excess energy carried in by the photon above 1.02 MeV required to create the pair goes into kinetic energy share by the positron and electron. Because the positron will subsequently annihilate after slowing down in the absorbing medium, two annihilation photons are normally produced as secondary products of the interaction. The two annihilation photons then track separately until they will be killed by Russian Roulette or detected by the detector.

Compton scattering

The interaction process of Compton scattering takes place between the

incident photon and electron in the absorbing material. It is the predominant interaction mechanism for low-energy gamma rays. The scattered photon energy can be calculated by the following equation,

$$E' = \frac{E}{1 + \frac{E}{m_0 c^2 (1 - \cos\theta)}} \tag{2.36}$$

Where m_0c^2 is the rest-mass energy of the electron (0.511MeV) and θ is angle between the direction of scattered photon with respect to its original direction. The photon transfers a portion of its energy to the electron named recoil electron. The recoil electron will deposit its all energy locally. The angular distribution of scattered gamma rays is predicted by the Klein-Nishina formula for the differential cross section $d\sigma / d\Omega$

$$\frac{d\sigma}{d\Omega} = Zr_0^2 \left(\frac{1}{1 + \alpha(1 - \cos\theta)} \right)^2 \left(\frac{1 + \cos^2\theta}{2} \right) \left(1 + \frac{\alpha^2 (1 - \cos\theta)^2}{(1 + \cos^2\theta)[1 + \alpha(1 - \cos\theta)]} \right) \tag{2.37}$$

Where $\alpha = h\nu / m_0 c^2$ and r_0 is the classical electron radius. Rejection method is used in CEARCPG to sample the angle θ.

Currently, Rayleigh scattering (coherent scattering) is not taken into account in CEARCPG. The coherent scattering is very important at low energy and for high Z materials when the electron must be considered bound. Only direction of photon will be changed after scattering. Figure 2-3 shows the photon cross section of sulfur. The data are from EPDL 97. The typical cutoff energy for photon transportation is 10 keV. From the figure 2-3, it can be seen that the dominant interaction for photon is photon-electron effect. Only below the 10.36 eV which is the binding energy of 3P shell of sulfur, the cross section mainly

comes from the photon incoherent scattering and coherent scattering. The low limitation of energy level Rayleigh scattering would be included depends on the binding energy of the most outside shell of element.

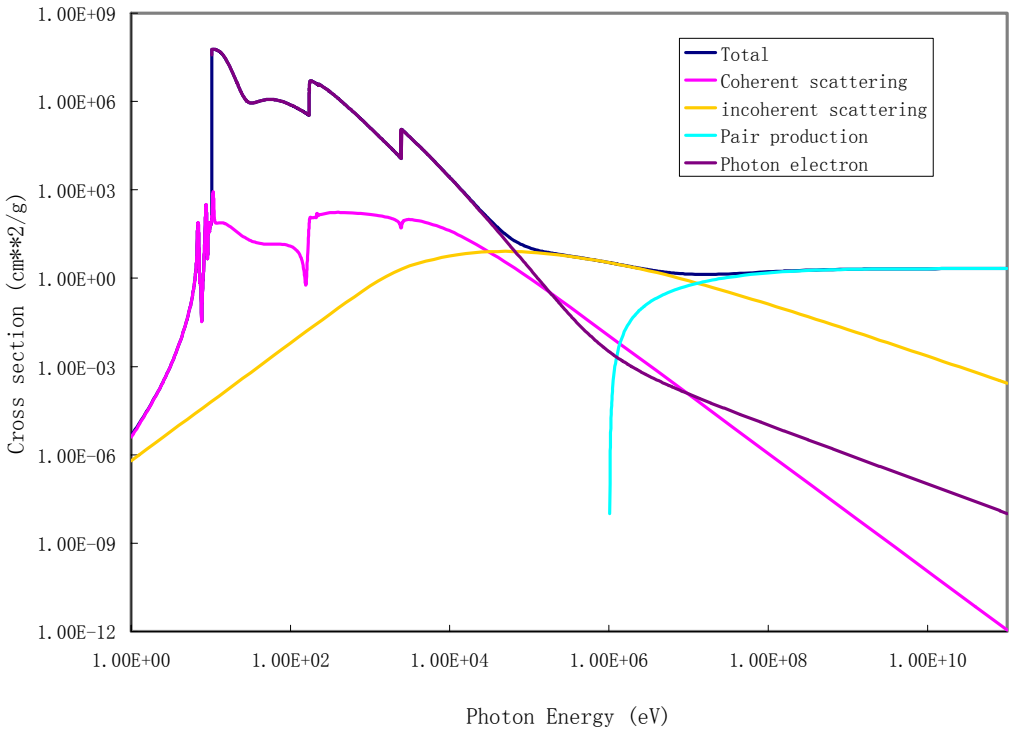

Figure 2- 3 The photon cross section of element sulfur

2.2.2 Photon transport

The method used to sample the path lengths of photons is the same as that of neutrons transportation described previously. The only difference is the cross section.

2.2.3 Photon sampling

In this part, five types of photon source are discussed separately. They are (1) photons from the neutron source, (2) photons from the neutron radioactive

capture reaction, (3) photons from neutron inelastic scattering, (4) photons from the natural background and (5) photons from the NaI detector activation.

Photons from neutron source

The default build-in neutron source is ^{252}Cf. The prompt fission gamma rays from ^{252}Cf is evaluated by Timothy E. Valentine (2001). In his work several fission neutron sources are evaluated including ^{233}U, ^{235}U, ^{239}Pu and ^{252}Cf. the average number of prompt fission gamma rays for spontaneous fission ^{252}Cf estimate to be 7.99±0.63 per spontaneous fission and the multiplicity distribution of gamma rays from fission can be described by the following equation.

$$\prod(G) = C_1 \frac{(C_2)^G e^{-C_2}}{G!} + (1 - C_1)\frac{(C_3)^G e^{-C_3}}{G!} \qquad (2.38)$$

For ^{252}Cf spontaneous fission source, C_1 = 0.675, C_2 = 6.78 and C_3 = 9.92. The multiplicity distribution is plotted in figure 2-4.

The gamma ray energy spectrum are plotted in the following figure 2-5 measured by V.V. Verbinski(1973). The procedure of sampling fission gamma rays is to sample the gamma rays number from the multiplicity distribution at first and then to sample the gamma rays energy from the fission gamma rays energy distribution. The angular distribution of fission gamma rays are regarded as isotropic. Because the average number of fission gamma rays of ^{252}Cf neutron source is about 7.99, it means there might be over one fission gamma rays to be sampled per fission. All these sampled fission gamma rays are regarded as in coincidence. Then the sampled fission gamma rays will be tracked independently.

If there are at least two gamma particles recorded by detector at the same time, one coincidence event of fission gamma rays is scored.

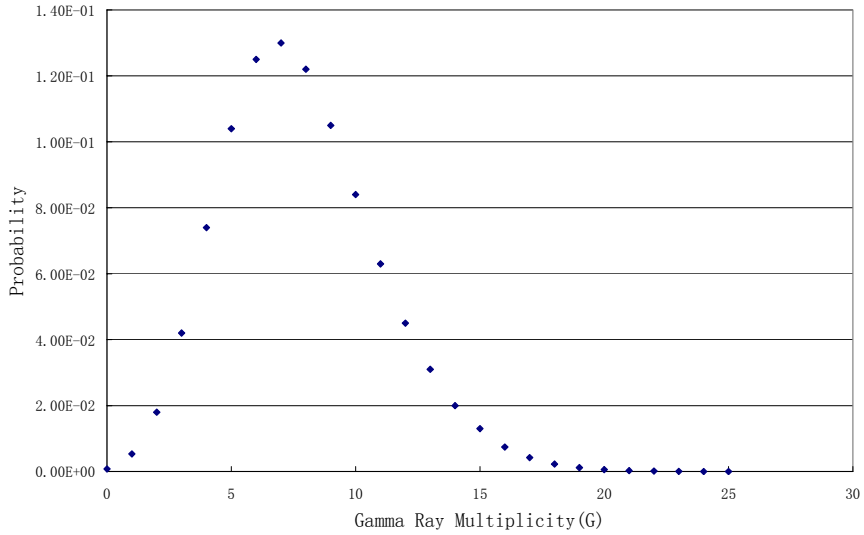

Figure 2- 4 The gamma ray multiplicity of ^{252}Cf neutron source

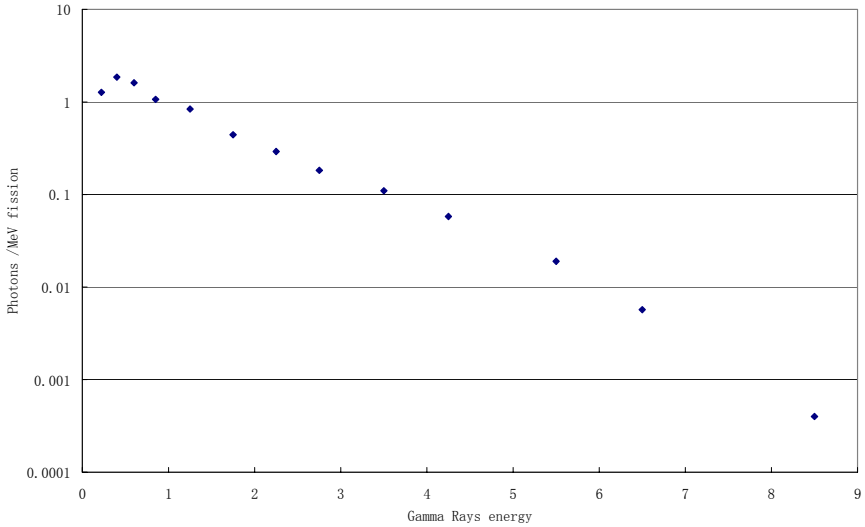

Figure 2- 5. The energy distribution of fission gamma rays of ^{252}Cf neutron source

Photons from neutron radioactive capture interaction

The algorithm of sampling the prompt gamma rays from the neutron

radioactive capture interaction has been described previously. The basic idea of sampling prompt gamma rays from the neutron radioactive capture interaction is using the nucleus excited scheme. Up to now, the angular distribution of prompt gamma rays from the neutron capture reaction is regarded as isotropic. The sampled gamma particle inherits the weight of neutron which induces the neutron capture reaction.

Photons from neutron inelastic scattering interaction

The algorithm of sampling the prompt gamma rays from neutron inelastic scattering interaction has mentioned previously. ENDF data are used to determine the excited level of the scattered nucleus. Once the excited level is determined, ENSDF data is used to sample the gamma rays generating from the neutron inelastic scattering reaction. Same as the prompt gamma rays from the neutron capture reaction, the gamma ray from neutron inelastic scattering reaction also inherits the weight of neutron that induces the inelastic scattering reaction. The angular distribution of prompt gamma rays is isotropic.

Photons from the natural background

The natural backgrounds are mainly from the ^{40}K , Uranium and Thorium decay chains. Usually the intensities of these spectra are very small compared to those of other elements of interest in the sample. However they are still useful in the calibration of the sample spectrum if high accuracy is desired. For example,

the 2.61 MeV gamma ray from the thorium chain and the 1.46 MeV gamma ray from ^{40}K are clearly identifiable in the measured background spectrum (Gardner et al., 2000). The approach used in CEARPGA II is still based on the linear analogy interpolation. In order to avoid the error which is introduced from the interpolation, CEARCPG tracks the real gamma rays from instead of the pseudo gamma rays. The decay gamma rays and their corresponding intensities for the ^{40}K , Uranium and Thorium decay chain are listed in table 2-3. Note that these spectra are not normalized like other elemental libraries since the associated average macroscopic cross section and contents are unknown.

Photons from NaI detector activation

When NaI detectors are used in the PGNAA measurement, they are also irradiated and activated by neutrons that penetrate the sample and the detector shielding materials. This activation results in the emission of prompt gamma rays from both I and Na. it also produces the decay gamma rays and beta particles from the radioisotopes ^{128}I and ^{24}Na that produced through the neutron capture reaction. Figure 2-6 plotted the decay mode of ^{128}I and ^{24}Na (Table of Isotopes, 2001). There are two decay modes of ^{128}I, 6.9 % of ^{128}I will decay to ^{128}Te through the EC mode and 93.1% will decay to ^{128}Xe through the β^- decay. The activation spectra of NaI detector were measured in the Gardner's work (2000). A Monte Carlo model was proposed in his work. In this work, the spectra of NaI detector activation are re-calculated. The approach is the same as that used in Gardner's work. The difference is that the schemes are used to generate the

prompt gamma rays and the decay gamma rays. The scheme files from ENSDF data library are used in this work to generate the spectra of NaI detector. The simulation results will be presented in the latter.

Table 2- 3 Decay gamma rays and their intensity of ^{40}K, Uranium and Thorium

Uranium		Thorium		^{40}K	
Energy (keV)	Intensity (%)	Energy (keV)	Intensity (%)	Energy (keV)	Intensity (%)
63.3	2.8	84.4	6.4	1461	100
92.8	3.2	129.1	1.2		
186.0	3.1	209.4	1.9		
295.2	13.3	238.6	19.4		
352.0	17.7	270.3	1.6		
609.4	20.8	300.1	1.4		
665.4	0.7	338.4	6.4		
768.4	2.7	463.0	1.9		
806.2	0.5	510.7	3.3		
934.0	1.5	593.1	12.5		
1001.1	0.4	727.3	2.7		
1120.4	8.1	794.8	2.0		
1238.2	3.7	860.5	1.7		
1377.7	2.5	911.1	12.1		
1408.0	2.0	968.9	9.6		
1509.3	1.5	1587.9	1.5		
1661.4	0.6	2614.5	14.5		
1764.5	9.7				
1847.6	1.1				
2118.7	0.6				
2204.3	2.6				
2448.0	0.8				

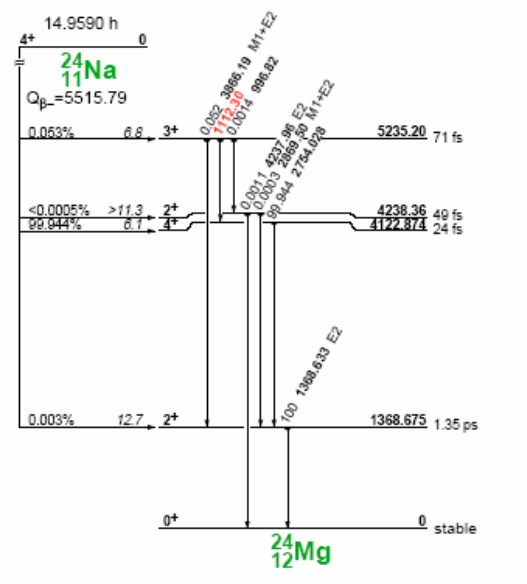

The scheme of ^{24}Na from β^- decay

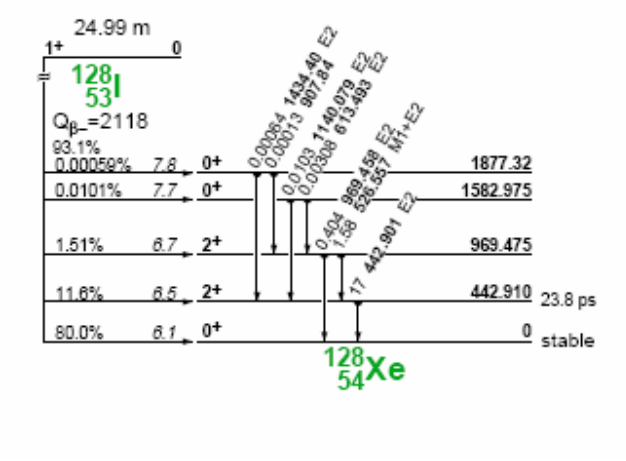

The scheme of ^{128}I from β^- decay

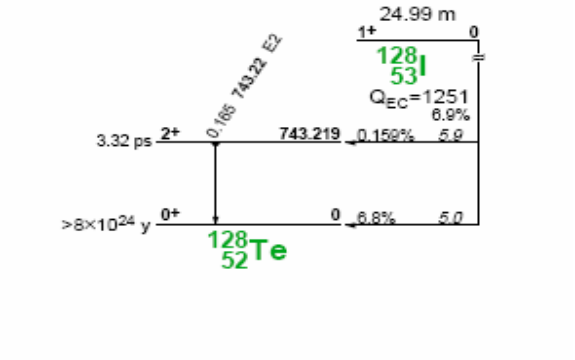

The scheme of ^{128}I from EC decay

Figure 2- 6 The decay scheme of ^{128}I and ^{24}Na

Sample the interaction type

Three types of gamma ray interactions predominate the energy range from 10 keV to 12 MeV. They are the photoelectric effect, the pair production and the Compton scattering. Of these three interactions, the photoelectric effect predominates in the lower energy range, the pair production is important only for gamma rays of higher energies and Compton scattering predominates in

intermediate energies. The photoelectric interaction of gamma rays is dealt with implicitly in the code since it leads to the loss of gamma rays. Therefore a weight adjusting factor is calculated to modify the gamma ray weight after sampling the interaction, which is given by

$$W = \frac{\Sigma_{pp} + \Sigma_c}{\Sigma_t} \qquad (2.39)$$

Where Σ_t is the total macroscopic cross section in the material, and Σ_{pp} is the macroscopic cross section of pair production and Σ_c is the macroscopic cross section of Compton scattering.

2.2.4 Recording the gamma rays

There are three ways to terminate gamma particle history. (1) Gamma particles escape the system; (2) Gamma particles are detected by the detector and (3) Gamma particles are killed by Russian Roulette.

Monte Carlo simulated NaI detector response function is used to convert the gamma rays record to the pulse-height spectrum after all neutron history finish. This technique was first introduced in code CEARPGA I. This technique is very powerful and can save as much as 50% of the total tracking time for each gamma ray history (Gardner 2000). The NaI detector response function is calculated by another Monte Carlo code named g03 that is developed by CEAR group (Gardner 2002). This code models the photon transport and electron transport. It also considers the NaI detector nonlinearity problem and the NaI detector variable flat continuum problem. The detailed information of code g03 can be referred Dr. Zhang's Ph.D thesis (2003). The problem of NaI detector

Nonlinearity and variable flat continuum problems are also discussed in his thesis.

2.3 Cross sections

2.3.1 Neutron Cross sections

The primary neutron libraries used in CEARCPG come from the ENDF/B-VI library and Japanese Atomic Energy Research Institute's (JAERI) JENDL library at 300 K. The neutron energy covers from 10^{-5} eV to 20 MeV. Unlike MCNP, CEARCPG can access the ENDF format directly. MCNP requires the data must be processed into ACE format at first. The very complex processing code used for this purpose is NJOY for evaluated data with ENDF format. As to CEARCPG, since users don't need to change the data format, it is easy for users to update the data library. Users only need to copy the new data file into the right directory. The isotopes covered in CEARCPG are presented in Appendix A.

2.3.2 Photon Cross Section

CEARCPG inherits the photon library used in CEARPGA II. It is NJOY pre-processing nuclear data. The photon cross section are extracted from EPDL library and are processed into three separate tables, which are total cross section table (Gtotal.xs), Compton scattering cross section table (Gcmptn.xs), and pair production table (Gpp.xs). These tables cover all the elements from Z=1 to 100 and the energy range now from 10 KeV to 20 MeV.

3 CEARCPG

3.1 Overview of CEARCPG

The CEARCPG code is a specific purpose Monte Carlo code which can be used for coincidence, anti-coincidence, time-of-flight, and normal (non-coincidence) PGNAA simulation for various applications. The code treats an arbitrary three-dimensional configuration of user defined materials bounded by first and second order surfaces. CEARCPG is written by Compaq Visual Fortran in Fortran 95. Dynamic memory allocation technique is used to store the data during the problem setup, such as the cross section, the angular distribution of scattered neutrons as well as the scheme data of the isotopes used in problem. CEARCPG is integrated by several modules. Each module can carry out different functions. For example, the function of geometry module is used to initiate the geometry of simulation problem and also can be used to determine the particles position and calculate the distance to the cell surface. Module Gamma pack can be used to track the gamma particle. The detailed description of each module is described in appendix C.

The flow chart of CEARCPG is plotted in figure 3-1. CEARCPG are composed of several major parts. They are the initialization part, which read the geometry input, the cross section data, set up variable dimensions and the dynamically allocated storage; the neutron transportation part; the gamma rays transportation part and the recording part. Each part is independent. The data which are exchanged among the different part are stored in the public memory

lots, the public common memory block.

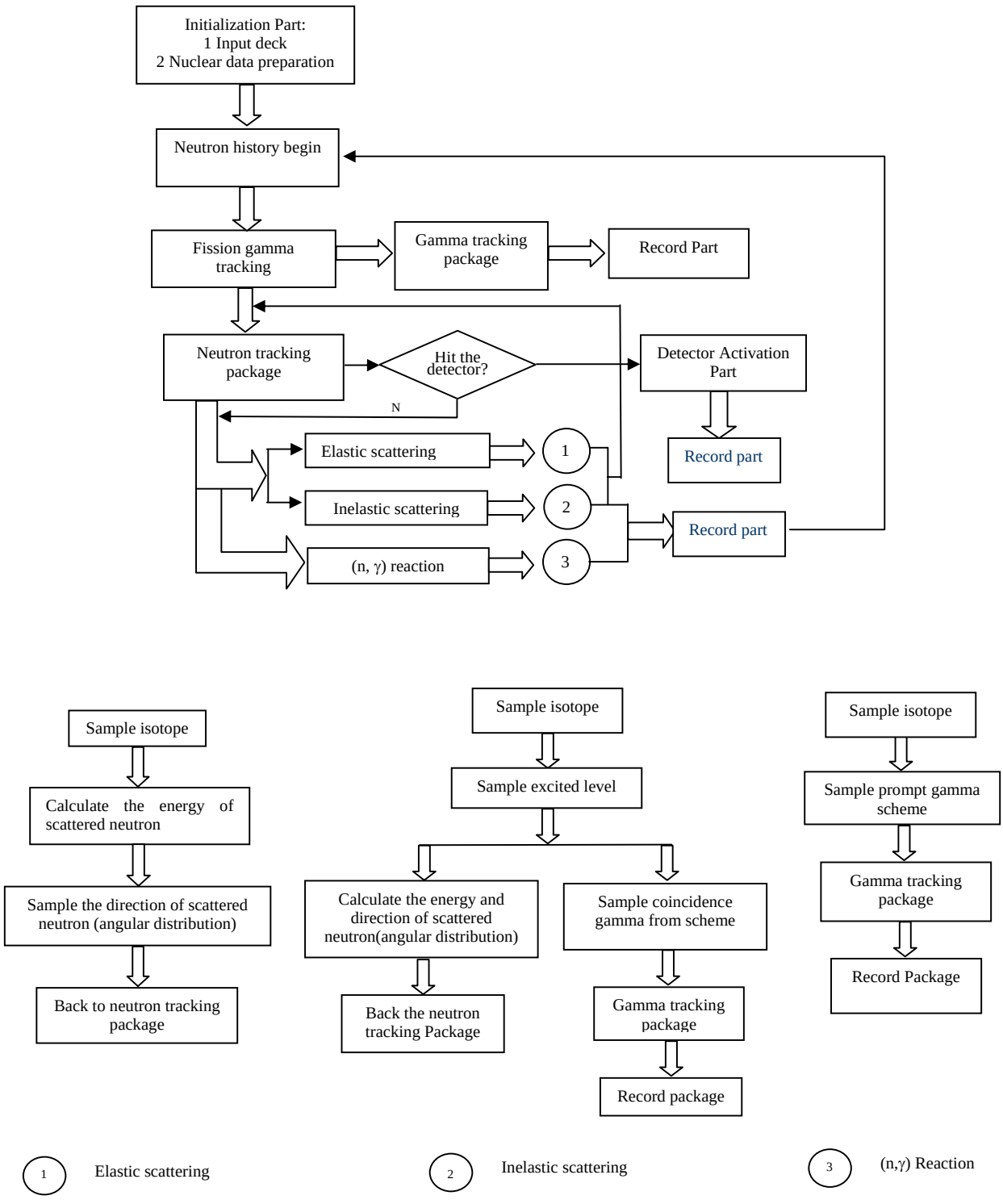

Figure 3- 1 The flow chart of CEARCPG

Each module can access the public data to do I/O operation during the simulation.

3.2 Features of CEARCPG

The main features of the CEARCPG code are listed as follows:

1. The neutron library includes 97 isotopes of practical interest. The neutron energy ranges from 10^{-11} to 20 MeV. Three sub-libraries are included.
   1) The neutron cross-section library, which is extracted from the ENDF/B-VI. 8 300K and the JENDL-3. 3 300K libraries. The angular distribution data of neutron elastic scattering and neutron inelastic scattering of each isotope is also included in this library,
   2) The (n,γ) scheme library, which is mainly extracted from the ENSDF library. This library is used to sample prompt gamma rays caused by the (n, γ) reaction, and
   3) The neutron inelastic scattering library. This library is used to sample the gamma rays that are induced by neutron inelastic scattering.
2. The library for gamma-rays include the elements Z=1 to 100, which come from the EPDL97 library. The gamma-ray energy range is from 0.01 to 20 MeV.
3. Most of the CEARCPG code input card takes the same form as those used in MCNP. By using the platform VisED of MCNP5, it is easy for user to design and check the geometry part used in the simulation.

CEARCPG is designed to record:

1. The total coincidence and single spectra of interested elements.
2. The single and coincidence library spectra

3. The single and coincidence spectra of fission gamma rays from the neutron source
4. The spectra of the natural background
5. The NaI detector activation spectra
6. The 2-D coincidence spectra

The simulated 2-D coincidence spectra are recorded in the KMAX (Sparrow 2005) format and the 2-D matrix format that can be plotted by MATLAB directly. The KMAX software is adopted to analyze the simulation results.

3.3 Geometry package of CEARCPG

A general geometry package is adopted. User can use input card to define the surface type and the cell specification. The geometry of CEARCPG treats an arbitrary 3-dimensions configuration user-defined materials in geometric cells bounded by the first or second – degree surface. The geometry configuration and definition of CEARCPG is the same as that of code MCNP. User can refer MCNP5 manual to get more information of how to define the surface and the cell. User even can use MCNP Visual Editor to design the geometry and check the geometry error. Unfortunately, the CEARCPG doesn't support the geometry operator and macrobodies which are widely used in MCNP.

The detailed description of surface type and the parameters of surface are presented in table 3-1

Table 3- 1 the surface card of CEARCPG

Surface Type		Description	Equation	Card Entries
Plane	P	General plane	Ax+By+Cz-D=0	ABCD
	PX	Plane normal to X	x-D=0	D
	PY	Plane normal to Y	y-D=0	D
	PZ	Plane normal to Z	z-D=0	D
Sphere	SO	Sphere centered at origin	$x^2+y^2+z^2-R^2=0$	R
	S	General	$(x-\bar{x})^2+(y-\bar{y})^2+(z-\bar{z})^2-R^2=0$	$\bar{x}\bar{y}\bar{z}R$
	SX	Centered on X-axis	$(x-\bar{x})^2+y^2+z^2-R^2=0$	$\bar{x}R$
	SY	Centered on Y-axis	$x^2+(y-\bar{y})^2+z^2-R^2=0$	$\bar{y}R$
	SZ	Centered on Z-axis	$x^2+y^2+(z-\bar{z})^2-R^2=0$	$\bar{z}R$
Cylinder	C/X	Parallel to X-axis	$(y-\bar{y})^2+(z-\bar{z})^2-R^2=0$	$\bar{y}\bar{z}R$
	C/Y	Parallel to Y-axis	$(x-\bar{x})^2+(z-\bar{z})^2-R^2=0$	$\bar{x}\bar{z}R$
	C/Z	Parallel to Z-axis	$(x-\bar{x})^2+(y-\bar{y})^2-R^2=0$	$\bar{x}\bar{y}R$
	CX	On X-axis	$y^2+z^2-R^2=0$	R
	CY	On Y-axis	$x^2+z^2-R^2=0$	R
	CZ	On Z-axis	$x^2+y^2-R^2=0$	R
Cone	K/X	Parallel to X-axis	$\sqrt{(y-\bar{y})^2+(z-\bar{z})^2}-t(x-\bar{x})=0$	$\bar{x}\ \bar{y}\ \bar{z}\ t^2\ \pm1$
	K/Y	Parallel to Y-axis	$\sqrt{(y-\bar{y})^2+(z-\bar{z})^2}-t(y-\bar{y})=0$	$\bar{x}\ \bar{y}\ \bar{z}\ t^2\ \pm1$
	K/Z	Parallel to Z-axis	$\sqrt{(y-\bar{y})^2+(z-\bar{z})^2}-t(z-\bar{z})=0$	$\bar{x}\ \bar{y}\ \bar{z}\ t^2\ \pm1$
	KX	On X-axis	$\sqrt{y^2+z^2}-t(x-\bar{x})=0$	$\bar{x}\ t^2\ \pm1$
	KY	On Y-axis	$\sqrt{y^2+z^2}-t(y-\bar{y})=0$	$\bar{y}\ t^2\ \pm1$
	KZ	On Z-axis	$\sqrt{y^2+z^2}-t(z-\bar{z})=0$	$\bar{z}\ t^2\ \pm1$

Table 3- 1 the surface card of CEARCPG (continued)

Ellipsoid Hyperboloid Paraboliod	GQ	Axes parallel to X-,Y-, or Z-axis	$A(x-\bar{x})^2+B(y-\bar{y})^2+C(z-\bar{z})^2+$ $D(x-\bar{x})+E(y-\bar{y})F(z-\bar{z})+G=0$	$ABCDEFG$ $\bar{x}\bar{y}\bar{z}$
Cylinder/ Cone Ellipsoid Hyperboloid Paraboloid	C	Axes not parallel to X-,Y-, or Z- axis	$Ax^2+By^2+Cz^2+Dxy+Eyz$ $Fzx+Gx+Hy+Jz+K=0$	$ABCDE$ $FGHJK$
Elliptical or circular torus. (Axes parallel to X-,Y-, or Z-axis)	K	$(x-\bar{x})^2/B^2+(\sqrt{(y-\bar{y})^2+(z-\bar{z})^2}-A)^2/C^2-1=0$ $(y-\bar{y})^2/B^2+(\sqrt{(x-\bar{x})^2+(z-\bar{z})^2}-A)^2/C^2-1=0$ $(z-\bar{z})^2/B^2+(\sqrt{(x-\bar{x})^2+(y-\bar{y})^2}-A)^2/C^2-1=0$		$\bar{x}\bar{y}\bar{z}\ ABC$

3.4 Input of CEARCPG

The format of input card is very similar to the input card of MCNP. Figure3-2 is an example of the typical input file. Most of the input card are the same as input file of MCNP (MCNP manual 2004). Only several specific cards used in CEARCPG are explained here.

1) Sdef card, which is used to define the neutron source. the default neutron source in CEARCPG is ^{252}Cf. CEARCPG also support the point neutron source, beam neutron and user-defined neutron source.
2) Number_detectors card is used to define the numbers of detector used in simulation.
3) Detector card is used to define the geometry information of detector, such as the size of the detector, position and so on.

4) Spect card is used to define the parameters of the output spectra, such as the number of channel for single and coincidence spectrum and the calibration of the spectrum.

5) Detcoin card is used to define the relationship among the detectors. In this example, detector 1 and detector 2 are used to record the coincidence spectrum.

```
Created on: Monday, December 29, 2003 at 22:50
    1      1  -11.34      -1  2  -4  5  -6  7
    2      1  -11.34      5  -4  -2  40  7  -6  8
         ......
   44      6  -1.06       -41  35  -27  30
   45      6  -1.06       -42  33  -27  29

    1         pz        23.5
    2         pz          23
    3         pz        13.3
         ......
   41        c/z          14           0         8.3
   42        c/z         -14           0         8.3

m1    82000              -1.0
        ......
m8    13027              -1
imp  1 1 1 1 1 1 1 1 1 1 1 1 1 1 1 1 1 1 1 1 1 1 1 1 1 1 1 1 1 1 1
     1 1 1 1 1 1 1 1 0 0 0 1 1 1
sdef   cf x=0.0  y=0.0  z=18  icel=3
nps    300000
number_detector 2
detector  -14.0 0 -25.8  7.62  15.24  16
          12.73 0 -24.53 7.62  15.24  21
sample   12
wcut 1d-6 1d-7 1d-10 1d-11 0.02
spect    2048 512 0 0  0.0055575  18000  0.0055575 0.02223
detcoin 1 ( 16 : 21 )
```

Figure 3- 2 The typical input of CEARCPG

Several variance reduction techniques are used in CEARCPG and they play important roles in CEARCPG. They are: Russian roulette; truncated exponential probability density function; discrete importance function Stratified

sampling approach; Detector response function and splitting. The definitions of theses technique have already been discussed in the introduction section.

Even though there are a lot of similarity between CEARCPG and MCNP, lots of difference still exist between CEARCPG and MCNP. Table 3-2 lists the difference between MCNP and CEARCPG.

Table 3- 2 The comparison between MCNP and CEARCPG

	CEARCPG	**MCNP**
Nuclear data	ENDF/B-VI ENSDF EPDL	ENDF/B-VI ENSDF with NJOY format EPDL
Neutron interaction	Neutron capture reaction	Same
	Neutron elastic scattering reaction (Free gas thermal Treatment)	Same
	Neutron inelastic scattering reaction (n, n' γ)	All inelastic scattering reaction, such as (n.n') (n,2n) etc.
Generation of neutron-induced photons	Sampling from isotope scheme	The number is function of neutron weight, photon limit weigh, photon production cross section, etc. Expanded photon production method &30X20 photon production method
Photon interaction	Simple Physics Treatment	Simple Physics Treatment & Detailed Physics Treatment
Variance reduction technique	Stratified sampling	general

4 Benchmark Experiments

Experimental benchmarks play very important roles for Monte Carlo code design. Several experiments have been done for benchmarking purposes. Both single and coincidence simulated spectrum are checked with experimental results. Usually, not only can the benchmark experiment be used to check the calculation, but also can be used to check the nuclear data used in the simulation.

4.1 Benchmark experiment 1-The ETI prototype

The ETI prototype PGNAA analyzer was designed to perform the on-line coal analysis. Its experimental configuration schematic for the Monte Carlo simulation is shown in figure 4-1. This analyzer consists of a ^{252}Cf radioisotope neutron source, a 5”×5” NaI(Tl) detector, and a rectangular coal chute located between the source and the detector. The cylindrical analyzer body is filled with neutron moderations and shielding materials such as polyethylene, paraffin, lead etc. the coal sample is composed of 17 major elements, including Hydrogen, Carbon, Nitrogen, Oxygen, Sodium, Magnesium, Aluminum, Silicon, Phosphorous, Sulfur, Chlorine, Potassium, Calcium, Titanium, Manganese, Iron and Nickel, but their exact contents are not available. The coal sample used in Monte Carlo simulation is assumed to have the average compositions of the coal sample and listed in table 4-1.

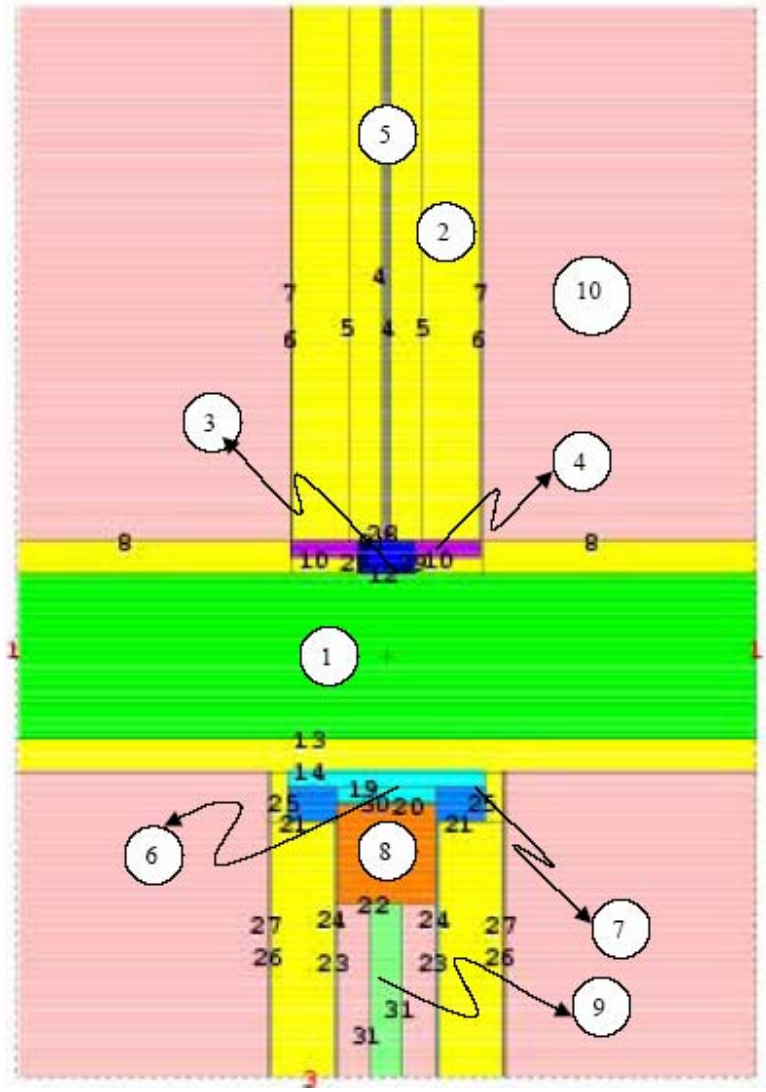

Figure 4- 1The geometry configuration of ETI prototype,
where 1 is coal sample, 2 the polyethylene, 3 bismuth with the neutron source, 4 air, 5 aluminum, 6 Lithium polyethylene, 7 lead, 8 NaI detector, 9 SiO_2 (PMT) and 10 is paraffin

The measured coal sample

Six coal sample with different weight fraction of sulfur are measured. The measured single spectrum of sample 1 is plotted in figure 4-2. The coal sample spectrum is shifted by using code GSHIFT according to the Hydrogen peak and the Nitrogen peak (2.223MeV and 1.829 MeV).

Table 4- 1 the assumed composition of coal sample

Number	Element	Weight fraction (%)
1	Hydrogen	5.2
2	Carbon	75.2865
3	Nitrogen	1.42
4	Oxygen	12.5513
5	Sodium	0.045
6	Magnesium	0.0595
7	Aluminum	1.164
8	Silicon	2.2612
9	Phosphorous	0.0097
10	Sulfur	0.77
11	Chlorine	0.11
12	Potassium	0.3277
13	Calcium	0.108
14	Titanium	0.0656
15	Manganese	0.0001
16	Iron	0.6212
17	Nickel	0.0001

The simulated spectra

Since there only one NaI detector is used, only single spectra are simulated by CEARCPG. Simulation is also done by using MCNP for comparison purpose. The results are plotted in figure 4-3. All the spectra are normalized at the nitrogen peak. Since the ^{252}Cf neutron source not only emits fission neutrons but also emits fission gamma rays, two simulations were done by using MCNP with different source. The materials used in MCNP are same as that used in CEARCPG. The agreement between CEARCPG and MCNP is quite different.

CEARCPG is much closer to the experimental spectrum. The MCNP model can not simulate the activation spectrum of NaI detector which is observed and measured by R.P. Gardner in 2000. Compared to the simulation results of CEARPGA II, the shape of CEARCPG is steeper than the spectrum of CEARPGA II. That can be explained by the algorithm used in CEARPGA II. In code CEARPGA II, only the high intensity prompt gamma rays are taken into account to apply the interpolation.

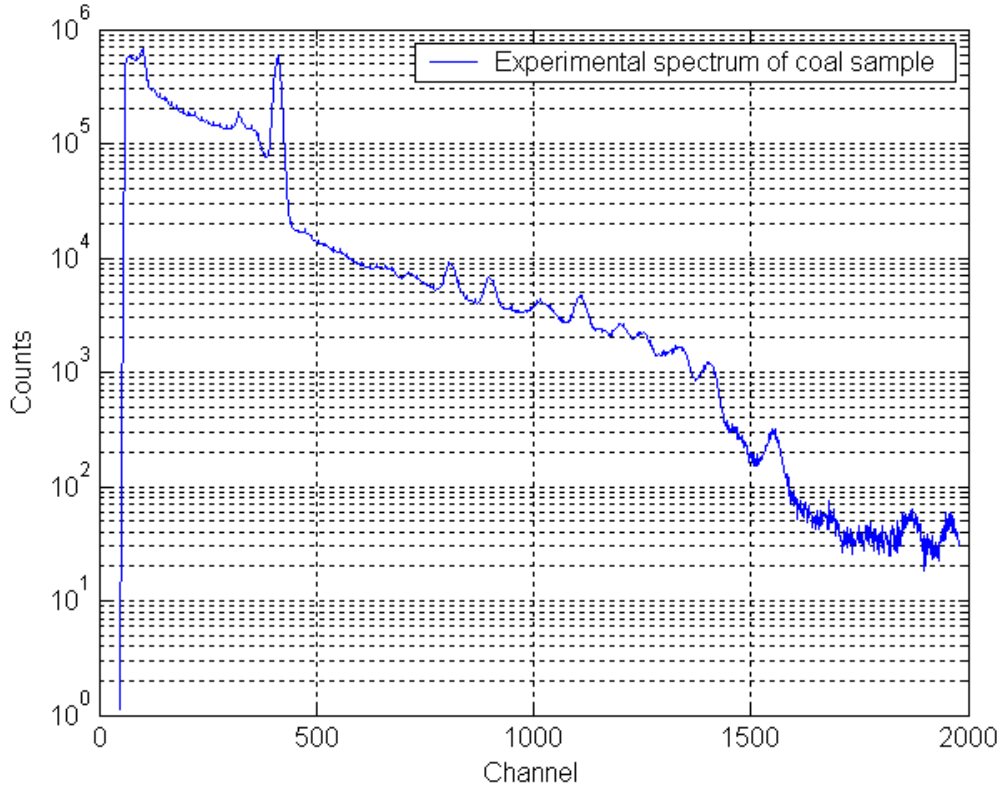

Figure 4- 2 The experimental single spectrum of coal sample 1

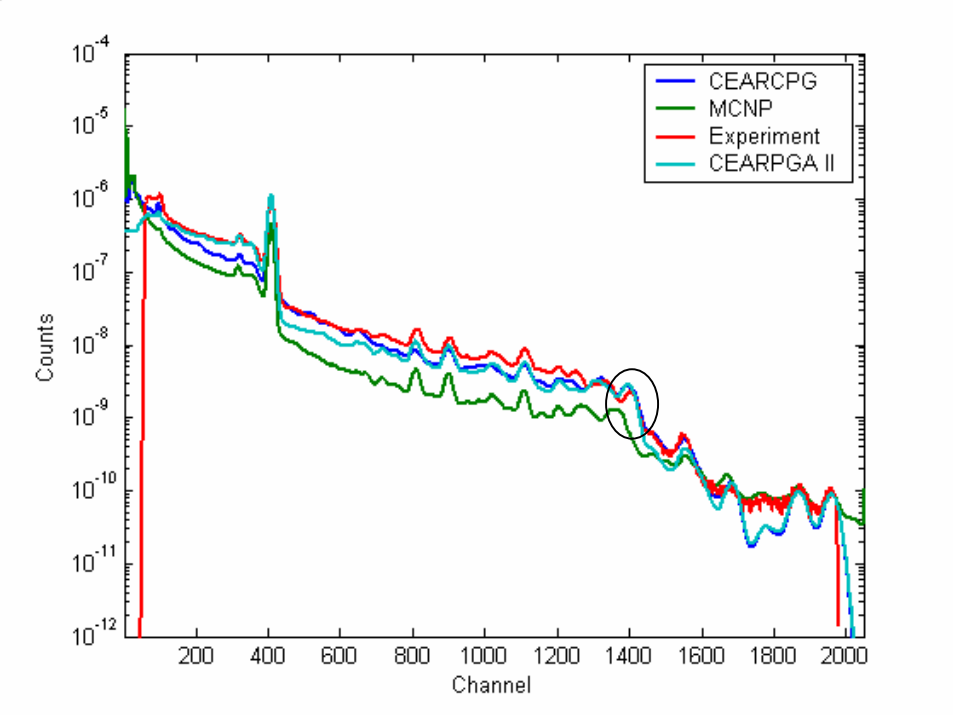

Figure 4- 3 The comparison of ETI prototype simulated spectra between code CAERCPG, code CAERPGAII and MCNP5

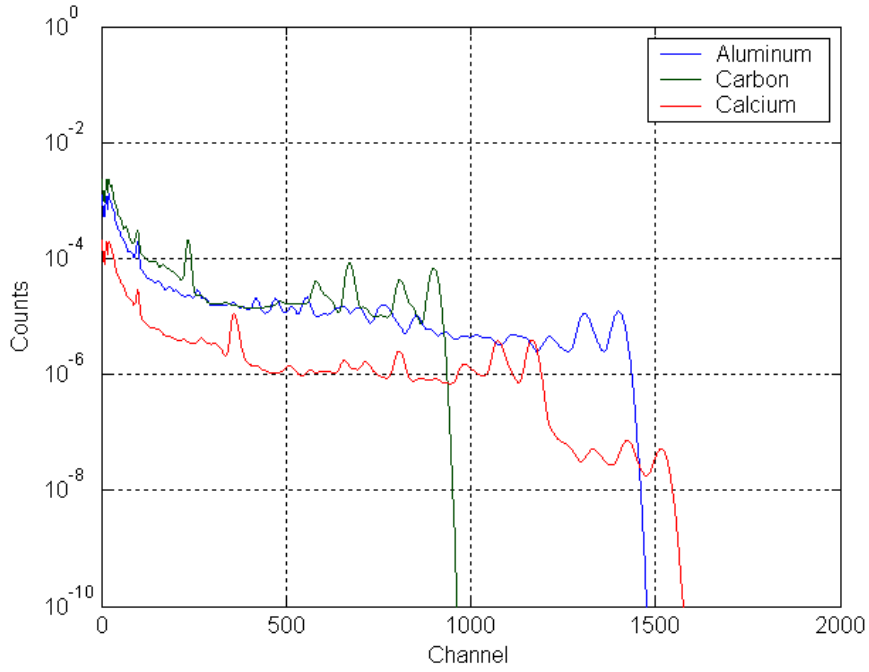

Figure 4- 4 Elemental library spectra of element Aluminum, Carbon and Calcium. Calculated by CEARCPG

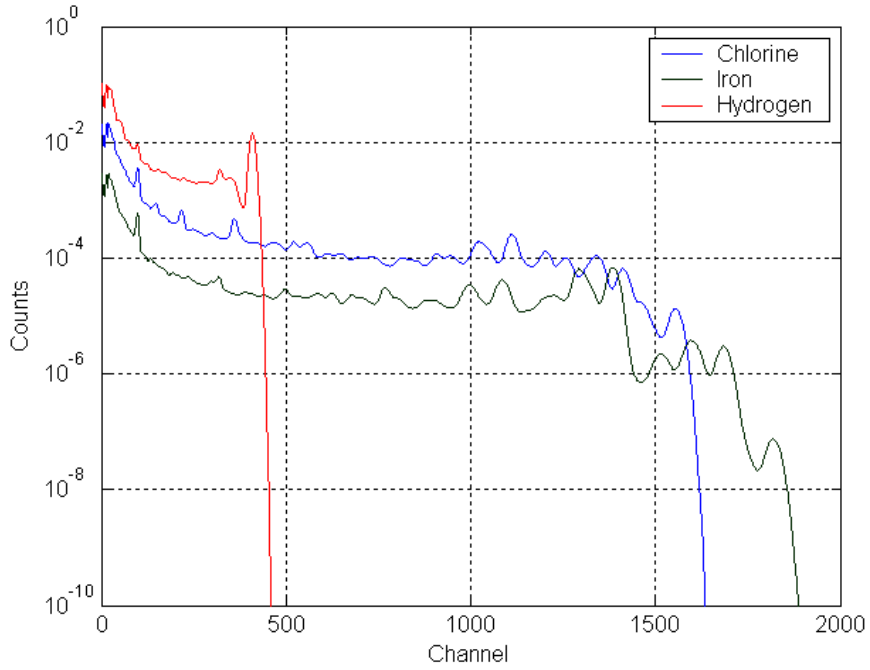

Figure 4- 5 Elemental library spectra of element Chlorine, Iron and Hydrogen. Calculated by CEARCPG

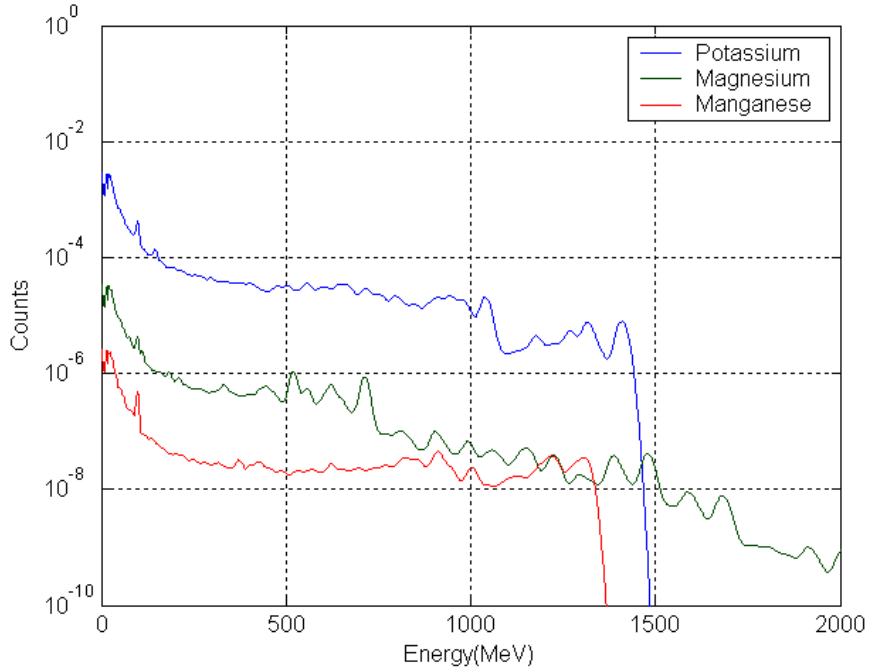

Figure 4- 6 Elemental library spectra of element Potassium, Magnesium and Manganese. Calculated by CEARCPG

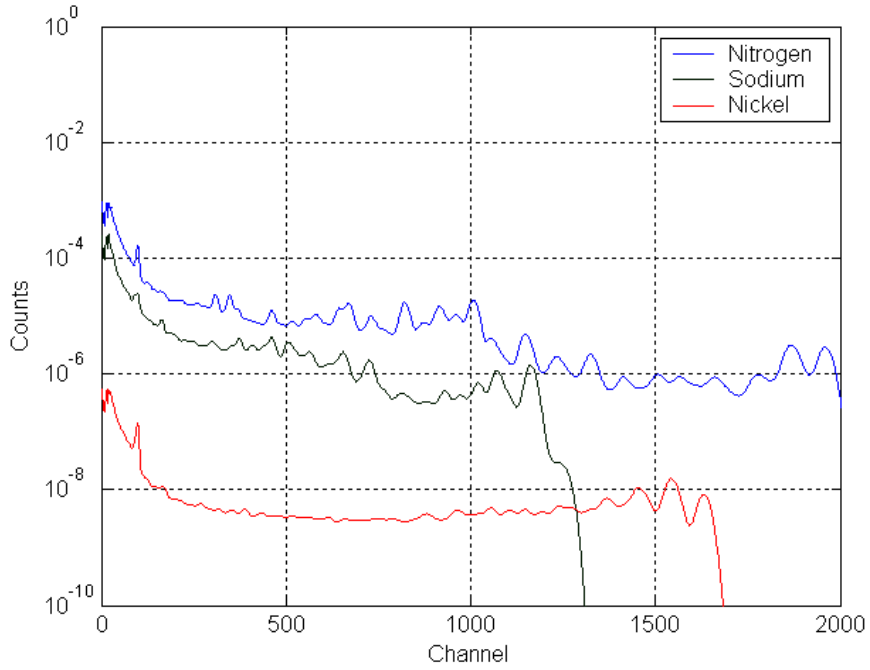

Figure 4- 7 Elemental library spectra of element Nitrogen, Sodium and Nickel. Calculated by CEARCPG

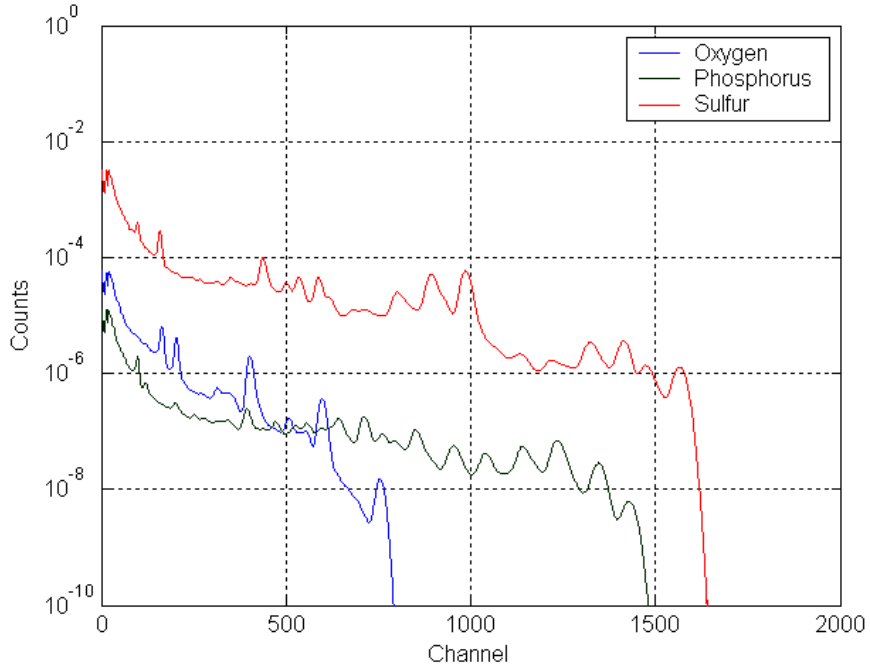

Figure 4- 8 Elemental library spectra of element Oxygen, Phosphorus and Sulfur. Calculated by CEARCPG

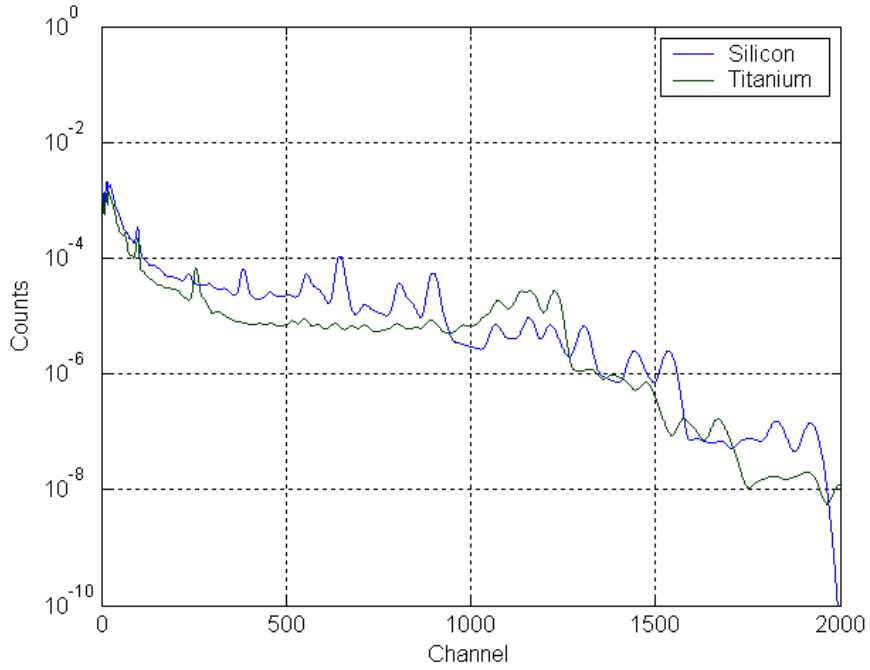

Figure 4- 9 Elemental library spectra of element Silicon and Titanium. Calculated by CEARCPG

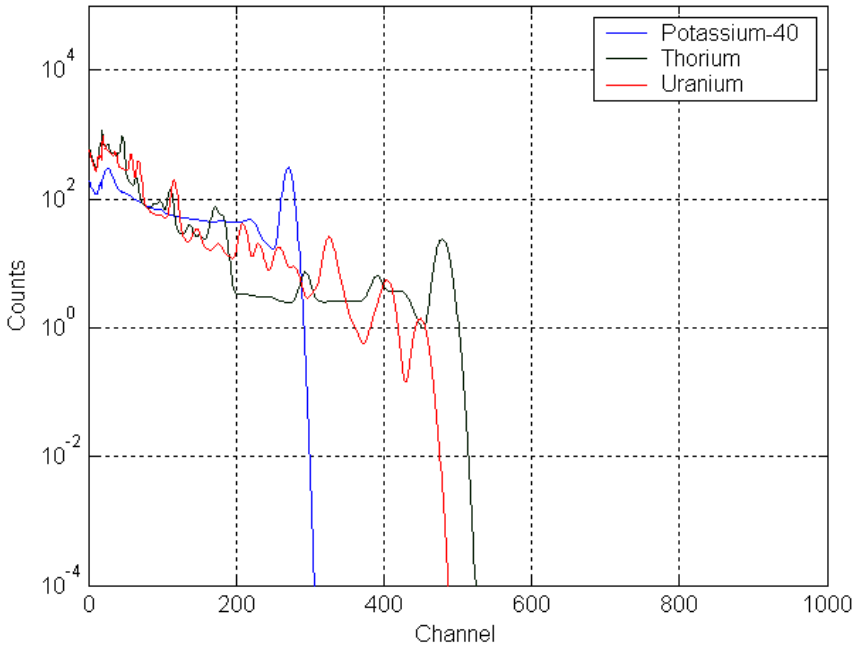

Figure 4- 10 Library spectra of natural background. Calculated by CEARCPG

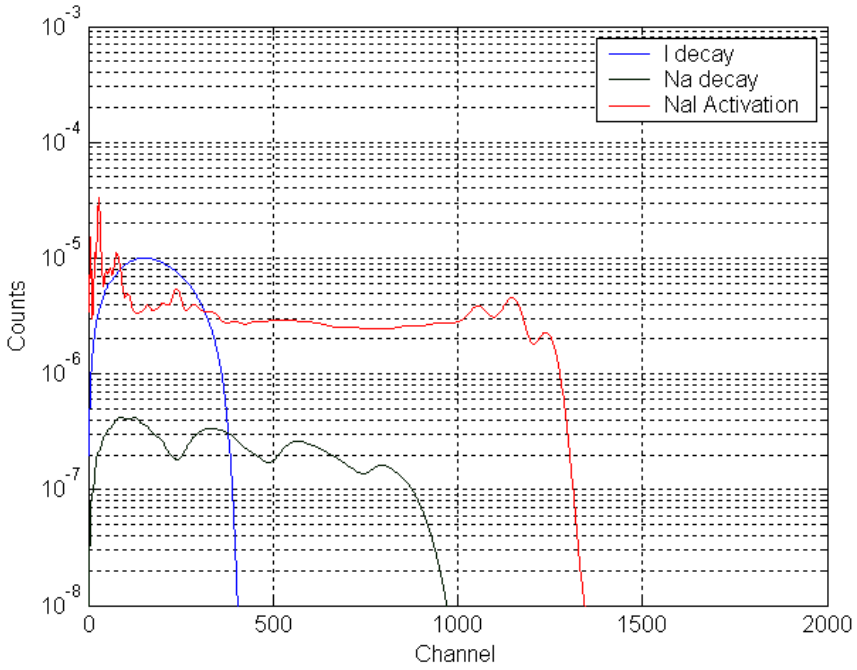

Figure 4- 11 Library spectra of NaI detector activation spectra. Calculated by CEARCPG

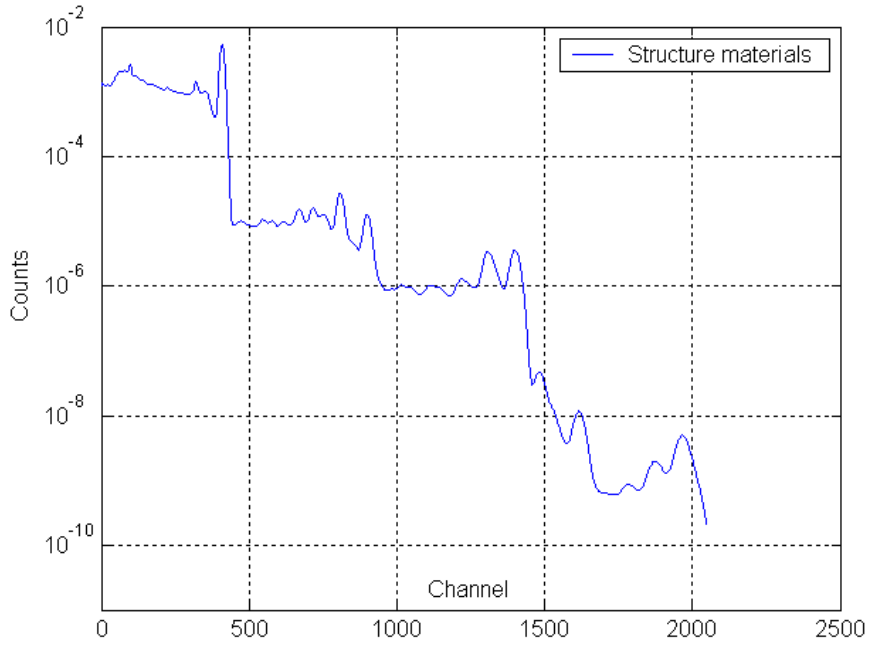

Figure 4- 12 Library spectra of structure materials. Calculated by CEARCPG

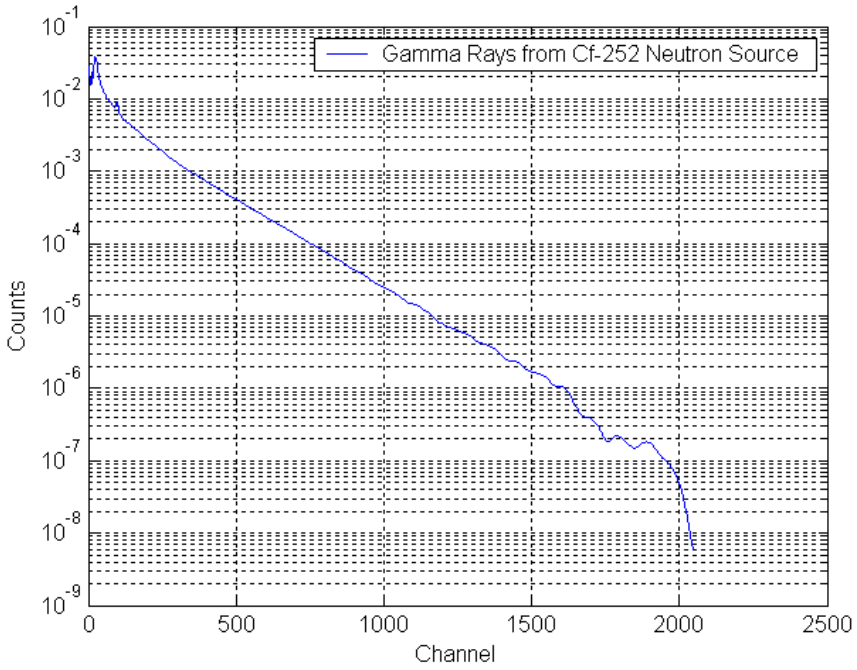

Figure 4- 13 Library spectra of fission gamma rays. Calculated by CEARCPG

However, in CEARCPG, all of the prompt gamma rays are taken into account since they are sampled from the scheme. Another improvement over the result of CEARPGA II is CEARCPG can predict the 511 KeV peak more accurate than CEARPGA II. It will be shown in the fitting results. The simulated elemental library spectra are listed from figure 4-4 to figure 4-13.

The Library Least-Square fitting

The MCLLS fitting result of coal sample is done with the simulated elemental library spectra. The fittings spectrum is plotted in figure 4-14. The reduced Chi-square is 26.

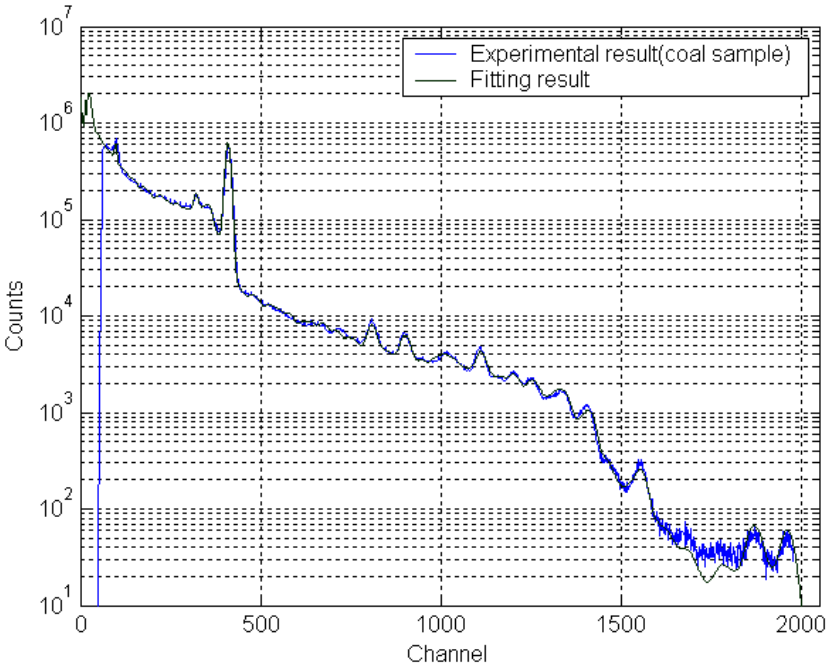

Figure 4- 14 the fitting result of ETI coal sample

The fitting spectrum is good agreement with the experimental spectrum. Compared to the result of code CEARPGAII (Zhang 2003), the fitting result of CEARCPG is better than the fitting of CEARPGA II at low energy region. Figure 4-15 shows the residuals over the deviation of each channel between the experimental spectrum and fitting spectrum. The maximum residuals peak is near to the Hydrogen peak. it might come from the Detector Response Function (DRF) used in CEARCPG. It looks like that the FWHM for Gaussian spreading is narrower than the true experimental spectra. All of the six experimental spectra are fitted by using Library Least-Square method. The Reduced Chi-Square is from 20-60. The calculated weight fraction of sulfur and the true value of each sample are listed in table 4-2. clearly, the MCLLS quantitative analysis for the sulfur composition are accurate.

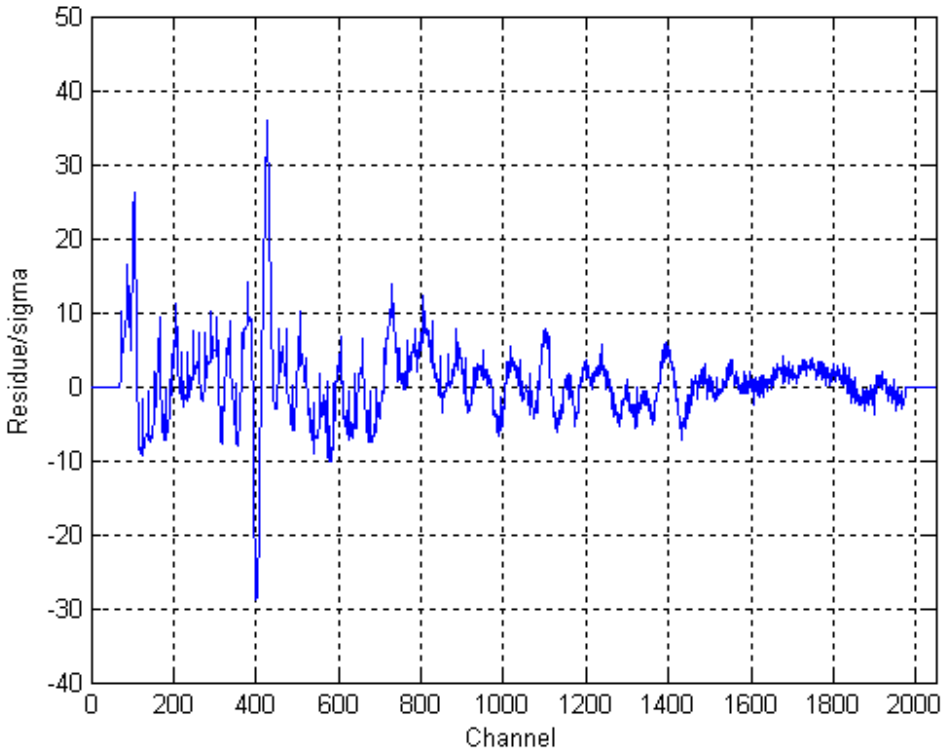

Figure 4- 15 the residue over deviation of channel for ETI coal sample fitting

Table 4- 2 MCLLS quantitative results for ETI coal sample measurements

Sample number	True weight fraction of sulfur (%)	Calculated weight Fraction (%)	Relative error (%)
1	0.57	0.59	3.51
2	0.68	0.745	9.56
3	0.36	0.492	36.67
4	0.78	0.707	9.36
5	0.61	0.543	10.98
6	1.19	1.06	10.92

4.2 Benchmark Experiment 2 – Pure Sulfur sample

4.2.1 Experiment electronics setup and results

The electronic schematic is plotted in figure 4-16. This experiment setup is composed of two 6”X6” NaI detectors. There are two circuits for each detector, the energy acquisition channel and timing channel. The output pulse of PMT is divided into two signals. One goes through the energy acquisition channel, through the preamplifier and the linear Amplifier then acts as input 1 of the Sparrow Multi-parameter Acquisition System. The other one will enter the timing channel. This channel is more complicated than the energy channel. Timing Filter Amplifier plus the CFD (Constant Fraction Discriminator) will pick up the time information of the incident pulse. The output signal of CFD is a logic pulse. The timing of detector 2 is almost the same as the situation of detector 1. The combination of timing filter and CFD offers precise timing information of each channel. Even though the timing information of two channels is close, extra delay is still needed to make sure that the two input logic pulses will arrive at the coincidence module within the resolving time. The coincidence module will generate a gate signal as input of Sparrow Multi-parameter Acquisition System. The gate signal will trigger the Sparrow Multi-parameter Acquisition System to be ready to receive the signals from the energy channel. If two signals arrive at the acquisition at the same time, one coincidence event is recorded. The coincidence events are temporarily buffered in an ADC module and finally are transferred to the computer with the acquisition software, KMAXNT.

In practice, the setting of timing channel is much more complicated. TAC (Time-to-Amplitude Converter) electronic modular is used to adjust the timing of two channels. Two parameters can be determined by TAC measured spectrum. One is the compensating time for delay time and the second is the FWHM of timing spectrum that can be used to set the window width of coincidence unit. The measured timing spectrum is plotted in figure 4-18. According to the timing spectrum, the compensating delay unit for the fast channel should be set to 50 ns and the window width of coincidence unit is about 20 ns.

The experiment setup is plotted in figure 4-17. ^{252}Cf neutron source is placed in 5cmX5cmX5cm lead shielding box. Paraffin wax worked as neutron slowing down materials. The fission neutron will be scatted and thermalizein the paraffin wax. A rectangular sample chute is located between the wax and the two 6”X6” NaI detectors.

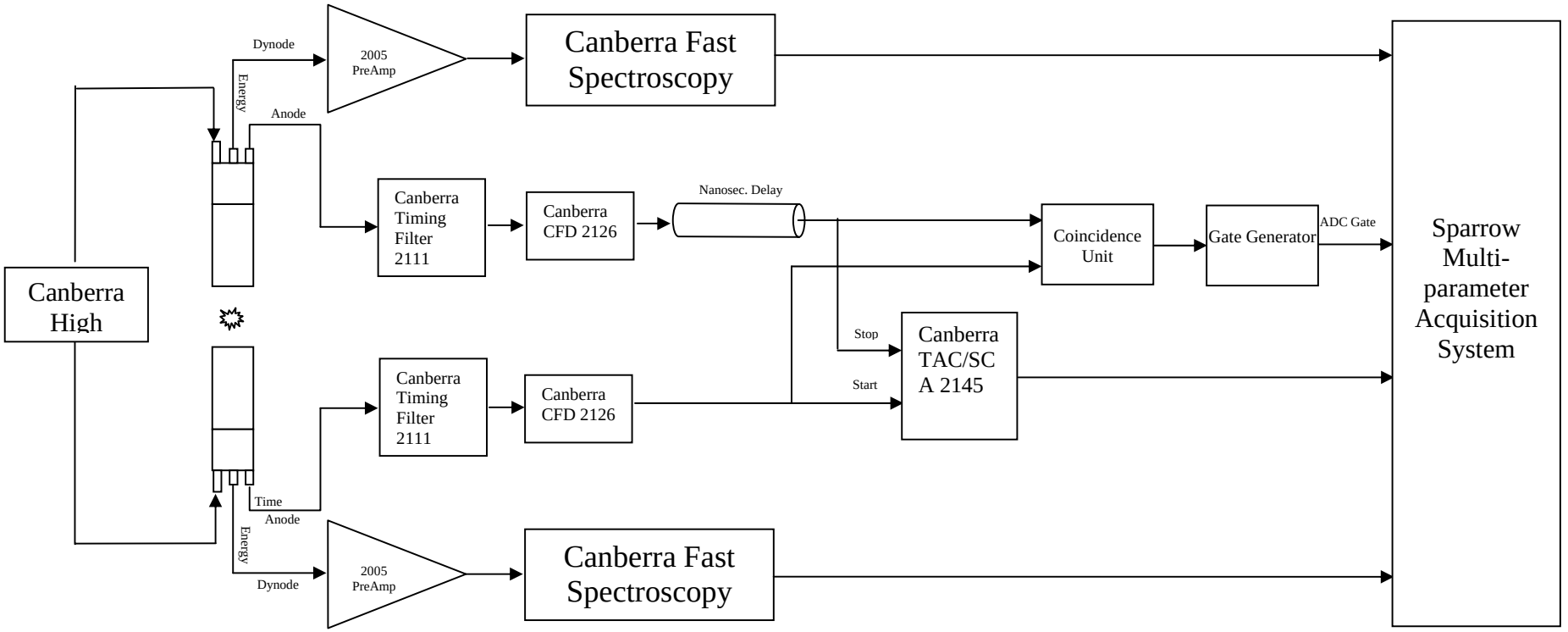

Figure 4- 16 Schematics of electronic connection of two 6”X6” NaI detector system.

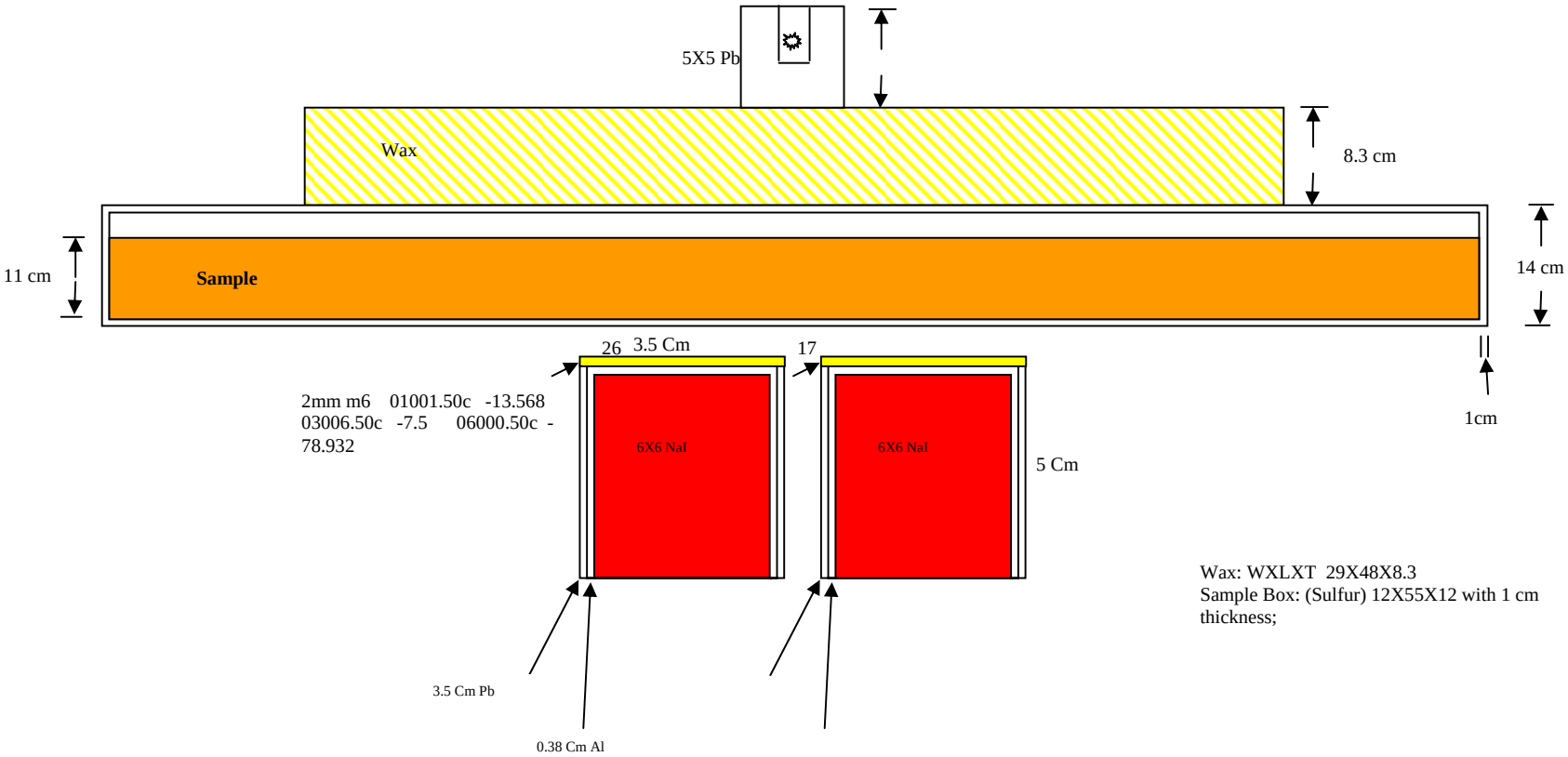

Figure 4- 17 Experimental setup for Sulfur sample

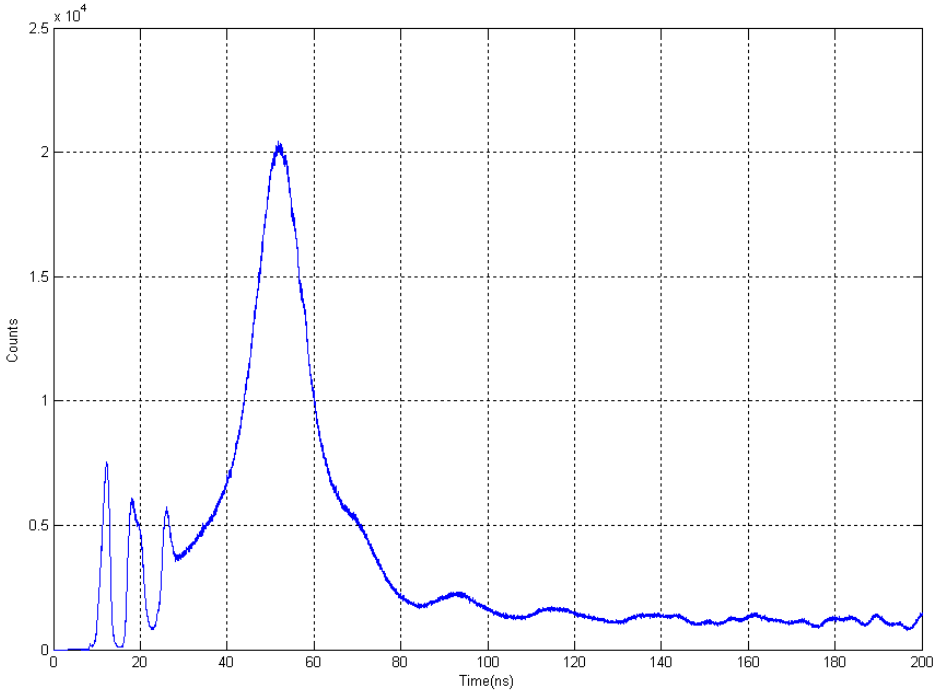

Figure 4- 18 Experiment timing spectrum with two 6"X6" NaI detector

4.2.2 The Experimental Results

The measured sulfur single and coincidence spectra are plotted in figure 4-19. The peaks which appear in the measured spectra are tabulated in table 4-3. The total coincidence spectrum is obtained experimentally by projecting the two-dimensional coincidence spectrum to the x-axis. Q-value diagonal projection is also applied on the two-dimensional coincidence spectrum. The projection energy window is plotted in figure 4-20. The energy of window is the Q value of ^{32}S (n, γ)^{33}S reaction, which is 8.641 MeV. The projection spectrum is plotted in figure 4-21. it can be seen that the Q-value diagonal projection spectrum has much better resolution and signal-to-noise ratio compared to ordinary single spectrum.

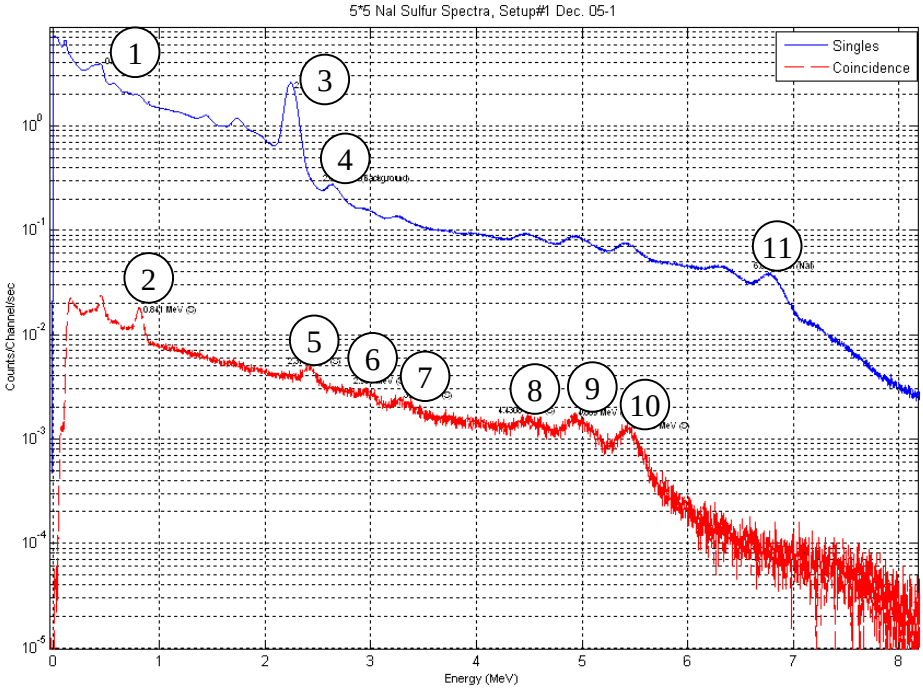

Figure 4- 19 The measured single and total coincidence spectra of pure sulfur sample.

Table 4- 3 Peaks of pure Sulfur sample

Peak	Energy (MeV)	Source
1	0.511	Pair Production
2	0.841	Sulfur
3	2.223	Hydrogen
4	2.61	Potassium-40
5	2.379	Sulfur
6	2.931	Sulfur
7	3.22	Sulfur
8	4.4308	Sulfur
9	4.869	Sulfur
10	5.4205	Sulfur
11	6.826	NaI

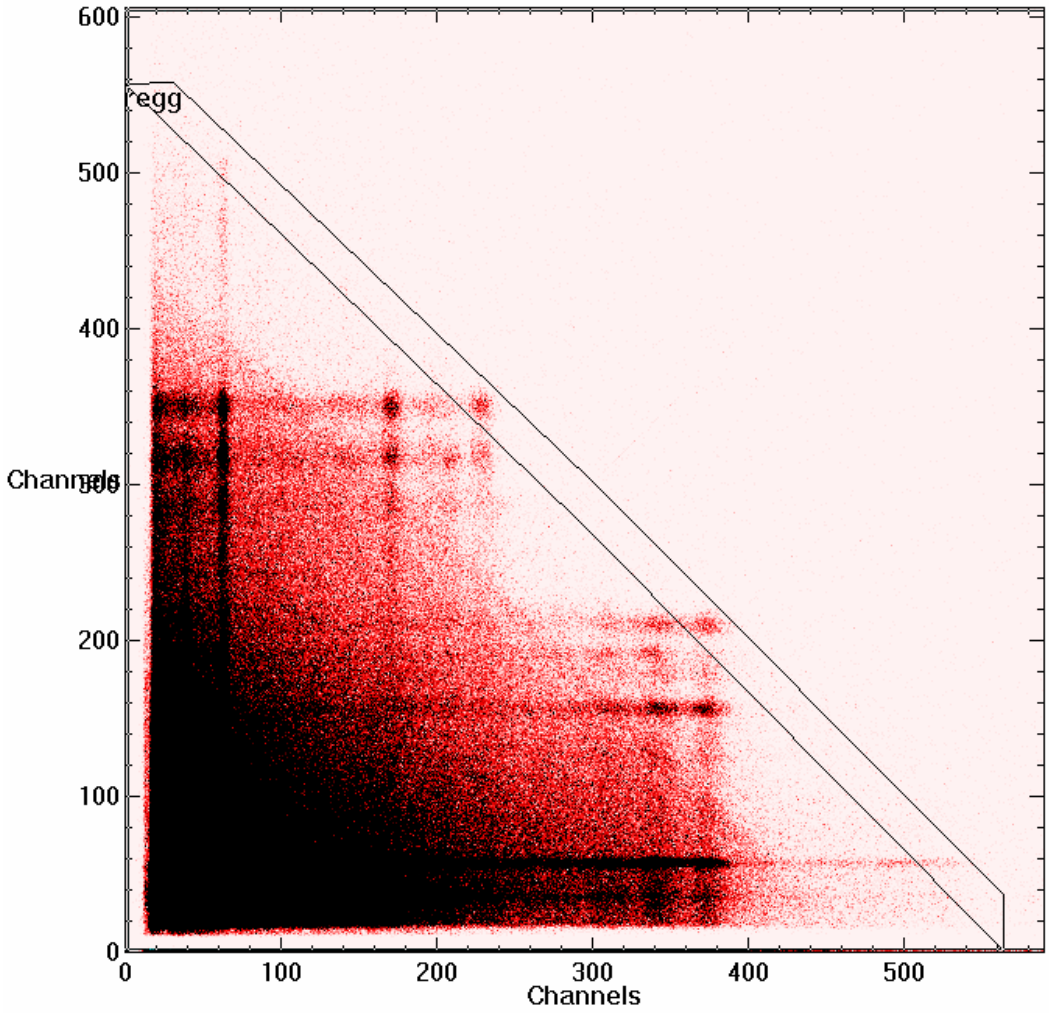

Figure 4- 20 the Q-value diagonal summation window for pure Sulfur sample

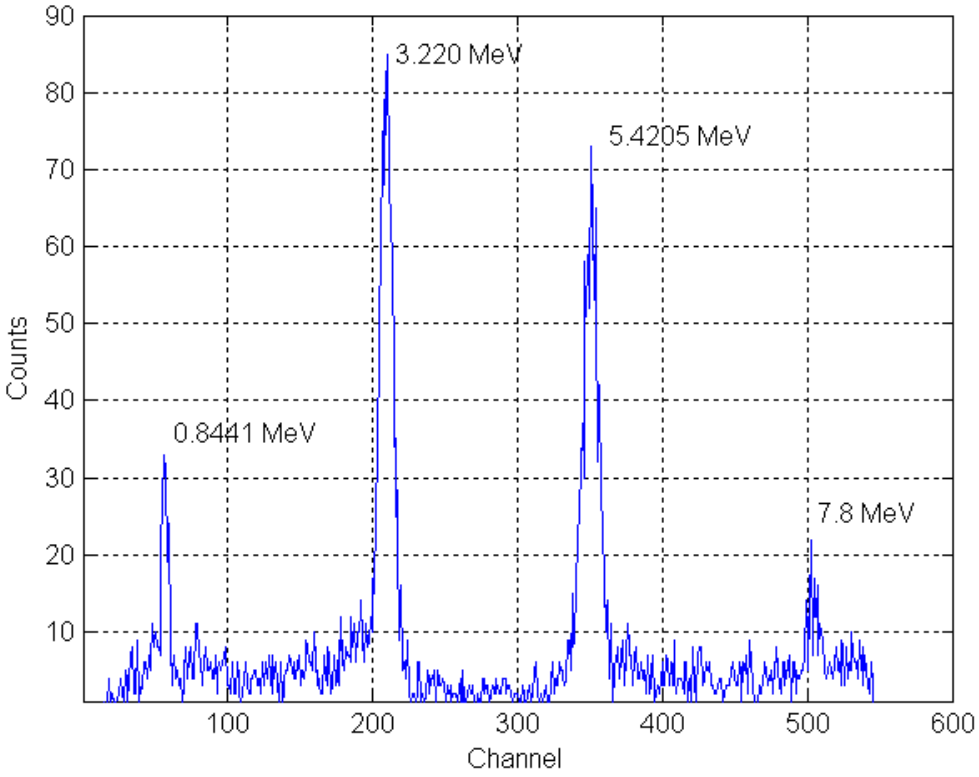

Figure 4- 21 The projection spectra of Q value diagonal summation for pure Sulfur sample

4.2.3 The Monte Carlo modeling

Single Spectra

This problem is also simulated by using general-purpose Monte Carlo code MCNP for comparison purpose. For MCNP, two simulations are done with different source. One is the fission neutron source and the other is for fission gamma source. For CEARCPG, only one simulation is needed since it already contains the fission gamma simulation. The final results are plotted in figure 4-22. it is the same as results of coal sample, the results of MCNP don't contain the

gamma rays which are from the natural background and the prompt gamma rays from the NaI detector activation.

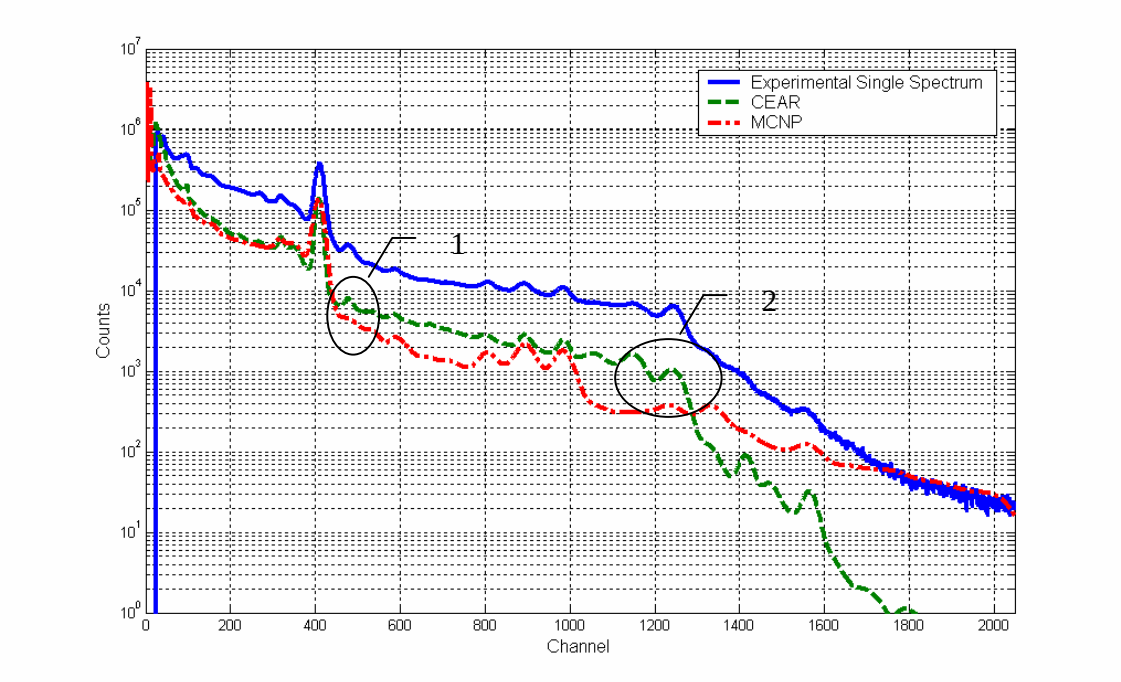

Figure 4- 22 The single spectra of pure sulfur sample. Where region 1 is the gamma rays from natural background and region 2 is the gamma rays from NaI detector activation

Coincidence spectra

Two-dimensional coincidence spectra are calculated by using CEARCPG. The detector response function of 6"X6" NaI detector is applied to convert the gamma flux spectra into the pulse-height spectra. The calculated two-dimensional coincidence spectrum is plotted in the figure 4-23. Horizontal projection and Q-value diagonal projection are also applied to get the total coincidence spectra and Q-value diagonal projection spectra. The projection spectra are plotted in figure 4-24 and figure 4-25. Library least-Square fitting is

applied on the single spectra, the total coincidence spectra and the Q-Value spectra. The libraries used in Least-Square fitting for single and coincidence are listed in table 4-4. The reduced Chi-Square for theses three fittings are 102, 55 and 2.1. The fitting spectra are plotted in figure 4-26, 4-27 and 4-24. Obviously, the fitting for the Q-value projection spectrum is much better than the other two fittings because there is only one interference source in the Q-value projection spectrum, the chance coincidence. Right now, CEARCPG can not generate the chance coincidence spectrum. The chance coincidence spectrum can be estimated with the experimental spectra by using the following equation,

$$R_c = R_1 \cdot R_2 \cdot \tau \qquad (4.1)$$

Where R_1 is the counting rate of detector 1 and R_2 is the counting rate of detector 2. τ is the resolving time of coincidence measurement. The calculated results show that the counts from chance coincidence are very low and can be ignored for the Q-value projection. Figure 4-28 shows the calculated two-dimensional chance coincidence and the projection spectrum.

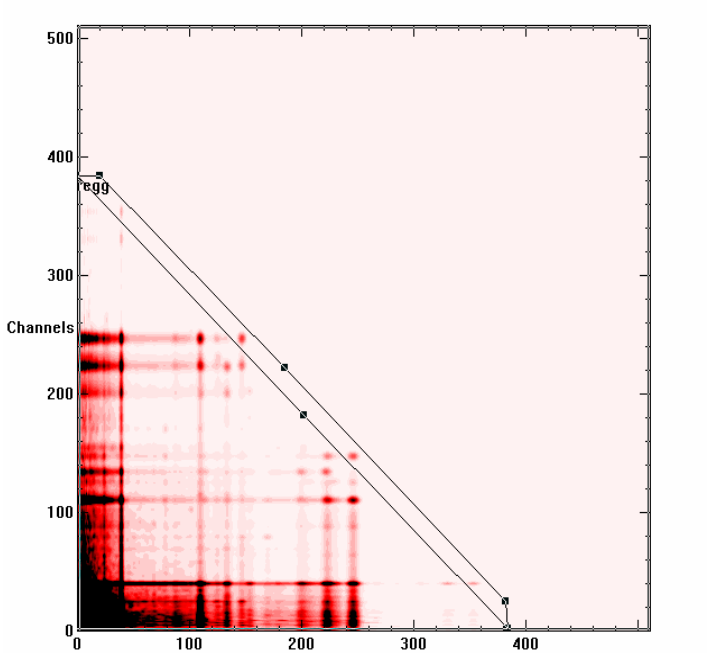

Figure 4- 23 The two-dimensional coincidence spectra of pure sulfur sample, calculated by CEARCPG

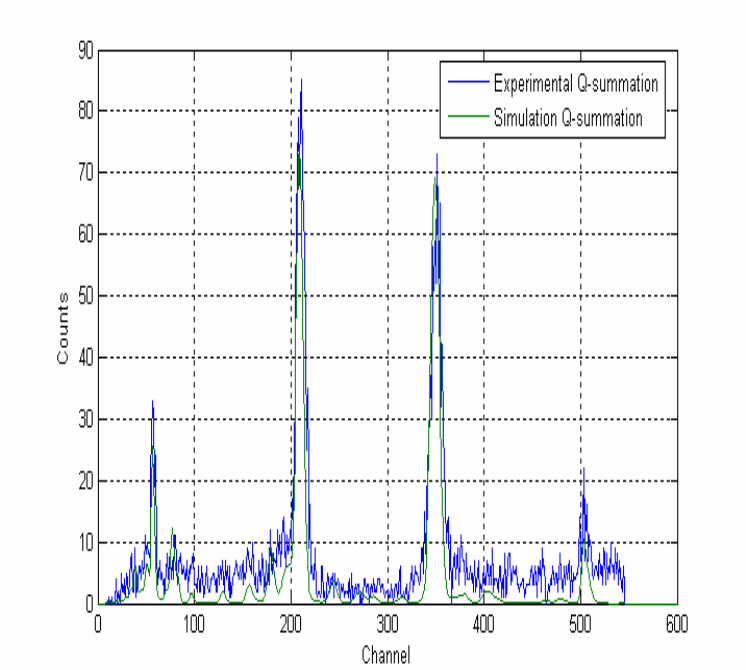

Figure 4- 24 The calculated Q-value projection spectrum .vs. experimental spectrum

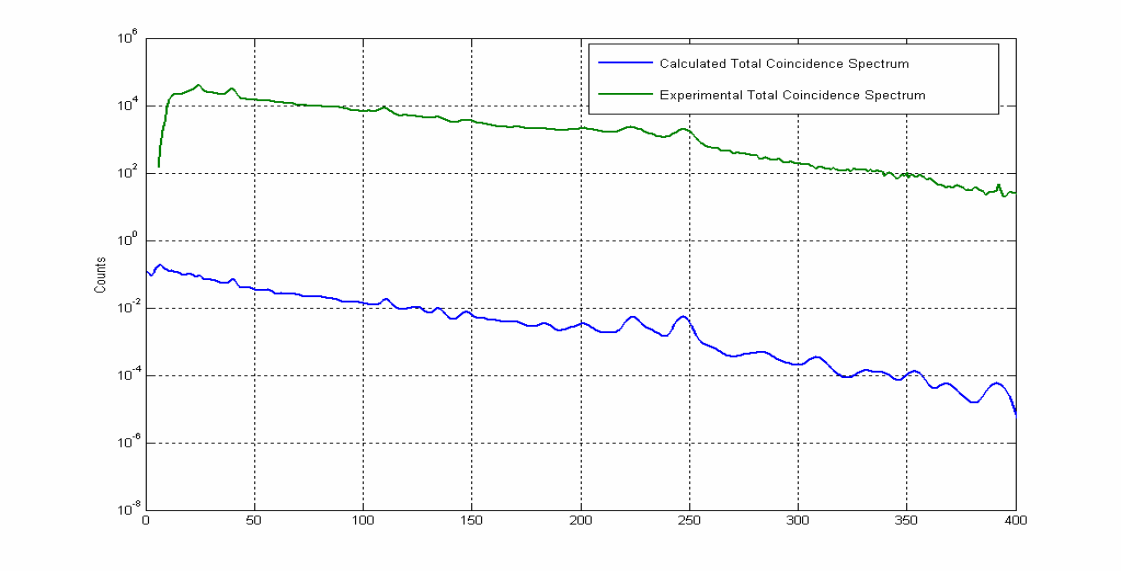

Figure 4- 25 The simulated Total coincidence spectrum of sulfur sample

Table 4- 4 The libraries used for Least-Square fitting of sulfur sample

Sources	**Single Spectrum**	**Total Coincidence spectrum**	**Q-value projection spectrum**
Sample	Sulfur	Sulfur	Sulfur
Natural background	Potassium-40		
	Thorium		
	Uranium		
Neutron source	Fission gamma rays	Fission gamma rays	
NaI detector	NaI activation spectrum		
	^{1287}I decay spectra		
	^{28}Na decay spectra		
		Chance Coincidence	

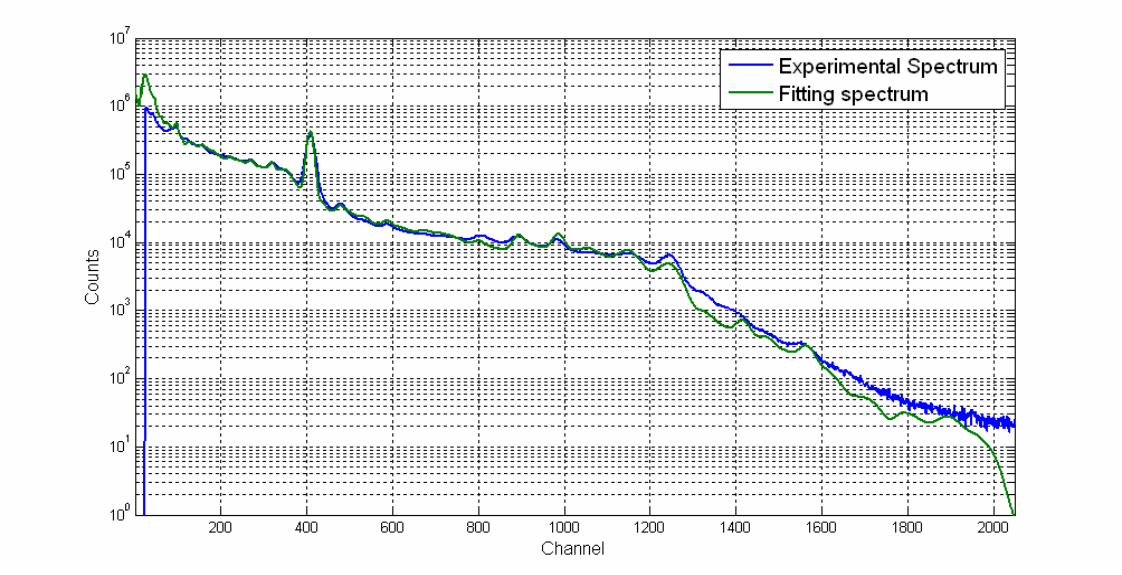

Figure 4- 26 The fitting spectrum of the single spectrum of sulfur sample

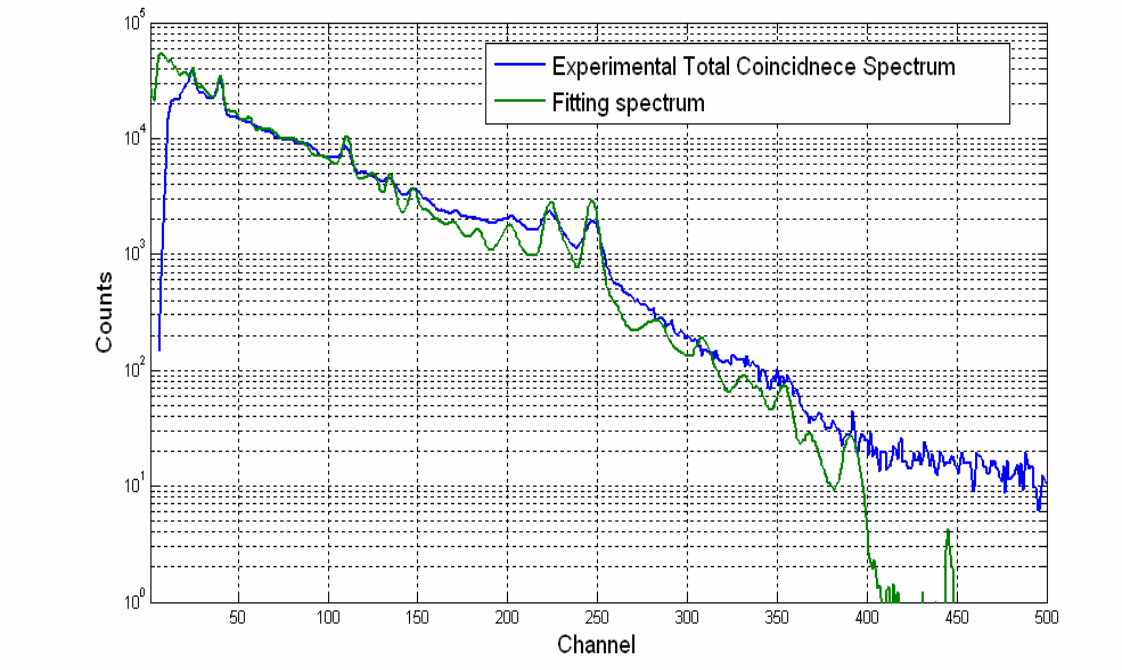

Figure 4- 27 The fitting spectrum of the total coincidence spectrum of sulfur sample

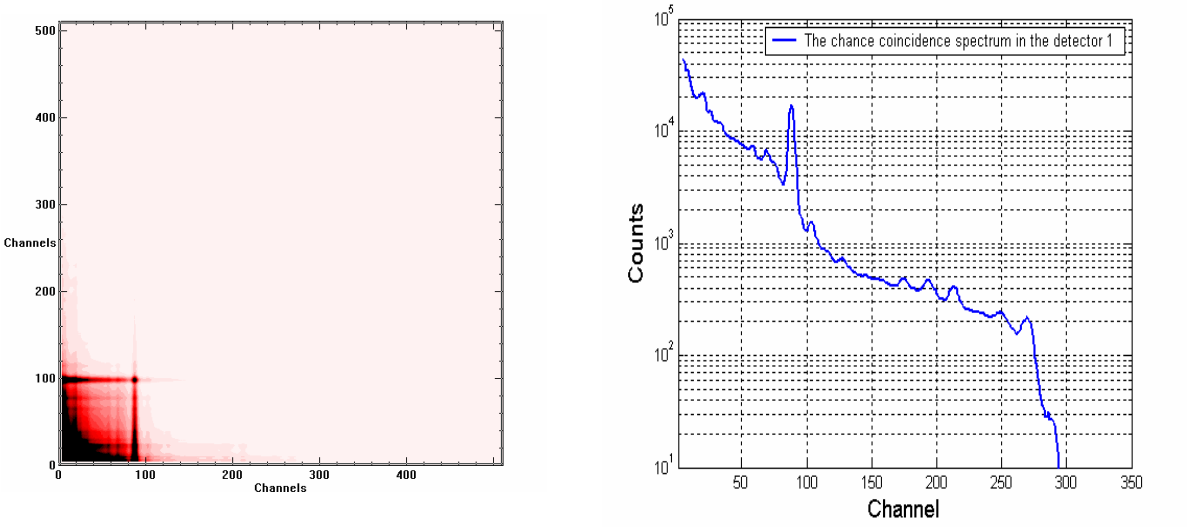

(a) (b)

Figure 4- 28 The Calculated chance coincidence spectrum (CountsX1000)

This benchmark experiment also can be used to explain the reason why the coincidence measurement can increase the signal-to-noise ratio quantitatively.

The pertinent treatment for improving (or not) the S/N ratio of a simple total counting rate radiation measurement is given in Knoll(1999). That treatment yields the relationship:

$$\frac{1}{T} = \frac{\varepsilon^2 S^2}{\left(\sqrt{(S+B)} + \sqrt{B}\right)^2} \qquad (4.1)$$

Where S and B are the signal and background (noise) counting rates, ε is the relative standard deviation of the signal (σ_S/S), and T is the total measurement time which is the sum of the gross counting rate time (T_{S+B}) and the background counting rate time (T_B), which have been optimized according to:

$$\frac{T_{S+B}}{T_B} = \left(\frac{S+B}{B} \right)^{1/2} \qquad (4.2)$$

The term 1/T can be considered to be a figure of merit.

In the case of the single PGNAA response for a typical on-line bulk analysis, the noise (N) is typically 90% or more of the gross counting rate when one considers the neutron source gamma rays, detector activation, prompt gamma rays from the construction materials of the analyzer, and the prompt gamma rays from hydrogen in the usual normal amount that is present. In this case one can use the limiting relationship for Eq. 4.1 given by:

$$\frac{1}{T} = \frac{\varepsilon^2 S^2}{4B} \quad \text{or} \quad \varepsilon = \frac{2\sqrt{B}}{S\sqrt{T}} \qquad (4.3)$$

For a value of S and B estimated from the results shown in Fig. 4-19 of 50,000 and 450,000, respectively, the value of ε for a unit value of T is 2.68%. In the case of the coincidence PGNAA response for the same case, the background or noise is much less than that for the signal. In this case one can use the limiting relationship for Eq 4.1 given by:

$$\frac{1}{T} = \varepsilon^2 S \quad \text{or} \quad \varepsilon = \sqrt{\frac{1}{ST}} \qquad (4.4)$$

For a value of S estimated from the results shown in Fig. 1 of 2,000, the value of ε for a unit value of T is 2.24%, which is slightly better than that from the singles response.

4.3 Benchmark Experiment 3 –pure mercury sample

The experiment was carried out on the Pulse Star research reactor at North Carolina State University. The demonstration of experiment setup is plotted in figure 4-29. The mercury has 7 natural stable isotopes. Table 4-5 shows some basic information of mercury. The normalized factor shows that there are almost 94% prompt gamma rays from ^{199}Hg. The Q value of ^{199}Hg(n,γ)^{200}Hg is 8.028 MeV. MC simulations are done by using MCNP and CEARCPG code separately. According to MCNP manual, the newest nuclear data library of mercury is 80000.40c and 80000.42c which are extracted from ENDL92. These Two nuclear data libraries are tested separately. The results of MCNP show that the nuclear data of mercury are not right. The results of MCNP are plotted in figure 4-30. The Gaussian spreading doesn't apply to the result. Table 4-6 lists the major prompt gamma rays of mercury [IAEA PGAA Database].

4.3.1 Experimental results

The experimental single spectrum and total coincidence spectrum are plotted in figure 4-31. The main peaks in the spectrum are labeled which are according to the label in table 4-6. The two-dimensional coincidence spectrum is plotted in figure 4-32. The Q-value projection spectrum is plotted in figure 4-33. It is the same as the projection spectrum of sulfur sample. The projection spectrum has a good resolution and much better signal-to-noise ratio. The dominant coincidence peak pairs are labeled in the figure 4-33 and their energies are listed in table 4-7.

4.3.2 Monte Carlo Modeling

The computer time is 23 hours. Since the simulation results of MCNP are not correct, only results of CEARCPG are plotted. Figure 4-34 shows the simulated single library spectrum of mercury before it is applied the detector response function. All the labeled peaks are listed in table 4-6. Figure 4-35 shows the simulated mercury library spectrum after it is applied the detector response function. The simulated total coincidence spectrum is plotted in figure 4-35 too. The simulated two-dimensional coincidence spectrum is plotted in figure 4-32 and the Q-value projection spectrum is plotted in figure 4-36 compared with the experimental Q-value projection spectrum. The Reduced Chi-Square is 4.3. The fitting spectrum and the experimental spectrum are in good agreement.

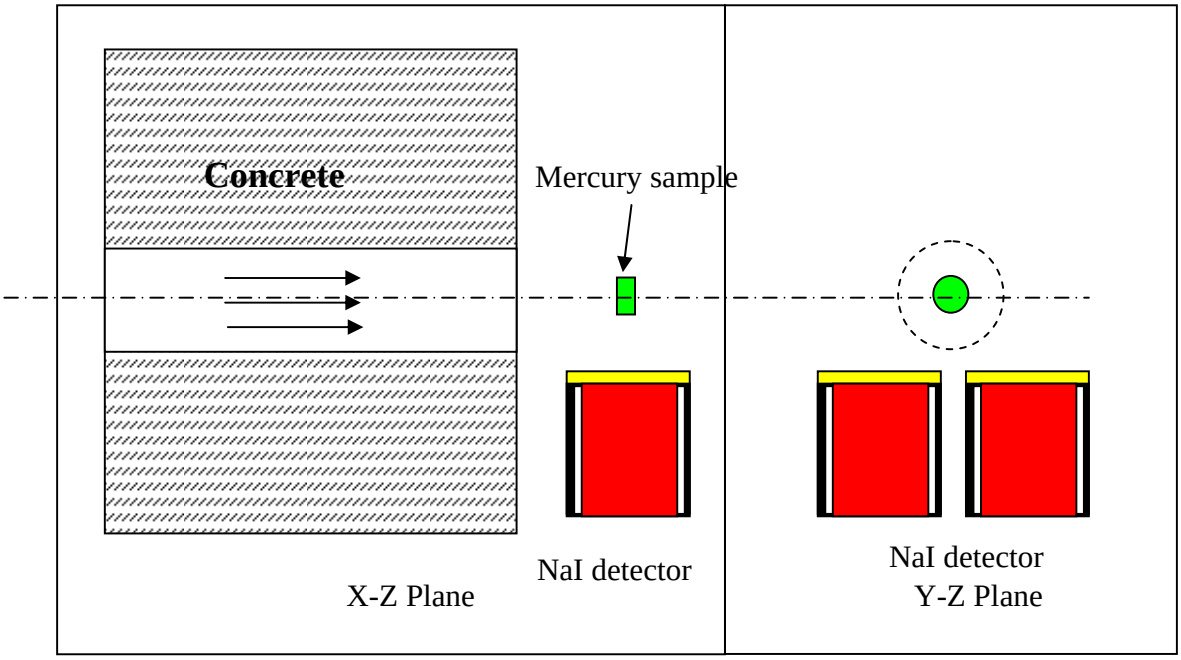

Figure 4- 29 The schematic of mercury experiment

Table 4- 5 Basic information of natural mercury

Isotope	Abundance(%)	σ_γ^Z (b)	Nγ	Factor (abundance*σ)	Normalized factor(%)
Hg-196	0.15	3190	10	478.5	1.246808
Hg-198	9.97	2.0	3	19.94	0.051957
Hg-199	16.87	2150	425	36270.5	94.50857
Hg-200	23.10	60		1386	3.611444
Hg-201	13.10	5.7	97	74.67	0.194565
Hg-202	29.86	4.9		146.314	0.381244
Hg-204	6.87	0.43	13	2.9541	0.007697

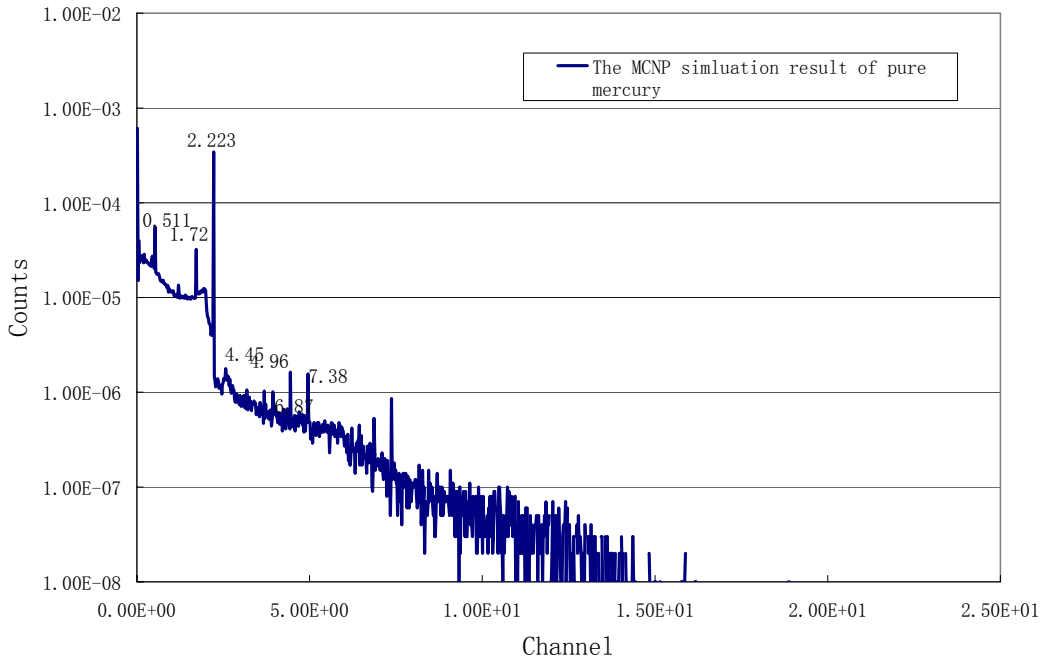

Figure 4- 30 The MCNP simulation result of pure mercury sample

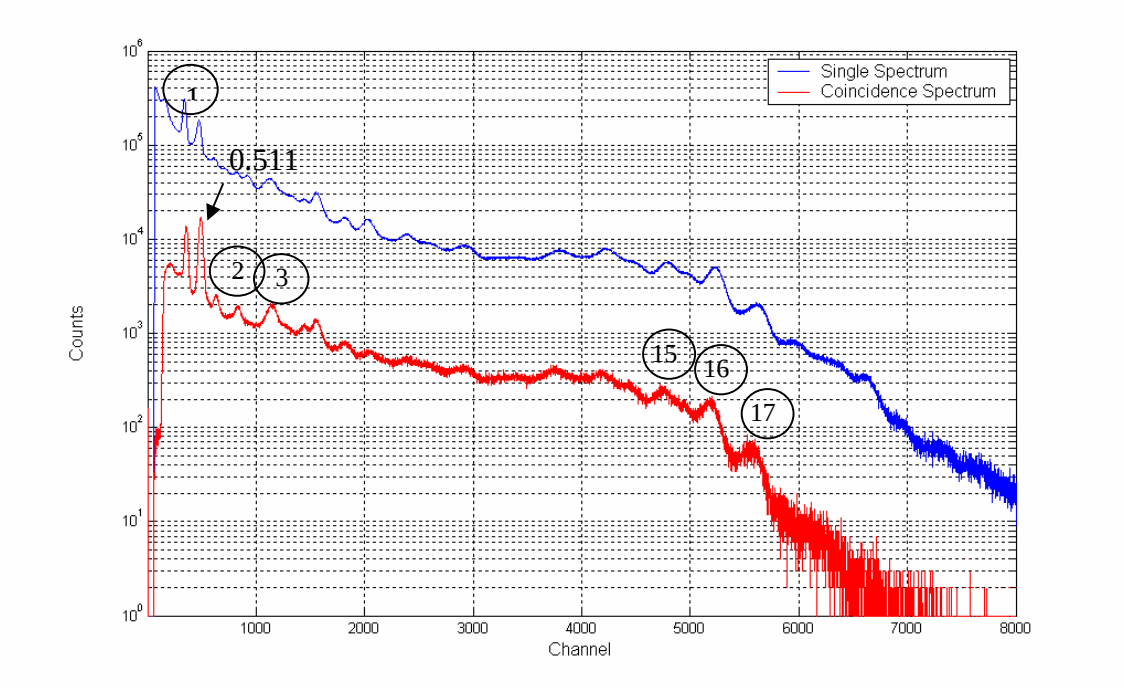

Figure 4- 31 The experimental spectra of pure mercury sample.
The peak index is accorded to the gamma rays in the table 4-6

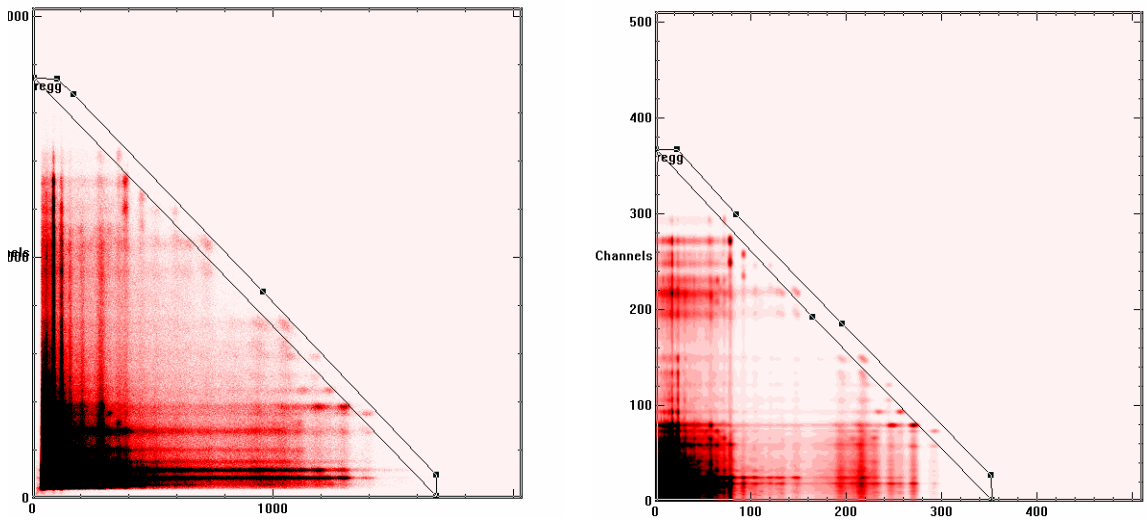

Figure 4- 32 The two-dimensional coincidence spectrum for pure mercury sample,
(a) is the experimental spectrum and (b) is the simulated spectrum

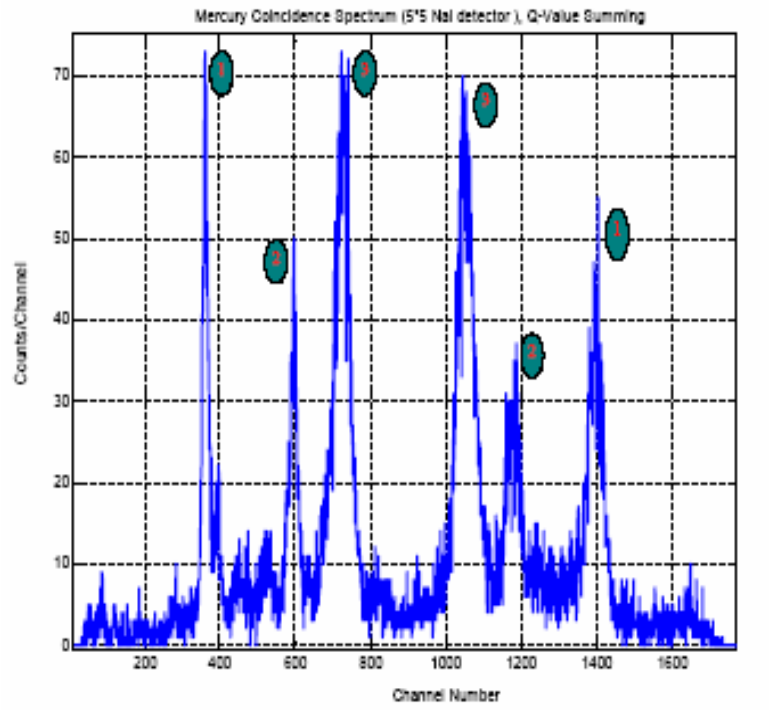

Figure 4- 33 The experimental Q-value projection spectrum of pure mercury sample

Table 4- 6 Energies adding up to 8.02 MEV in the ^{200}Hg activation decay

Pair #	Energy(MeV)
1	1.571 and 6.457
2	2.639 and 5.387
3	and 4.739 3.185 and 4.841

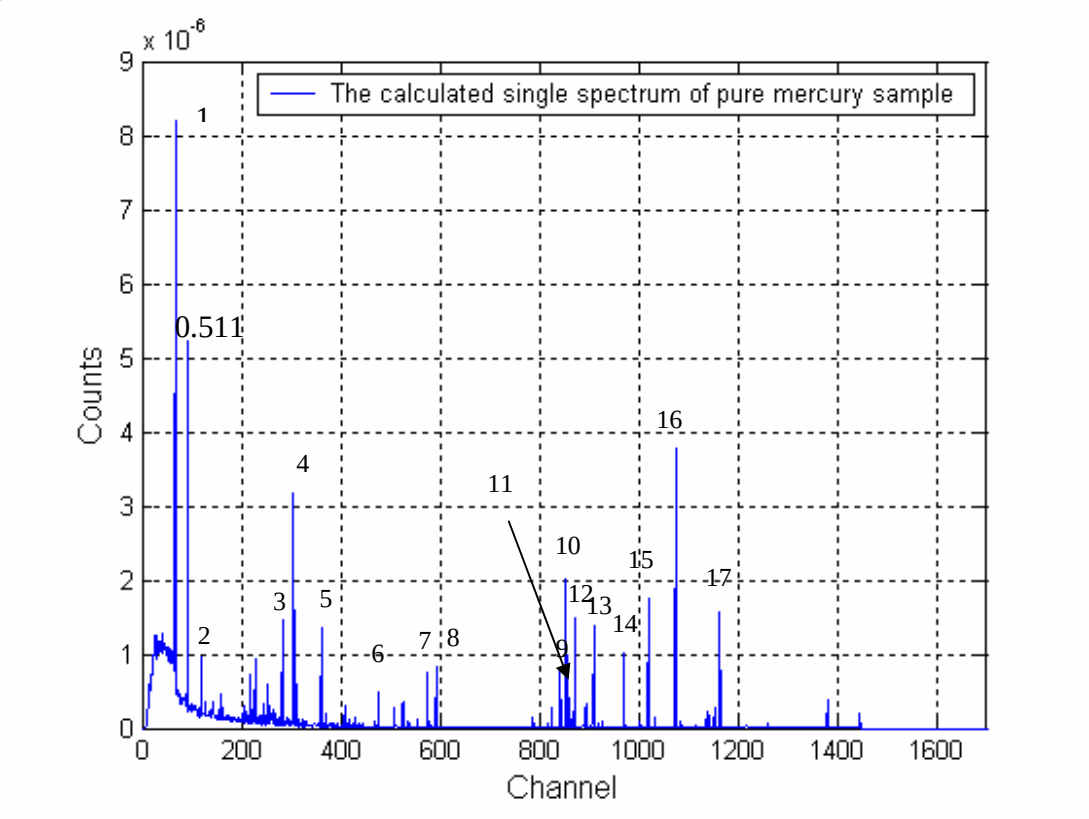

Figure 4- 34 The calculated single spectrum of pure mercury sample

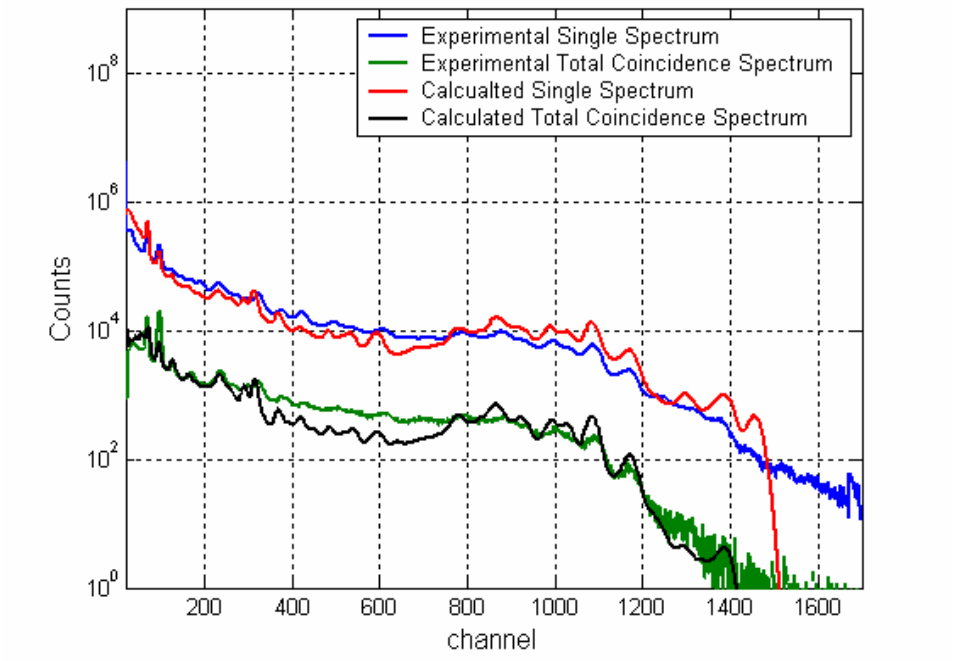

Figure 4- 35 The simulated spectra of pure mercury sample

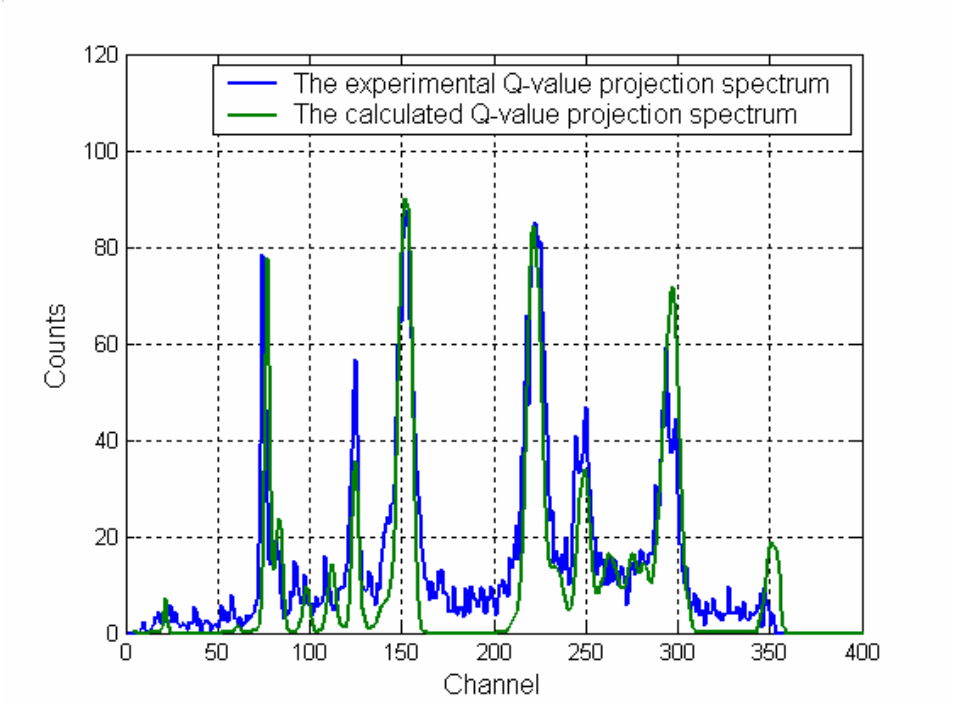

Figure 4- 36 The calculated Q-value projection spectrum of pure mercury

Table 4- 7 The major prompt gamma rays of mercury

#	Energy(MeV)	Relative Intensity	#	Energy(MeV)	Relative Intensity
1	0.367	3.79	10	4.739	0.455
2	0.661	0.337	11	4.759	0.187
3	1.570	0.447	12	4.842	0.302
4	1.693	0.849	13	5.050	0.302
5	2.002	0.367	14	5.388	0.264
6	2.639	0.175	15	5.658	0.415
7	3.186	0.171	16	5.967	0.944
8	3.288	0.201	17	6.457	0.349
10	4.675	0.196			

In general, the simulated Q-value projection spectrum matches the experimental spectrum better than the total coincidence spectrum and the single spectrum since the Q-value projection spectrum has better SNR (Signal-to-Noise Ratio) and little interference. This conclusion is also approved by the results of the pure sulfur sample.

5 Optimization of the Coincidence PGNAA Application

Coincidence PGNAA analysis is a newly developing technique for elemental analysis of bulk sample. The main disadvantage is that this method is time consuming due to the low coincidence counts rating. Since there is little study about quantitative analysis of the coincidence results, How to improve the analysis accuracy and speed up the coincidence measurement become the objectives of optimization. Since the diagonal projection spectrum has better characteristic over the single spectrum and the total coincidence spectrum, using the diagonal projection spectrum might be a possible way to improve the accuracy. How to select the best energy window to apply the diagonal projection should be the first task of the optimization. The second is how to optimize the physical experiment setup in order to get the “highest” coincidence measurement efficiency. As we know, the biggest disadvantage of the coincidence measurement is its low counting rate. Even the new electronic device have been developed rapidly in the past ten yeas, the low counting rate of the coincidence measurement is still the “bottle neck”.

5.1 Optimization for the energy window of diagonal projection

In order to optimize the energy window of diagonal projection, a mixture sample is assumed. The composition of assumed sample is listed in table 5-1. The interested element is mercury and sulfur since mercury is a toxic chemical element in the coal and sulfur can produce acid rain. From table 5-1 we can estimate that there are almost 92% prompt gamma rays from the thermal

neutrons interacting with mercury. Among the isotopes of mercury, there are almost 94% prompt gamma rays from ^{199}Hg. Figure 5-1 shows the coincidence library spectra and the total coincidence spectrum. Poisson noise is added in the total coincidence spectrum. The coincidence spectrum not only contains the coincidence gamma rays from the sample. But also contains the coincidence gamma-rays from the structure materials. The spectrum of structure materials is treated as “unknown” part since, in practice, there are always some unknown parts in the measurement spectrum. The simulated results also prove that the most of the gamma spectrum comes from the contribution of mercury. Several energy windows are used to get the different elemental library spectrum. Library Least-Square fitting will be done with these elemental coincidence library spectra. According the Table 5-1, the first window is outlined which energy covers from 8 – 11 MeV, which is plotted in figure 5-2, It contains the gamma –rays from elements Cl, Hg, S, Si, N and Al. although the Q value of Al is less than 8 MeV, there is still some counts from Al because of energy spreading. The projection elemental library spectra are plotted in figure 5-3. it is clear that the most important elements are Hg and Cl, which take nearly 99% out of all counts. The second attempt is that the energy of window is from 6 to 8 MeV. In this region, seven elemental libraries are included. They are Al, Cl, Hg, N, Na, S, and Si. The third window is applied with energy from 6 to 11 MeV. The number of elemental spectra is 7 and they as the same as the second case. The energy of the last window is from 0 to 11 MeV. All 9 elemental spectra are included. The information and MCLLS fitting results are listed in table 5-2.

Based on the Reduced Chi-Square and the fitting results, the best fitting results is the first one. This result is reasonable since there is little interference in the high-energy window. For gamma-rays measurement, most of interferences concentrate in the low-energy region. The high-energy window projection can get a good resolution spectrum and have fewer peaks. It already has been proved in the sulfur and mercury experiment.

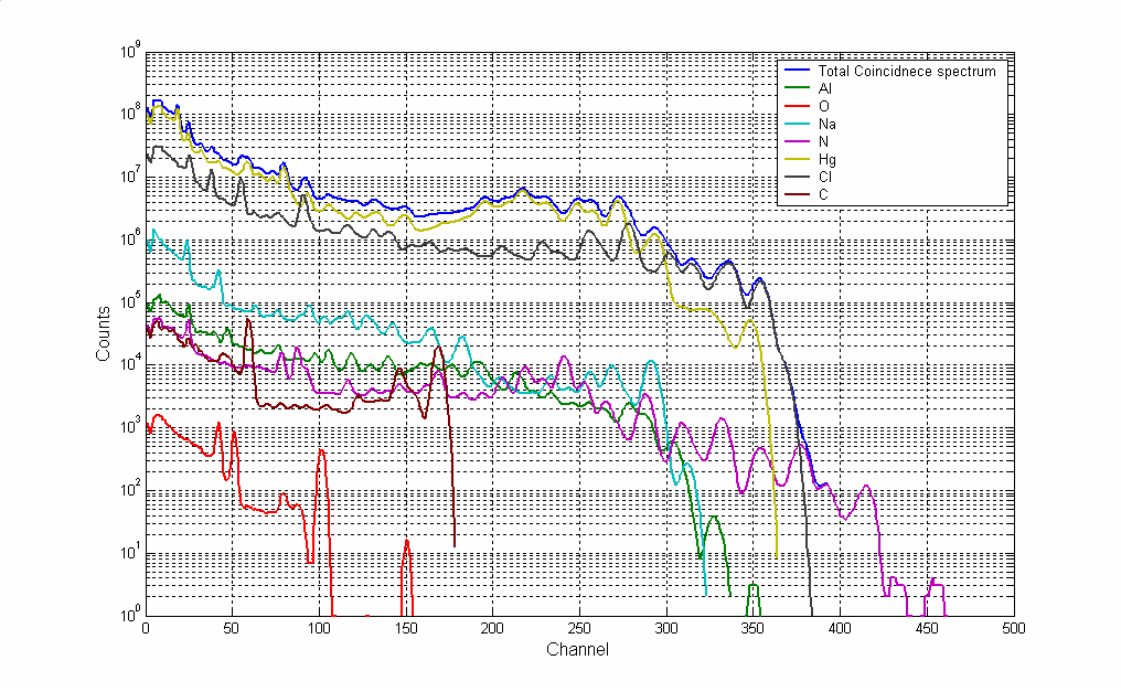

Figure 5- 1 The simulated spectra of mixture sample

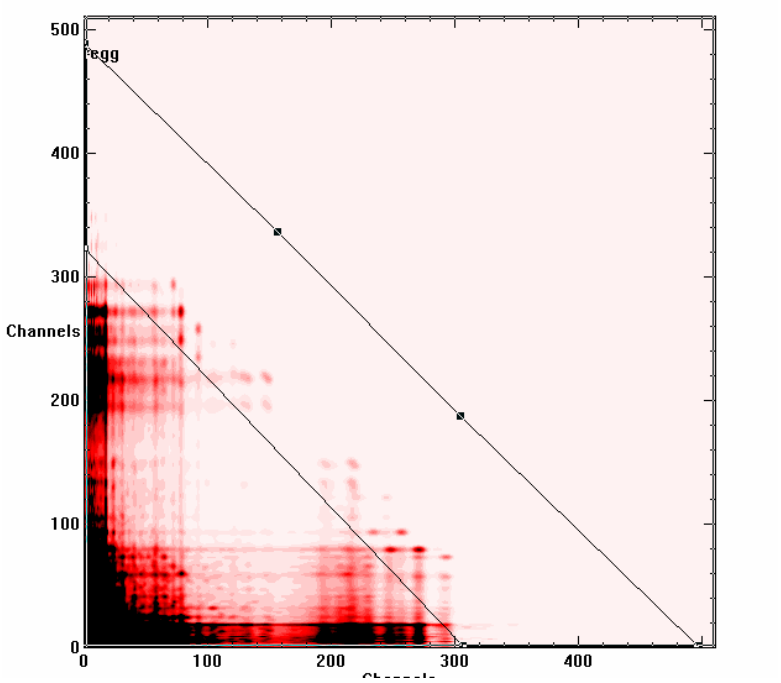

Figure 5- 2 The energy window is from 8-11 MeV

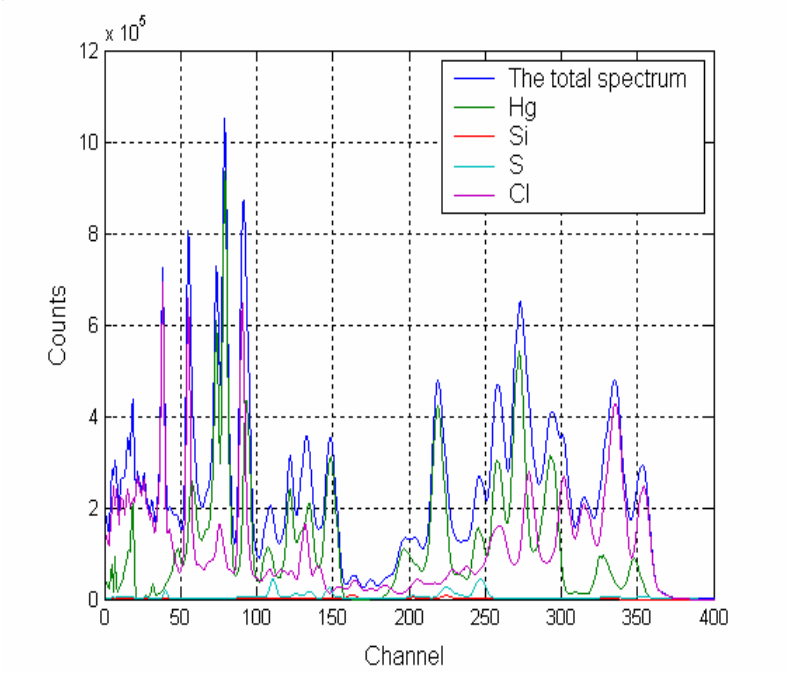

Figure 5- 3 The projection library spectra with window 8-11 MeV

Table 5- 1 Data of mixture sample

Elements		Q-value (MeV)	Thermal neutron cross section (b)	Weight fraction (%)	Factor	Normalized factor
Cl	Cl-35(75.78%)	8.579	43.5	1.729	33.068	7.90
	Cl-37(24.22%)	6.107	0.43			
Hg	Hg-196(0.15%)	6.785	3190	2.168	383.789	91.65
	Hg-198(9.97%)	6.664	2.0			
	Hg-199(16.87%)	8.028	2150			
	Hg-200(23.10%)	6.230	60			
	Hg-201(13.10%)	7.754	5.7			
	Hg-202(29.86%)	5.992	4.9			
	Hg-204(6.87%)	5.588	0.43			
Na		6.959	0.53	1.121	0.53	0.13
O		4.143	0.00019	5.487	0.00019	0.00
S		8.641	0.548	5.6	0.548	0.13
Si		8.473	0.177	1.943	0.177	0.04
H		2.224	0.3326	2.892	0.3326	0.08
C		4.946	0.00353	75.28	0.00353	0.00
N		10.833	0.0798	1.4	0.0798	0.02
Al		7.725	0.231	2.38	0.231	0.06

Table 5- 2 The fitting results of mixture sample with different windows

Window (MeV)	Reduced Chi-Square	Libraries	Fitting results	Relative error (%)
8-11	0.400024	Al	0.204682E+01	105
		Cl	0.101788E+01	1.7
		Hg	0.100831E+01	0.8
		N	0.157843E+01	57
		S	0.105871E+01	5.8
		Si	0.970995E+00	3
6-8	0.112989	Al	0.204054E+01	104
		Cl	0.101532E+01	1.5
		Hg	0.100200E+01	0.2
		N	0.190646E+01	90.1
		Na	0.861058E+00	13.9
		S	0.106766E+01	6.8
		Si	0.903131E+00	9.7
6-11	0.332224	Al	0.217254E+01	117
		Cl	0.101891E+01	1.9
		Hg	0.100127E+01	0.13
		N	0.157218E+01	57.2
		Na	0.793817E+00	20.6
		S	0.107016E+01	7.01
		Si	0.878273E+00	12.2
0-11	0.304072	Al	0.179594E+01	79.6
		C	0.375249E+01	275
		Cl	0.102086E+01	2.1
		Hg	0.999694E+00	0.1
		N	0.157241E+01	57.2
		Na	0.810371E+00	19
		O	-.357616E+02	
		S	0.101069E+01	1.1
		Si	0.851775E+00	14.2

5.2 Optimization of the coincidence PGNAA application

As mentioned previously, the biggest disadvantage of coincidence measurement is its low counting rate. One possible improvement is studied by using CEARCPG. The proposed schematic is plotted in figure 5-4. Six 3”X3” NaI detectors surround a 6”X6” central NaI detector. The surrounding NaI detectors will work as “Trigger”.

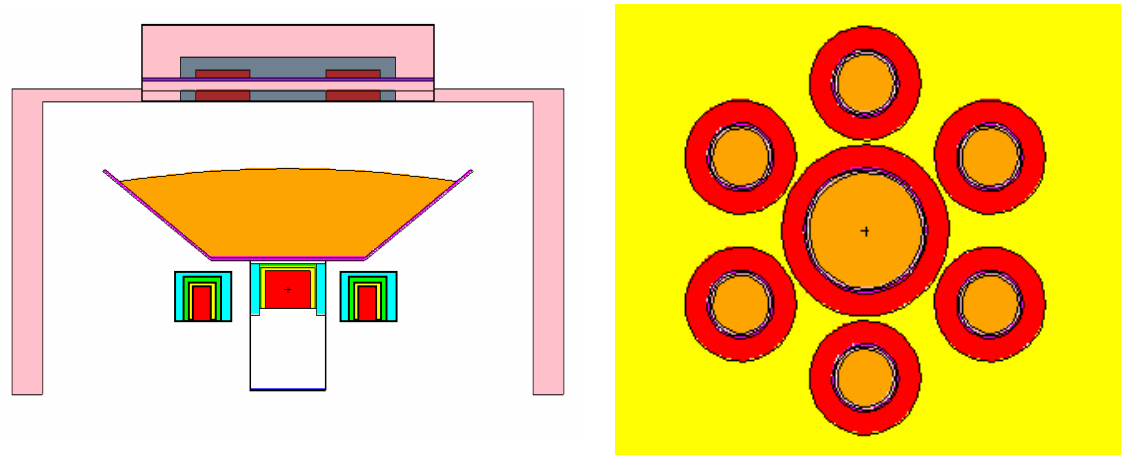

Figure 5- 4 The optimized coincidence PGNAA application

Sulfur sample is used to check the new geometry setup. The simulation results are plotted in Figure 5-5. The results of the old geometry which in presented in figure 4-17 is also plotted in figure 5-6. The total neutron history is 3E+05. The coincidence counts is 21378 and the simulation time is 32.8 hours by using P-IV Intel PC. The red numbers in figure indicate that the neutron distribution which penetrate through the sample and hit the detector directly. The dotted line indicates the position of sample and neutron source. It is obvious that the distribution of neutron should be symmetrical. For the old geometry setup, the total neutron history is 1E+06 and the simulation time is 28.4 hours. The coincidence counts are 22478. If the coincidence counts are normalized by neutron history, the efficiency of the new geometry is 3.23 times higher than the old geometry setup. The only expansion is computation time, which is 1.89 times higher than the computation of ole setup. But in practice, the new geometry setup can substantially increase the coincidence counting rate.

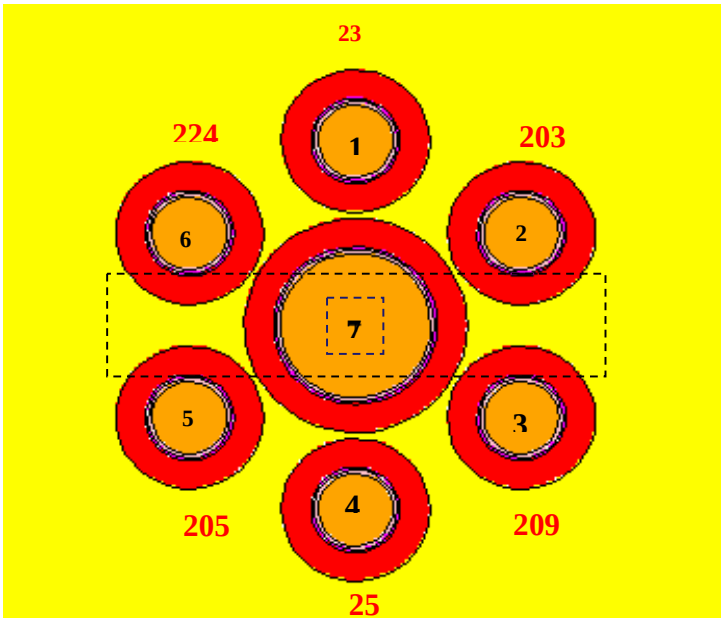

Figure 5- 5 Neutron distribution of the optimized coincidence PGNAA application

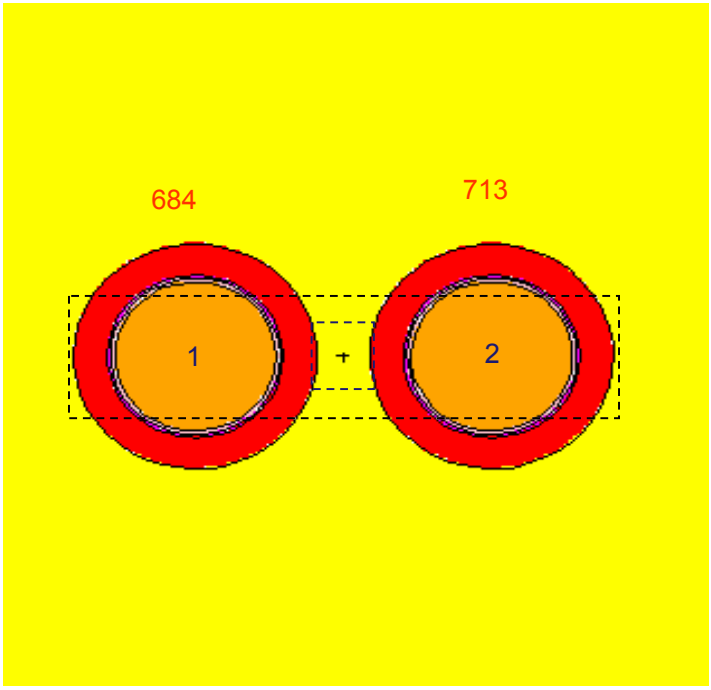

Figure 5- 6 Neutron distribution of the old coincidence PGNAA application

6 Conclusion and Discussion

CEARCPG is the first specific code that can be used to simulate the single/coincidence spectrum of coincidence PGNAA. This code is relatively complicated, which include the collection of nuclear data, evaluation of the nuclear data, investigations of neutron/photon physics, implementation of variance reduction techniques, benchmark experiments, data analysis, etc. CEARCPG is different from the CEARPGA I and CEARPGA II. Compared to code CEARPGA I, CEARCPG abandoned expected value splitting approach which plays important rules in CEARPGA I since it induced the big weight problem. Compared to code CEARPGA II, CEARCPG abandoned the analog linear interpolation approach which is the key point of code CEARPGA II since it also introduces error when applying the interpolation to get the true prompt gamma-rays spectra. These two codes can not be used to simulate the coincidence spectrum. Lots of improvement were done in CEARCPG, they are:

1) It is a new Monte Carlo code and is written with Fortran 95. Dynamic memory allocation technique and public memory allocation make it easy to regulate and update.
2) It is modularized. It makes the users easy to write their own patch or implement the module of CEARCPG into the other code.
3) CEARCPG gets rid of the pre-calculated gamma table and follows all the prompt gamma rays produced from neutron interaction. The mechanisms used to track the neutrons and photons in CEARCPG completely follow the

principles of nuclear physics. It proves that the simulation results of CEARCPG are more accurate and reliable.

4) It solves the problem to generate the gamma rays from neutron inelastic scattering reaction.
5) It can be used to simulate the single/coincidence spectrum of coincidence PGNAA.

Several cases are simulated by using CEARCPG. The simulation results are accurate versus the results of the benchmark experiments. The results of benchmark experiments also indicate that the coincidence PGNAA analysis can significantly remove the interference from the background, natural gamma-rays or the gamma-rays from the structural materials of PGNAA applications. For single spectra, two Monte Carlo codes were designed to generate the background spectrum, such as natural background spectra of ^{40}K, Uranium and Thorium, the activation spectrum from NaI detector and the decay spectrum of ^{128}I, ^{24}Na. All these background spectra are used in the library Least-Square fitting to help get more accurate fitting results.

With the two-dimensional coincidence spectrum, a new data analysis method, the diagonal projection, is checked in this work. The advantages of this approach include,

1) The projection spectrum has better resolution.
2) The high-energy diagonal projection can remove the interference from the other low Q-value element.
3) Increase the accuracy of analysis

Combining with the Monte Carlo Library Least-Square fitting approach, the simulated single and coincidence spectra are successfully used to quantitatively determine the sulfur concentration of the coal sample. (Table 4-2). The calculated results are accurate compared to the certified value.

A proposed optimized geometry is presented in this project. The simulation results show the optimized setup could improve the coincidence counts 3.23 times higher than the old coincidence PGNAA setup.

Two of advantages of CEARCPG need to be mentioned here. One is the input decks and the nuclear data library used in CEARCPG. Most of the input decks used in CEARCPG are the same as those used in MCNP. There is no difficulty for MCNP users to use this code. The other is CEARCPG can access the ENDF/ENSDF data library directly. It is convenient for users to update the nuclear data. The users only need to copy the newer nuclear data into the right directory

The most contributions of this ph.D work is a new algorithm is developed to sample the neutron-produced coincidence gamma-rays. Before this work, the commonly used method to generate prompt gamma rays in Monte Carlo codes, such as MCNP, was to sample the prompt gamma rays from the pre-calculated gamma-ray table for every photon-producing neutron interaction. By using this method, the information among the gamma rays is lost even we know the energy and intensity of each prompt gamma ray. The algorithm limits the existing Monte Carlo code to be extended to coincidence simulation. The algorithm developed in this thesis makes it possible to simulate the coincidence spectrum by using the

Monte Carlo method. Actually, this algorithm can also be extended to sample the decay gamma-rays of radioisotope produced during the PGNAA measurement.

There have some issues still needed to be discussed deeply. The first is the coincidence events which are caused by multiplicities of fission neutrons. Since there are more than one fission neutrons emitted per spontaneous fission, these fission neutron also can reduce the prompt gamma-ray to emit simultaneously. The second is the Rayleigh scattering (Coherent scattering) for low-energy photons. Theses two parts will be discussed as follows.

Coincidence events reduce by fission neutron

According the ENDF/B-VI data library, the average prompt fission neutron per spontaneous fission is 3.759 ± 0.0048, the average delay neutron per spontaneous fission is 0.0086 ± 0.0010 and the total average neutrons per spontaneous fission is 3.7676 ± 0.004. The neutron yield of ^{252}Cf is 2.31x10^{12} neutrons/(second∗gram). In order to estimate the coincidence events introduced by fission neutrons, one extremely case is assumed. In this case, 1 mg ^{252}Cf is used as neutron source. A simple geometry setup is assumed and plotted in the figure 6-1 and sample is sulfur. There are several assumptions about neutron. The neutrons are total thermalized before they enter the sample. It is assumed that the fission neutrons arrived at the sample at the same time. The typical resolving time of coincidence unit is 20ns which is the same as that used in experiments. The neutrons emission rate in the resolving time is 46.2. According to ENDF data library, the microscopic cross section of neutron in sulfur sample is 1.712 barn and atomic density is 3.91021X10^{-2}/(cm*barn). The mean free path

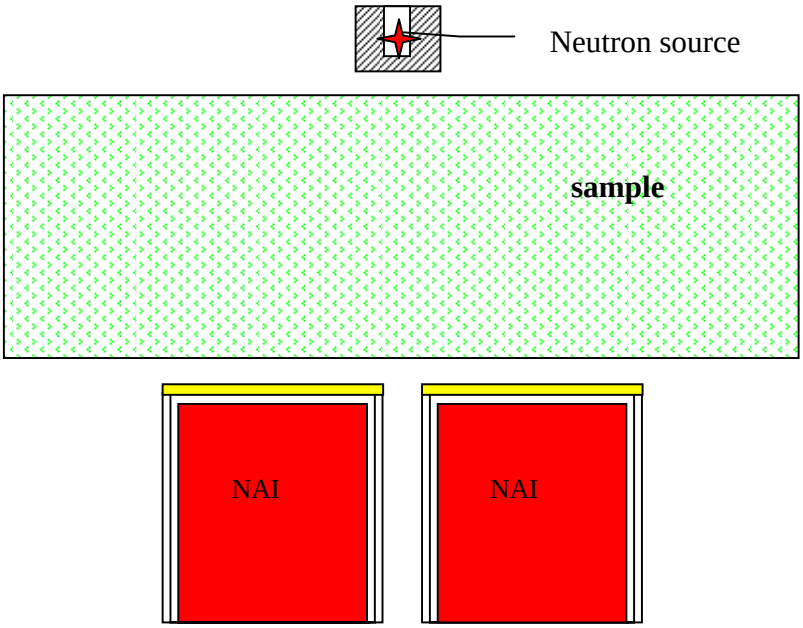

Figure 6- 1 The geometry setup used for estimation of neutron coincidence

($1/\Sigma_{Tot}$) of thermal neutrons (velocity=2200 m/s) in sulfur is 14.942 cm. The travel distance of thermal neutron in resolving time is $4.4X10^{-3}$ cm. Since the low velocity of thermal neutron, the travel distance of thermal neutron is enough to discriminate them in timing. The biggest chance for thermal neutrons to induce "false" coincidence events is two or more thermal neutrons interact at the "same location". The pdf of neutron flight distance is described by equation 2.8. At first, only two thermal neutrons are considered to interact at the "same location". Based on the equation 2.8, the probability for the first thermal neutron interact at flight distance *x* is

$$p(x) = \Sigma_{Tot} e^{-\Sigma_{Tot} x} \qquad (6.1)$$

Where Σ_{Tot} is the macroscopic cross section and *x* is the neutron flight distance. For the second thermal neutron, it must travel from x - Δx to x - Δx, where Δx is the thermal neutron travel distance in the resolving time, for thermal neutron, it is

$4.4X10^{-3}$ cm. since these two thermal neutrons are totally independent, the probability of the first thermal neutron interacted at location x with the second thermal neutron interacted from x - Δx to x - Δx can be calculated by using following equation.

$$p(x) = \Sigma_{Tot} e^{-\Sigma_{Tot} x} \cdot \int_{x-\Delta x}^{x+\Delta x} \Sigma_{Tot} e^{-\Sigma_{Tot} x'} dx' = \Sigma_{Tot} e^{-\Sigma_{Tot} x} (e^{-\Sigma_{Tot}(x-\Delta x)} - e^{-\Sigma_{Tot}(x+\Delta x)}) \quad (6.2)$$

The probability is a function of x. if let x be the mean free path the probability of two thermal neutrons interacted in the range [x - Δx, x + Δx] is $5.334X10^{-6}$. It proves that the “false” coincidence caused by neutron multiplicities can be ignored for coincidence PGNAA analysis. In the real, the interaction and scattering of neutron in the wax already detach the neutrons which are emitted simultaneously.

The probabilities of “false” coincidence event of the gamma-ray induce fast neutron inelastic scattering reaction also be estimated. The setup is the same as that described previously except the neutron source. The energy of neutron is 14 MeV. Extremely case is assumed. There is no any other interaction before the fast neutrons interact with sample. The microscopic cross section of sulfur for fast neutron is 1.952 barn and the mean free path is 13.103 cm. the velocity of fast neutron is $5.163X10^{7}$ m/s. the distance of fast neutrons traveling in the resolving time is 103.26 cm. The probability of the first thermal neutron interacted at location x with the second thermal neutron interacted from x - Δx to x - Δx calculated by using equation 6.2. For the mean free path, the probability is 0.028. it is needed to be pointed out, extreme case is estimated. In the real, we need to

consider the probability of neutron inelastic scattering reaction, which is around 50 % out of the total cross section for 14 MeV fast neutrons. Multiple scattering or interaction might be occurred before the fast neutrons interact with sample. The detection efficiency of gamma-ray also needs to be taken into account. All these effect might decrease the probabilities two or three order. In general, the “false” coincidence events reduced by the neutron multiplicities can be ignored in the measurement. Actually, there is no “false” coincidence peaks observed in the experimental measurement.

7 Future Work

There are two main work needed to done in the future. One is to implement the differential operator into CEARCPG. The differential operator is a powerful tool for the measurement sensitivity study and the system optimization. This technique has already been implemented into another Monte Carlo code developed at CEAR which can be used to study the X-ray fluorescence analysis (Guo, 2004). The results show this technique is useful and accurate.

The basic idea of differential operator is that a measured spectrum of an unknown sample can be described in a Taylor series expansion with zeroth, first and second order derivatives calculated at reference state (or composition). These differential responses can be used to re-adjust the calculated library spectra if there have some big difference between the initial guess and the true value of unknown sample. Unlike the X-ray, for PGNAA analysis, the measured unknown sample spectra not only contain the photon contributions, but also have the contributions of neutron. In general, the algorithm used in EDXRF can not be used in PGNAA analysis directly, a new algorithm to implement the differential operator is need to be investigated.

Currently, CEARCPG can not be used to simulate the decay gamma-ray of radioisotopes. Actually, ENSDF nuclear data library already have the information of decay gamma-rays of radioisotope. The algorithm used to sample the prompt gamma-ray also can be used to sample the decay gamma-ray of radioisotope. Figure 7-1 shows the ENSDF file of ^{28}Al. From ENSDF file, we can get the following information, such as the decay mode of radioisotopes, level structure

information of decay gamma-ray, intensities of decay gamma-ray. This feature will be implemented into CEARCPG in the future.

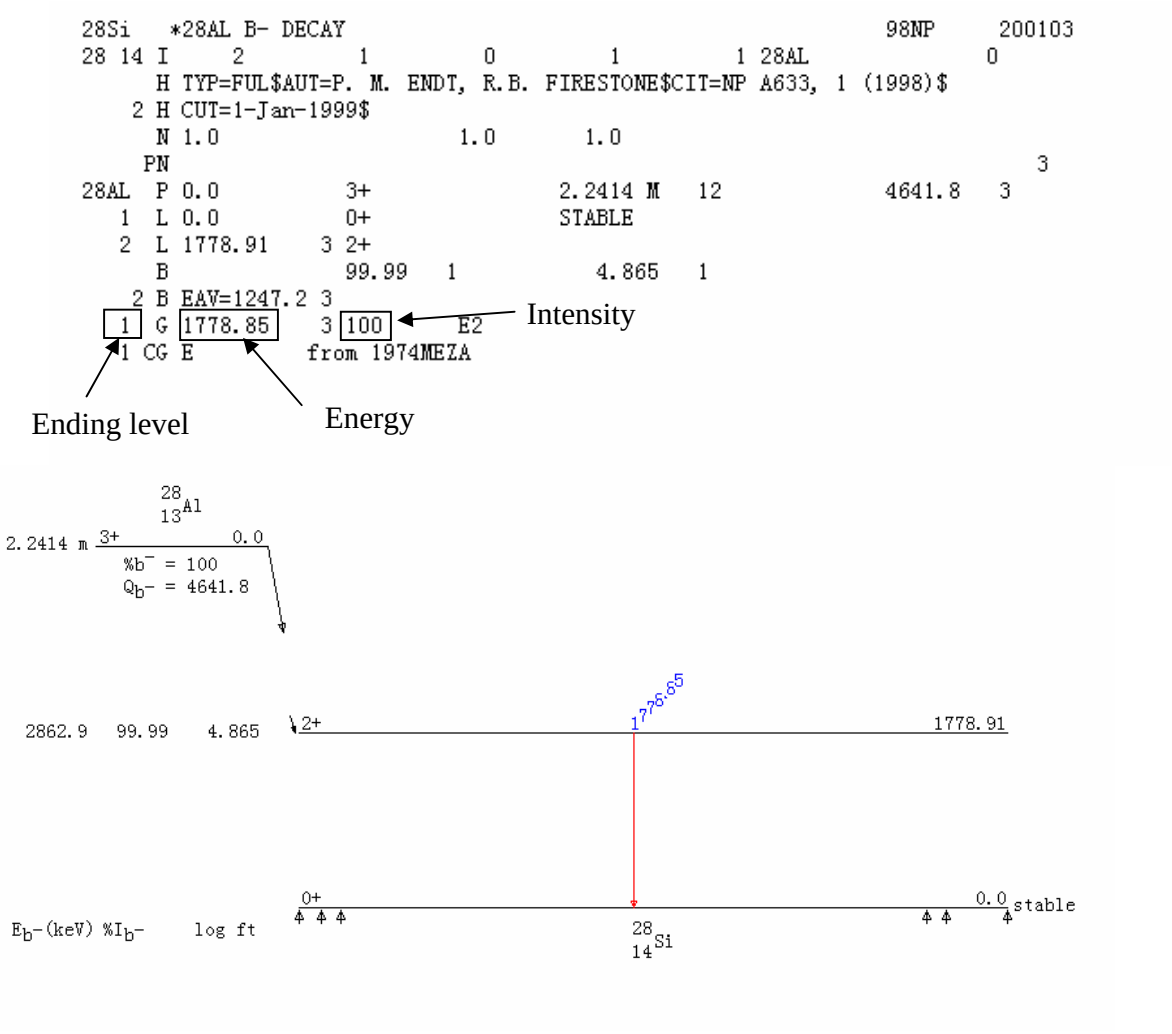

Figure 7- 1 The ENSDF file of decay gamma-ray of ^{28}Al

General-purpose Monte Carlo code MCNP is widely used and has more complicated and detailed considerations of neutron/photon/electron transportation. Another advantage is that MCNP is a public and source free software. There are lots of MCNP users on global, and they can help to benchmark the code. Challenge is how to implement the algorithm into MCNP. Right now, pre-calculated gamma-rays tables are used in MCNP to generate the

neutron-induced prompt gamma-rays. If this new algorithm is going to be integrated into MCNP, the ENSDF nuclear structure data should be evaluated carefully. Fortunately, there was a CRP project about database development of prompt gamma-ray neutron activation analysis which was proposed by IAEA in Oct. 1998. This project can provide the necessary nuclear data for this implementation. Another improvement of MCNP is to modify the tally part of MCNP, so each elemental library spectrum can be tallied directly by using MCNP.

Reference

Arinc, F., Gardner, R. P., Wielopolski, L., and Stiles, A. R. (1975). "Applications of the least-squares method to the analysis of XRF spectral intensities from atmospheric particulates collected on filters." Advances in X-ray Analysis, 19, pp. 367-380.

Bertin, E. P. (1978). Introduction to X-ray spectrometric analysis, Plenum Press, New York.

Brookhaven National Laboratory, Evaluated Nuclear Structure Data File (ENSDF) http://www.nndc.bnl.gov/ensdf/ (2005)

Carter, L..L.., and Cashwell E.D., 1975. Particle-Transport Simulation with the Monte Carlo Method, Energy Research and Development Administration Critical Review Series, TID-26607, U.S. Department of Energy Chemistry, 40, pp. 1080-1086.

Clark, T. C., Gardner, R. P., and Verghese, K., 1982. A Monte Carlo Model for In-Situ Prompt Gamma-Ray Analysis Probs, Nucl. Instru. Methods, 193, 365, (1982).

Criss, J. W., and Birks, L. S. (1968). "Calculation Methods for Fluorescence X-Ray

Duffy, D., Cox, S.A., Heraenberg, C.L., N.M., Fallon, O., and Wiggins, P.F. , Coal Analytical Assembly Using Catpure Gamma Rays From Accelerator

Ehmann, W.D., Vance, D.E., 1991. Radiochemistry and Nuclear Methods of Analysis. Wiley-Interscience, New York, pp. 302-303 (Chapter 9.6.4).

Ember, P., Belgya, J. L. and Molnar, G. L., Improvement of the capabilities of PGAA by coincidence techniques, Applied Radiation and Isotopes, Volume 56, Issue 3, March 2002, Pages 535-541.

Ember, P., Belgya, T., Weil, J. L. and Molnar, G. L., A practical test of a - coincidence measurement setup for PGAA , Nuclear Instruments and Methods in Physics Research Section B: Beam Interactions with Materials and Atoms, Volume 213, January 2004, Pages 406-409

Ember, P., Belgya, T., Weil, J. L. and Molnar, G. L., Coincidence measurement setup for PGAA and nuclear structure studies, Applied Radiation and Isotopes, Volume 57, Issue 4, October 2002, Pages 573-577

ENDF - 6, revised April 2001, BNL-NCS-44945-01/04-Rev. National Nuclear Data Center, Brookhaven National Laboratory, Upton, N.Y. 11973-5000

Firestone, Richard B., Table of Isotopes, Eighth Edition, 2001

Fluorescence." British Journal of Applied Physics, 3, pp. 358.

Gardner, R. P., 2000. A Report on the Contract: Software Design for a PGNAA Coal Analyzer Prototype, North Carolina State University.

Gardner, R. P., 2002. A Monte Carlo Simulation Approach for Generating NaI Detector Response Functions (DRF's) that Accounts for Nonlinearity and Variable Flat Continua, A Report to Sabia, Inc, North Carolina State University.

Gardner, R. P., Mayo, C. W., El-Sayyed, E. S., Metwally, Zheng, W. A., Y. and Poezart, M., A feasibility study of a coincidence counting approach for PGNAA applications, Applied Radiation and Isotopes, Volume 53, Issues 4-5, 15 November 2000, Pages 515-526

Gardner, R.P., Sood, A., Wang, Y. Y., Liu, L., Guo, P.J., and Cehrek, R. J., Single Peak Versus Library Least-Squares Analysis Method for PGNAA Analysis of Vitrified Waste. Appl. Radiat. Isot. Vol. 48, No. 10-12, pp. 1331-1335, 1997

Gardner, R.P.. A Report on the Contract: Software Design for a PGNAA Coal Analyzer Prototype, North Carolina State University. 2000 Radioisotopes, Department of Nuclear Engineering, North Carolina State University.

Gardner, Robin P., A Monte Carlo Simulation Approach for Generating NaI Detector Response Function(DRF's) that Accounts for Nonlinearity and Variable Flat Continua. A report to Sabia. Inc. North Carolina State University 2002.

Gardner, Robin P., El-Sayyed, Zheng, Yuanshui, Hayden, Stephanie and Mayo, Charles W., NaI detector neutron activation spectra for PGNAA applications, Applied Radiation and Isotopes, Volume 53, Issues 4-5, 15 November 2000, Pages 483-497

Gillam, E., and Heal, H. T. (1952). "Some Problems in the Analysis of Steels by X-ray

Gozani, T., Bozorgmanesh, H., Brown, D., Elias, E., Maung, T., and Reynolds, G., Coal Elemental Analysis by Prompt-Neutron Activation Analysis

Gozani, T., Elias, E., Orphan, V., Reed, J., and Shreve, D., Prompt - Neutron Activation Analysis - Applications to Coal Analysis, Trans. Am. Nucl. Soc. 26, 160, (1977)

Green, L., Mitchell, J. A., and Steen, N.M., 1973. The Californium - 252 Fission Neutron Spectrum from 0.5 to 13 MeV

Guo, P., 1997. CEARPGA User's Guide, Center for Engineering Application of Radioisotopes

Guo, Weijun, Ph.D thesis, North Carolina State University. 2004

IAEA Database for Prompt Gamma-ray Neutron Activation Analysis, http://www-nds.iaea.org/pgaa (2005)

Jakubek, J., Nuiten, P., Pluhar, J.,Popsil, S., Sinor, M., Stekl, I., Timorack!y, S., Vobeck!y, M., 1998. Coindence gammagamma spectroscopy system for instrumental neutron activation analysis. Nucl. Instrum. Methods A 414, 261-264.

Jenkins, R. (1988). X-ray fluorescence spectrometry, J. Wiley, New York.

Kim, J.I. and Hoste, J.. Non-destructive Neutron Activation Determination of Silver and Antimony in Bismuth by gamma-gamma Coincidence Spectrometry, Analytica. Chimica. Acta 33 (1965) 449-458

Kim, J.I. Speecke and Hoste, J., Neutron Activation Analysis of Copper in Bismuth by gamma-gamma Coincidence Measurement. Analytica Chimica Acta 33(1965) 123-130

Koeberl, Ch., Huber, H., 2000. Optimalization of the multiparameter g-g coincidence spectrometry for the determination of iridium geological materials. J. Radioanal. Nucl. Chem 244, 655-660.

Lux, Ivan and Koblinger, Laszlo, Monte Carlo Particle Transport Methods: Neutron and Photon Calculations, CRC Press, Boca Raton (1991)

Marshall , J.H. III and Zumberge, J.F., on-line Measurements of Bulk Coal Using Prompt Gamma Neutron Activation Analysis, nucl. Geophys. 3(4), 445, (1989)

Metwally, Walid A., Ph.D thesis, North Carolina State University, 2003

Metwally, W. A., Gardner, R. P. and Mayo, C. W., Two-dimensional diagonal summing of coincidence spectra for bulk PGNAA applications , Nuclear Instruments and Methods in Physics Research Section A: Accelerators, Spectrometers, Detectors and Associated Equipment, Volume 525, Issue 3, 11 June 2004, Pages 511-517

Metwally, Walid A., Gardner, Robin P. and Mayo, Charles W., Elemental PGNAA analysis using gamma-gamma coincidence counting with the library least-squares approach, Nuclear Instruments and Methods in Physics Research Section B: Beam Interactions with Materials and Atoms, Volume 213, January 2004, Pages 394-399

Metwally, Walid A., Gardner, Robin P., Mayo, Charles W., Elemental PGNAA analysis using gamma-gamma coincidence counting with the library least-squares approach, Nucl. Instru. Methods, B, In press, 2004

Metwally, Walid A., Gardner, Robin. P., Mayo, Charles W., Elemental PGNAA analysis using gamma-gamma coincidence counting with the library least-squares approach. Nuclear Instrument and Methods in Physics Research B 213 (2004) 394-399.

Meyer, G., Piccot, S., Rocchia, R., Toutain, J.P.J., 1993. Simultaneous determination of Ir and Se in K-T boundary clays and volcanic sublimates. Radioanal. Nucl. Chem. 168, 125-131

Meyer, G., Piccot, S., Rocchia, R., Toutain, J.P.J., 1993. Simultaneous determination of Ir and Se in K-T boundary clays and volcanic sublimates. Radioanal. Nucl. Chem. 168, 125-131.

Meyer, G.J., 1987. Multiparameter coincidence spectrometry applied to the instrumental activation analysis of rocks and minerals. Radioanal. Nucl. Chem. 114, 223-230

Mickael , M., Gardner, Robin P. and Verghese, K., McDNL: A new Specific Purpose Monte Carlo Code for Simulation of Dual Spaced Neutron Porosity Logd. SPWLA 29th Annual logging Symposium, San Antonio, TX, June 1988

Mickael M., Gardner R. P., and Verghese K., 1988. McDNL: A New Specific Purpose Monte Carlo Code for Simulation of Dual Spaced Neutron Porosity Logs, SPWLA 29th Annual logging Symposium, San Antonio, TX, June 1988.

Molnar, G., Lindstrom, R.M., 1998. Nuclear Methods in Mineralogy and Geology, Plenum Press, New York, London, pp. 145-164 (Chapter 3).

Molnar, G.L., Risvay, Zs., Veres, A., Simonits, A., Rausch, H.,1993. Cold neutron facility for prompt gamma neutron activation analysis. J. Radioanal. Nucl. Chem. 167, 133-137.

National Nuclear Data Center, Brookhaven National Laboratory, ENDF-102 DATA FORMATS AND PROCEDURES FOR THE EVALUATED NUCLEAR DATA FILE ENDF-6, April 2001

Peplow, D.E., Gardner, R.P., Verghese, K., 1994. Sodium Iodide Detector Response Functions Using Simplified Monte Carlo Simulation and Principal Components, Nuclear Geophysics, Vol. 8, No. 3, pp. 243-259.

Perry, D. L., Firestone, R. B., Molnar , G. L., Kasztovszky, Zs., Rlvay, Zs. , Belgya, T., PGAA investigation of mineral deposits from deep sea vents on the Pacific floor, BNC Experimental Report, 20.12.1999

Reynolds, G. , Bozorgmanesh, H., Elias, E. , Gozani, T. , Maung, T. , and Orphan, V., Nuclear Assay of Coal- Volume I, Coal Composition by Prompt Neutron Activation Analysis - Basic Experiment, Report EPRI EP-989, Vol. 1 (1979)

Shyu C. 1991 . Development of Monte Carlo Library Least-Square Method of Analysis for Neutron Capture Prompt Gamma Ray Analyzer. Ph.D thesis, North Carolina State University.

Shyu C. M., Gardner R. P. and Verghese K. (1993) Development of the Monte Carlo library least-squares method of analysis for neutron capture prompt gamma-ray analysers. Nuclear Geophysics 7(2), 241-268.

Shyu, C., 1991. Development of the Monte Carlo - Library Least-Squares Method of Analysis for Neutron Capture Prompt Gamma-Ray Analyzer, PhD Dissertation, North Carolina State University.

Shyu, C.M., Gardner, R.P., Verghese , K.. Nuclear Geophys. 7 (2) 1993 241

Shyu, C.M., He, T., Verghese, K. and Gardner, R.P. (1988) Monte Carlo-library least-squares principle for nuclear analysers. Transactions of the American Nuclear Society, Suppl. 3, 56, 4446.

Sparrow Corporation, multi-parameter data acquisition and instrument control software KMAX, http://www.sparrowcorp.com/

Valentine, Timothy E., Evaluation of prompt fission gamma rays for use in simulation nuclear safeguard measurement. Annals of Nuclear Energy 28 (2001) 191-201.

Verbinski, V. V., Weber, Hans, and Sund, R. E., Prompt Gamma Rays from 236U(n,f), 239Pu(n,f) , and spontaneous fission of 252Cf. Physics Review C, Volume 7, number 3, March 1973

Wapstra, A.H., 1979. Alpha-, Beta- and Gamma-ray Spectroscopy, 5h Edition, North-Holland Publishing Company, Amsterdam, New York, Oxford, Vol. I, pp. 539-555 Chapter VIII/C). .P. Ember et al. / Applied Radiation and Isotopes 56 (2002) 535-541 541.

Wapstra, A.H., 1979. Alpha-, Beta- and Gamma-ray Spectroscopy,5th Edition, North-Holland Publishing Company, Amsterdam, New York, Oxford, Vol.1 pp 539-555 (Chapter VIII/C)

Zhang, Wenchao, Gardner, Robin P.. The analog linear interpolation approach for Monte Carlo simulation of PGNAA : The CEARPGA code. Nuclear Instruments and Methods in physics Research B. 213 (2004) 116-123

Zhang, Wenchao, The analog Linear Interpolation Approach for Monte Carlo Simulation of Prompt Gamma-Ray Neutron Activation Analysis, Ph.D Thesis, North Carolina State University, 2003

Zhou, Chunmei, Prompt gamma-ray Data Evaluation of Thermal- Neutron Capture. China Nuclear data Center, 1999

Appendix A: The ENDF files in CEARCPG

ISOTOPE	NEUTRON_CS LIB	ISOTOPE	NEUTRON_CS LIB
1001.	ENDF/B-VI 300K	29063.	ENDF/B-VI 300K
2004.	ENDF/B-VI 300K	29065.	ENDF/B-VI 300K
3006.	ENDF/B-VI 300K	30064.	JENDL-3 300K
3007.	ENDF/B-VI 300K	30066.	ENDF/B-VI 300K
4009.	ENDF/B-VI 300K (No inelastic CS)	30067.	ENDF/B-VI 300K
5010.	ENDF/B-VI 300K	30068.	ENDF/B-VI 300K
5011.	ENDF/B-VI 300K	31069.	JENDL-3 300K
6012.	ENDF/B-VI 300K	31071.	JENDL-3 300K
7014.	ENDF/B-VI 300K	32070.	JENDL-3 300K
8016.	ENDF/B-VI 300K	32072.	ENDF/B-VI 300K
9019.	ENDF/B-VI 300K	32073.	ENDF/B-VI 300K
11023.	ENDF/B-VI 300K	32074.	ENDF/B-VI 300K
12024.	ENDF/B-VI 300K	32076.	ENDF/B-VI 300K
12025.	JENDL-3 300K	40090.	ENDF/B-VI 300K
12026.	JENDL-3 300K	40091.	ENDF/B-VI 300K
13027.	ENDF/B-VI 300K	40092.	ENDF/B-VI 300K
14028.	ENDF/B-VI 300K	40094.	ENDF/B-VI 300K
14029.	ENDF/B-VI 300K	40096.	ENDF/B-VI 300K
14030.	ENDF/B-VI 300K	41093.	ENDF/B-VI 300K
15031.	ENDF/B-VI 300K	42092.	ENDF/B-VI 300K
16032.	ENDF/B-VI 300K	42094.	ENDF/B-VI 300K
16034.	JENDL-3 300K	42095.	ENDF/B-VI 300K
17035.	ENDF/B-VI 300K	42096.	ENDF/B-VI 300K
17037.	ENDF/B-VI 300K	42097.	ENDF/B-VI 300K
19039.	JENDL-3 300K	42098.	ENDF/B-VI 300K
19041.	ENDF/B-VI 300K	42100.	ENDF/B-VI 300K
20040.	JENDL-3 300K	45103.	ENDF/B-VI 300K
20044.	JENDL-3 300K	48106.	ENDF/B-VI 300K
22046.	ENDF/B-VI 300K	48110.	ENDF/B-VI 300K
22047.	ENDF/B-VI 300K	48111.	ENDF/B-VI 300K
22048.	ENDF/B-VI 300K	48112.	ENDF/B-VI 300K
22049.	JENDL-3 300K	48113.	ENDF/B-VI 300K
22050.	ENDF/B-VI 300K	48114.	ENDF/B-VI 300K
23051.	ENDF/B-VI 300K	48116.	ENDF/B-VI 300K
24050.	ENDF/B-VI 300K	56134.	ENDF/B-VI 300K
24052.	ENDF/B-VI 300K	56135.	ENDF/B-VI 300K
24053.	ENDF/B-VI 300K	56136.	ENDF/B-VI 300K
24054.	ENDF/B-VI 300K	56137.	ENDF/B-VI 300K
25055.	ENDF/B-VI 300K	56138.	ENDF/B-VI 300K

26054.	ENDF/B-VI 300K	63151.	ENDF/B-VI 300K
26056.	ENDF/B-VI 300K	63153.	ENDF/B-VI 300K
26057.	ENDF/B-VI 300K	73181.	ENDF/B-VI 300K
27059.	ENDF/B-VI 300K	74182.	ENDF/B-VI 300K
28058.	ENDF/B-VI 300K	74183.	ENDF/B-VI 300K
28060.	ENDF/B-VI 300K	74184.	ENDF/B-VI 300K
28061.	ENDF/B-VI 300K	74186.	ENDF/B-VI 300K
28062.	ENDF/B-VI 300K	79197.	ENDF/B-VI 300K
82206.	ENDF/B-VI 300K	83209.	ENDF/B-VI 300K
82207.	ENDF/B-VI 300K		
82208.	ENDF/B-VI 300K		

The data format is ZZAAA

Appendix B: ENSDF files in CEARCPG

Element	Z	Isotopes	#
H	1	^{1}H(99.985)	1
He	2	^{4}He(100)	1
Li	3	^{6}Li(7.5) ^{7}Li(92.5)	2
Be	1	^{9}Be(100)	1
B	5	^{10}B(19.9) ^{11}B(80.1)	2
C	6	^{12}C(98.9) ^{13}C(1.10)	2
N	7	^{14}N(99.63)	1
O	8	^{16}O(99.76)	1
F	9	^{19}F	1
Na	11	^{23}Na(100)	1
Mg	12	^{24}Mg(78.99) ^{25}Mg(10.00) ^{26}Mg(11.01)	3
Al	13	^{27}Al(100)	1
Si	14	^{28}Si(92.23) ^{29}Si(4.67) ^{30}Si(3.10)	3
P	15	^{31}P(100)	1
S	16	^{32}S(95.02) ^{33}S(4.21)	2
Cl	17	^{35}Cl(75.77) ^{37}Cl(24.23)	2
K	19	^{39}K(93.2581) ^{41}K(6.7302)	2
Ca	20	^{40}Ca(96.941) ^{44}Ca(2.086)	2
Ti	22	^{46}Ti(8) ^{47}Ti(7.3) ^{48}Ti(73.8) ^{49}Ti(5.5) ^{50}Ti(5.4)	5
V	23	^{51}V(100)	1
Cr	24	^{50}Cr(4.345) ^{52}Cr(83.79) ^{53}Cr(9.50) ^{54}Cr(2.365)	4
Mn	25	^{55}Mn(100)	1
Fe	26	^{54}Fe(5.9) ^{56}Fe(91.72) ^{57}Fe(2.1)	3
Co	27	^{59}Co(100)	1
Ni	28	^{58}Ni(68.077) ^{60}Ni(26.223) ^{61}Ni(1.140) ^{62}Ni(3.634)	4
Cu	29	^{63}Cu(69.17) ^{65}Cu(30.83)	2
Zn	30	^{64}Zn(48.6) ^{66}Zn(27.9) ^{67}Zn(4.1) ^{68}Zn(18.8)	4
Ga	31	^{69}Ga(60.108) ^{71}Ga(39.892)	
Ge	32	^{70}Ge(21.23)^{72}Ge(27.66)^{73}Ge(7.73)^{74}Ge(35.94) ^{76}Ge(7.44)	5
Zr	40	^{90}Zr(51.45) ^{91}Zr(11.22) ^{92}Zr(17.15) ^{94}Zr(17.38) ^{96}Zr(2.8)	5
Nb	41	^{93}Nb(100)	1
Mo	42	^{92}Mo(14.84) ^{94}Mo(9.25) ^{95}Mo(15.92) ^{96}Mo(16.68) ^{97}Mo(9.55) ^{98}Mo(24.13) ^{100}Mo(9.63)	7
Rh	45	^{103}Rh(100)	1
Cd	48	^{106}Cd(1.25) ^{110}Cd(12.49) ^{111}Cd(12.80) ^{112}Cd(24.13) ^{113}Cd(12.22) ^{114}Cd(28.73) ^{116}Cd(7.49)	7
I	53	^{127}I(100)	1
Ba	56	^{134}Ba(2.42) ^{135}Ba(6.593) ^{136}Ba(7.85) ^{137}Ba(11.23)	5

		^{138}Ba(71.70)	
Eu	63	^{151}Eu(47.81) ^{153}Eu(52.19)	2
Ta	73	^{181}Ta(100)	1
W	74	^{182}W(26.3) ^{183}W(14.28) ^{184}W(30.7) ^{186}W(28.6)	4
Au	79	^{197}Au(100)	1
Pb	82	^{206}Pb(24.1) ^{207}Pb(22.1) ^{208}Pb(52.4)	3
Bi	83	^{209}Bi(100)	1

Appendix C: The main modules in CEARCPG

Modules	Purpose
CEARCPG	The main code of CEARCPG. Initialization part will be done in this part
Cf252	Sampling of neutron from ^{252}Cf neutron source. neutrons' energy, direction will be sampled in this modular
Function	Several functions used in CEARCPG are stored in this part
Gamma pack	Will simulate the gamma rays tracking part, including the fission gamma rays from neutron source
Gamma cross section read	The gamma rays cross sections f the used elements are read in this part
Neutron cross section	The neutrons cross section of the interested elements will be read in this part
Geometry pack	This package will calculate the particles track in cell. The data such as the distance to the cells surface and which cell is the next cell that particles will enter are calculated in this package
Interpolation	Package is used to interpolate the cross section from the previously stored cross section file. The cross section include the cross section of neutron and gamma rays
MCNP Random	The random number generator part. This random number generator is adopted from MNCP5 code
Neutron package	Neutron interaction part. Neutron scattering will be simulated in this part. This package the subroutines that are used for neutron elastic scattering, inelastic scattering as well neutrons thermal scattering
Parameters	The parameters used in CEARCPG, such as the maximum number of detectors allowed to use in code CAERCPG and the maximum number of arrays that are used to store the cross section data.
Record package	This package will record the single spectra and coincidence spectra of interested elements.
Scheme	The prompt gamma rays from neutron radioactive capture reaction and neutron inelastic scattering reaction will be sampled in the part
Sub	Several subroutines used in CEARCPG are store in the package
Sub_input	The geometry input file will be read in this package
Sub_NaI	The NaI detector response function will be calculated in this package